Euscorpius

Occasional Publications in Scorpiology

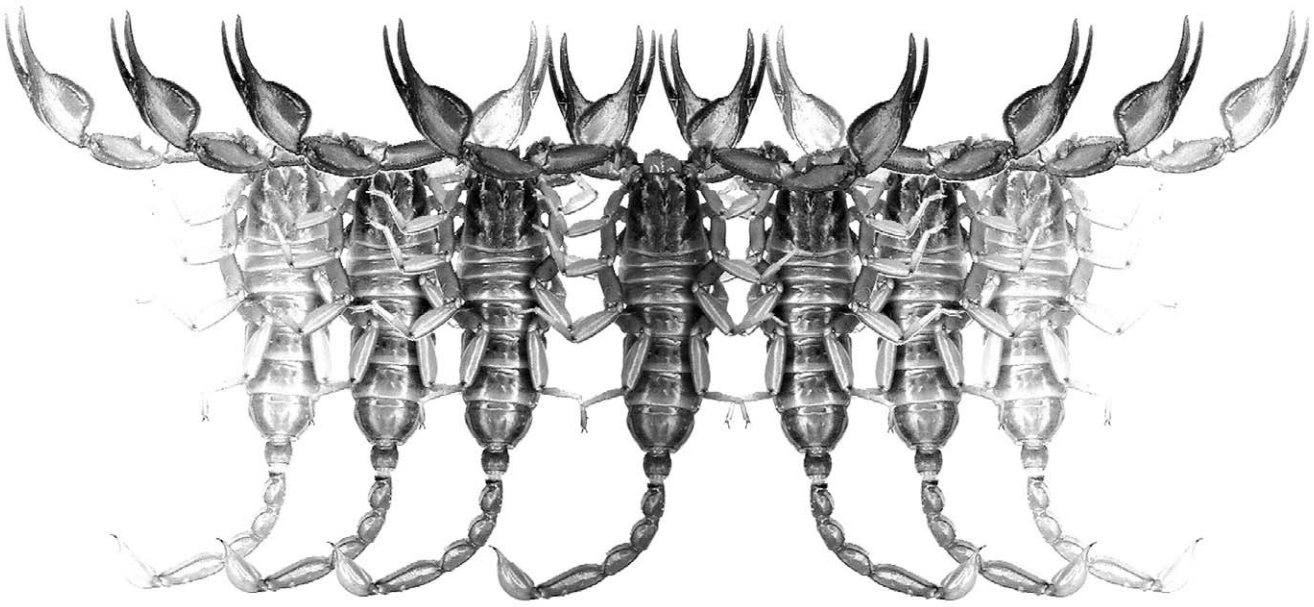

The Genera *Butheolus* Simon, 1882 and *Xenobuthus* gen. nov. (Scorpiones: Buthidae) in Oman

Graeme Lowe

May 2018 – No. 261

Euscorpius

Occasional Publications in Scorpiology

EDITOR: **Victor Fet**, Marshall University, **'fet@marshall.edu'**
ASSOCIATE EDITOR: **Michael E. Soleglad, 'soleglad@znet.com'**

Euscorpius is the first research publication completely devoted to scorpions (Arachnida: Scorpiones). ***Euscorpius*** takes advantage of the rapidly evolving medium of quick online publication, at the same time maintaining high research standards for the burgeoning field of scorpion science (scorpiology). ***Euscorpius*** is an expedient and viable medium for the publication of serious papers in scorpiology, including (but not limited to): systematics, evolution, ecology, biogeography, and general biology of scorpions. Review papers, descriptions of new taxa, faunistic surveys, lists of museum collections, and book reviews are welcome.

Derivatio Nominis

The name ***Euscorpius*** Thorell, 1876 refers to the most common genus of scorpions in the Mediterranean region and southern Europe (family Euscorpiidae).

Euscorpius is located at: **http://www.science.marshall.edu/fet/Euscorpius**

(Marshall University, Huntington, West Virginia 25755-2510, USA)

ICZN COMPLIANCE OF ELECTRONIC PUBLICATIONS:

Electronic ("e-only") publications are fully compliant with ICZN (*International Code of Zoological Nomenclature*) (i.e. for the purposes of new names and new nomenclatural acts) when properly archived and registered. All ***Euscorpius*** issues starting from No. 156 (2013) are archived in two electronic archives:

- **Biotaxa,** http://biotaxa.org/Euscorpius (ICZN-approved and ZooBank-enabled)
- **Marshall Digital Scholar**, http://mds.marshall.edu/euscorpius/. (This website also archives all *Euscorpius* issues previously published on CD-ROMs.)

Between 2000 and 2013, ICZN did not accept online texts as "published work" (Article 9.8). At this time, *Euscorpius* was produced in two identical versions: online (*ISSN 1536-9307*) and CD-ROM (*ISSN 1536-9293*) (laser disk) in archive-quality, read-only format. Both versions had the identical date of publication, as well as identical page and figure numbers. Only copies distributed on a CD-ROM from ***Euscorpius*** in 2001-2012 represent published work in compliance with the ICZN, i.e. for the purposes of new names and new nomenclatural acts.

In September 2012, ICZN Article 8. *What constitutes published work*, has been amended and allowed for electronic publications, disallowing publication on optical discs. From January 2013, ***Euscorpius*** discontinued CD-ROM production; only online electronic version (*ISSN 1536-9307*) is published. For further details on the new ICZN amendment, see http://www.pensoft.net/journals/zookeys/article/3944/.

Publication date: 25 May 2018

http://zoobank.org/urn:lsid:zoobank.org:pub:BDB28370-E60B-49B0-A2DA-F30D6E89D6D0

Euscorpius — Occasional Publications in Scorpiology. 2018, No. 261

The genera *Butheolus* Simon, 1882 and *Xenobuthus* gen. nov. (Scorpiones: Buthidae) in Oman

Graeme Lowe

Monell Chemical Senses Center, 3500 Market St, Philadelphia, USA

http://zoobank.org/urn:lsid:zoobank.org:pub:BDB28370-E60B-49B0-A2DA-F30D6E89D6D0

Summary

The genus *Butheolus* Simon, 1882 is revised based on new material from Dhofar Province in Oman. *B. gallagheri* Vachon, 1980 is redescribed, and a related new species, *B. harrisoni* **sp. n.**, is also described. The species *B. anthracinus* (Pocock, 1895) is redescribed and moved to a new genus *Xenobuthus* **gen. n.**, that is differentiated from *Butheolus* by size, pedipalp finger dentition, setation, granulation and hemispermatophore structure, and a related new species, *X. xanthus* **sp. n.**, is also described. Revised diagnoses are provided for the genus *Butheolus*, and for the species *B. thalassinus* Simon, 1882, and *B. villosus* Hendrixson, 2006, a key is given for the species examined in this study, and the status of other related species discussed.

Introduction

The Old World buthid genus *Butheolus* includes several small to medium-sized scorpions endemic to the Arabian Peninsula. Its composition has varied since it was originally created by Simon (1882) for two species: *B. thalassinus* from Aden, Yemen, and *B. aristidis* from Nubia, Egypt. A number of other small scorpions were described under *Butheolus*, but were subsequently moved into different genera, i.e. *Orthochirus* Karsch, 1892, *Microbuthus* Kraepelin, 1898 and *Neobuthus* Hirst, 1911 (Kovařík & Lowe, 2012). Two African genera, *Neobuthus* and *Nanobuthus* Pocock, 1895, have been considered either as subgenera or synonyms of *Butheolus* (Kovařík, 2003, 2004; Vachon, 1975), or as separate genera (Lourenço, 2001). Kovařík & Lowe (2012) showed that *Neobuthus* and *Butheolus* were distinct according to several diagnostic characters used in scorpion taxonomy at the genus level. Apart from *B. thalassinus*, other species described more recently under *Butheolus* are: *B. gallagheri* Vachon, 1980, from south coastal Dhofar Province of Oman; *B. villosus* Hendrixson, 2006, from the sand desert of central Saudi Arabia; *B. arabicus* Lourenço & Qi, 2006 from the Hijaz mountains of western Saudi Arabia; and *B. hallani* Lourenço & Rossi 2017 (= *B. pallidus* Lourenço & Duhem, 2012) from the United Arab Emirates. Simon (1910) indicated that *Buthus anthracinus* Pocock, 1895, from the Hadramaut, Yemen, might belong to *Butheolus*, and it was so listed by Fet & Lowe (2000).

The taxonomy of *Butheolus* has received relatively little attention over the years, as specimens were rare in museum collections. The genus is revised here based on study of substantial additional material, collected from the Dhofar Province of southern Oman mostly in expeditions by the author together with Michael D. Gallagher in 1993–1995, and by Alex & Birgit Winkler in 1999–2001. Detailed descriptions are provided for both sexes of *B. gallagheri*, which was originally based on a single male holotype. A closely related species, *B. harrisoni* **sp. n.**, is also described. The species *Buthus anthracinus* differs from *Butheolus* in some key characters and is transferred into a new genus, *Xenobuthus* **gen. n.**, which also includes a second new species, *X. xanthus* **sp. n.**

Abbreviations

Specimen depositories: AMNH, American Museum of Natural History, New York, USA; BMNH, Natural History Museum, London, UK; FKCP, private collection of František Kovařík, Prague, Czech Republic; GL, private collection of Graeme Lowe, Pennsylvania, USA; MCSN, Museo Civico de Storia Naturale "Giacomo Doria", Genoa, Italy; MCZ, Museum of Comparative Zoology, Cambridge, Massachusetts, USA; MNHN, Muséum National d'Histoire Naturelle, Paris, France; NHMB, Naturhistorisches Museum, Basel, Switzerland; ONHM, Oman Natural History Museum, Muscat, Oman; USNM, United States National Museum of Natural History (Smithsonian Institution), Washington, DC, USA; WDS, private collection of W. David Sissom, Canyon, Texas, USA; ZMUH, Zoologisches Institut und Zoologisches Museum, Universität Hamburg, Germany; ZSM, Zoologische Staatssammlung, Munich, Germany. *Biometrics*: L, length; W, width; D, depth. *Material*: juv, juvenile(s).

Materials & Methods

Material examined was either loaned from museums or collected by the author or other collectors. Collections were made in daytime by rock rolling, or at night by ultraviolet (UV) detection and locality coordinates were recorded either by Global Positioning System (Garmin GPS50) or estimated from published records and maps. Collected material was preserved in the field as described in Williams (1968). Specimens were studied under a dissecting microscope, viewing reflected white light or blue-green fluorescence under UV LED illumination. Biometrics were measured with an ocular reticule or digital camera as described in Lowe et al. (2014). Anatomical terminology generally follows Stahnke (1971), that of metasomal carination, Lowe et al. (2014), of tarsal segments and setation, Haradon (1984). Hemispermatophore terminology follows Kovařík et al. (2018). Illustrations were prepared from digital images acquired with reflected or trans-illuminated white light, or UV epifluorescence illumination (Prendini, 2003; Volschenk, 2005). Image frames from different focal planes were merged by focus stacking software (Zerene Stacker 1.02). Anatomical figures were prepared by merging color patterns under white light with cuticular surface topography revealed by UV fluorescence, except where indicated. Adult specimens are depicted except in Fig. 270. Summary statistics of variables are expressed as: range = minimum – maximum, and mean ± SD (standard deviation). Species diagnoses and descriptions are based on adults except for certain ontogenetically invariant meristic counts (i.e. pectine teeth and chela finger dentition) which also include juveniles.

Systematics

Genus ***Butheolus*** Simon, 1882

Butheolus Simon, 1882: 248.

Butheolus: Karsch, 1886: 76; Pocock, 1890: 121–122 (part); Pocock, 1892: 47; Laurie, 1896: 131; Lönnberg, 1897b; 194 (part); Kraepelin, 1899: 34 (part); Pocock, 1900: 28 (part); Kraepelin, 1905: 337, 353; Simon, 1910: 77; Hirst, 1911: 462, 464; Birula, 1917a: 164; Birula, 1917b: 55; Werner, 1934:145, 266, 270, 294, 299; Kästner, 1941: 231; Sreenivasa-Reddy, 1970: 18; Stahnke, 1972: 127, 129, fig. 12 (part); Vachon, 1974: 906; Vachon, 1975: 1598 (part); Vachon, 1980: 253 (part); Francke, 1985: 6, 15; Vachon & Kinzelbach, 1987: 92 (part); Sissom, 1990: 97, 101 (part); El-Hennawy, 1992: 97, 101, 104, 114 (part); Nenilin & Fet, 1992: 17; Lourenço & Vachon, 1995: 297; Kovařík, 1996: 177–178; Kovařík, 1998a: 117; Kovařík, 1998b: 105 (part); Fet & Lowe, 2000: 88 (part); Lourenço, 2001: 179; Kovařík, 2003: 137–138 (part); Soleglad & Fet, 2003: 88; Kovařík, 2004: 2–3, 25 (part); Fet & Soleglad, 2005: 11; Fet, Soleglad & Lowe, 2005: 3, 11, 22, fig. 23 (part); Lourenço, 2005: 26–28; Prendini & Wheeler, 2005: 481; Hendrixson, 2006: 56 (part); Lourenço & Qi, 2006: 91–93 (part); Dupré, 2007: 4, 12, 17 (part); Kovařík, 2009: 23, 31; Hennawy, 2009: 126 (part); Lowe, 2010a: 37, 44; Lourenço & Leguin, 2011: 1; Kovařík & Lowe, 2012: 1–2, 18–23 (part); Kovařík et al., 2013: 4; Yang et al., 2013: 5; Loria & Prendini, 2014: 25, tab. 5; Lowe et al., 2014: 120, fig. 98; Lowe & Kovařík, 2016: 1, 43; Loria & Prendini, 2018: tab. 1.

TYPE SPECIES. *Butheolus thalassinus* Simon, 1882, by subsequent designation (Kraepelin, 1895: 5; Pocock, 1895: 295).

Simon (1882) described *B. thalassinus* as a new species under *Butheolus*, but did not explicitly designate it as the type species. In the appendix to the same publication, he described a second new species under the same genus (*B. aristidis*), leaving ambiguity about which was the type species. Later, Birula (1898: 292) transferred *B. aristidis* to *Orthochirus*. According to Fet & Lowe (2000: 88), *B. thalassinus* was established as the type species of *Butheolus* by subsequent designation of Simon (1910: 77). However, a subsequent designation according to ICZN Art 69.1.1 had already been made earlier by Kraepelin (1895: 5) and Pocock (1985: 295) when they referenced *B. thalassinus* as the type species of *Butheolus*, and it was also cited as the type species by Pocock (1900: 28).

DIAGNOSIS**.** Small buthids (Kovařík, 2009; Sissom, 1990), adults 24–36 mm in length; carapace strongly trapezoidal, ratio of posterior W/ anterior W 1.9–2.5, preocular area inclined downwards towards anterior margin, surface densely granular, without distinct carinae; tergites densely granular, tergites I–III lacking carinae or with weak median carina, IV–VI weakly tricarinate with median and paired lateral carinae; tergite VII with broad median carina, two pairs of lateral carinae; posterior margins of sternites III–VI armed with fringe of non-contiguous digitate denticles that are larger in males; metasomal segments nearly uniform in width and depth, robust with granulated carinae, segments II–V densely granular on lateral and ventral intercarinal surfaces; metasoma I–III with 10 carinae, IV with 4 or 6 complete carinae (ventrosubmedian, ventrolateral pairs complete, dorsosubmedian pairs may be complete, dorsolateral pairs weak or incomplete), V with 2 complete carinae (ventrolateral pairs); ventrolateral carinae on metasoma V without enlarged lobate dentition; telson with slightly elongated ovoid vesicle, with or without a

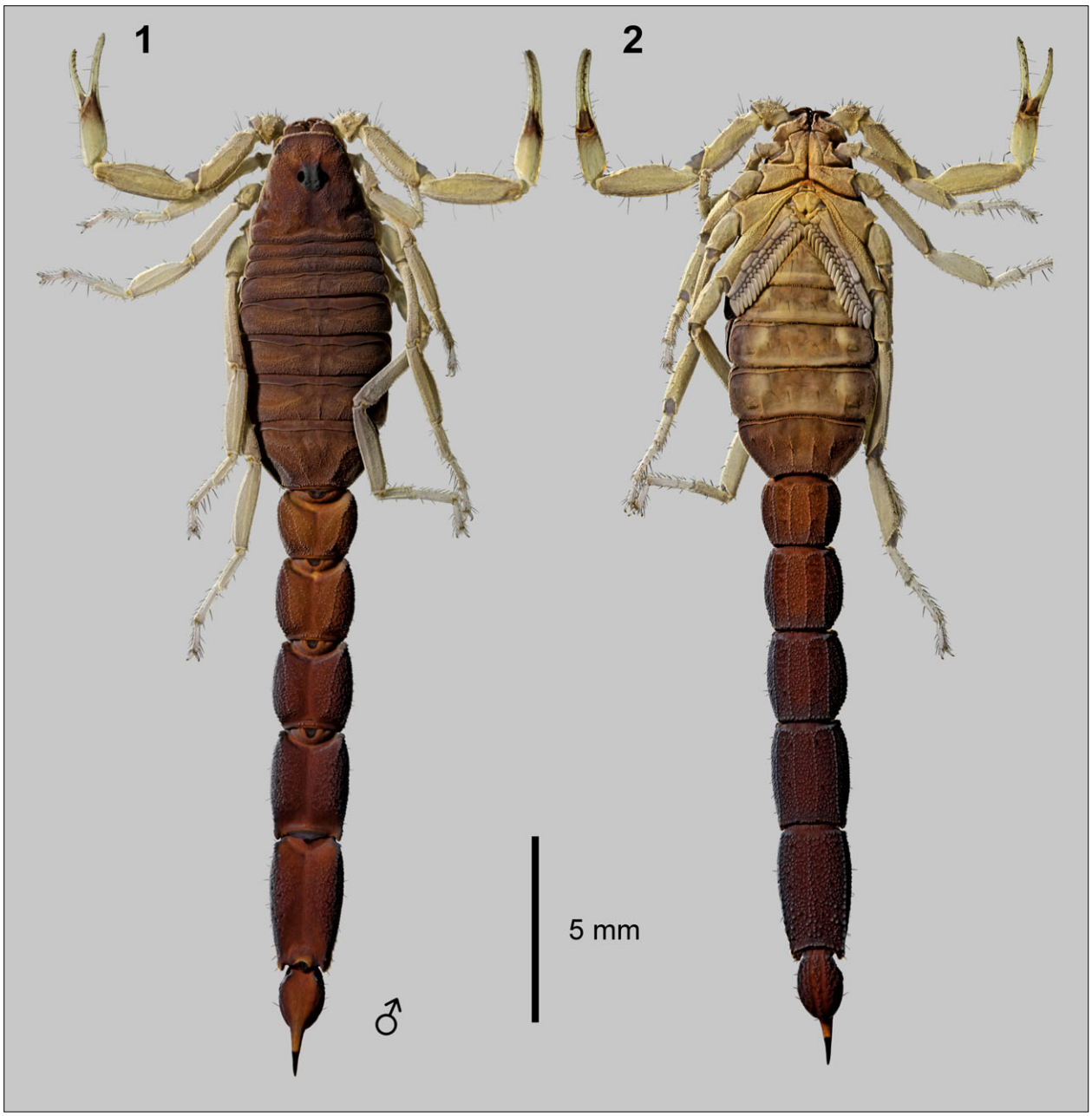

Figures 1–2: Habitus of male *Butheolus gallagheri* Vachon, 1980. **Fig. 1.** Dorsal aspect. **Fig. 2.** Ventral aspect. Oman, wadi above Khor Rori Beach, E. of Taqah, 17°3.2'N 54°25.33'E, 18.X.1993, leg. G. Lowe. Scale bar: 5 mm.

blunt subaculear tubercle, aculeus shorter than vesicle; pectines with fulcra; hemispermatophore with flagellum separated from a 3-lobed sperm hemiduct, basal lobe a small, narrow, hook-like process; chelicerae with characteristic buthid pattern of dentition (Vachon, 1963), two denticles on ventral aspect of fixed finger; pedipalps orthobothriotaxic, type Aβ (Vachon, 1974, 1975), patella with d_3 internal to dorsomedian carina, chela manus with V_2 not strongly displaced internally, V_1–V_2 axis nearly collinear with long axis of chela, chela fixed finger with *db* on proximal half of finger between *esb* and *est*, *it* near tip; pedipalps short, chelae small with carinae reduced or obsolete, dentate margins of fingers armed with 6–7 (rarely 8) non-imbricated linear subrows of primary denticles; subrows flanked by mid-row internal and proximal external accessory denticles; movable finger with 3 enlarged subdistal denticles; males without recess or scalloping of dentate margins at base of pedipalp fingers, with chela manus narrower than females; tergites lacking macrosetae; tibial spurs

Figures 3–4: Prosoma and mesosoma of male *Butheolus gallagheri* Vachon, 1980. **Fig. 3.** Dorsal aspect, carapace and tergites. Same locality data as male in Figs. 1–2. **Fig. 4.** Ventral aspect, coxosternal area and sternites. Oman, Salalah, leg. A. Ullrich. Scale bar: 1 mm.

present on legs III–IV; basitarsi I–III with regular series of long macrosetae on retrosuperior, retroinferior and inferior margins; ventral surfaces of telotarsi with paired rows of macrosetae; prolateral and retrolateral tarsal spurs present on all legs; moderate sexual dimorphism in setation, macrosetae on carapace, pedipalps, legs, sternites and metasoma longer in females than males.

REMARKS. Sexual dimorphism in setation is apparent in *Butheolus*, but is not as pronounced as it is in *Neo-*

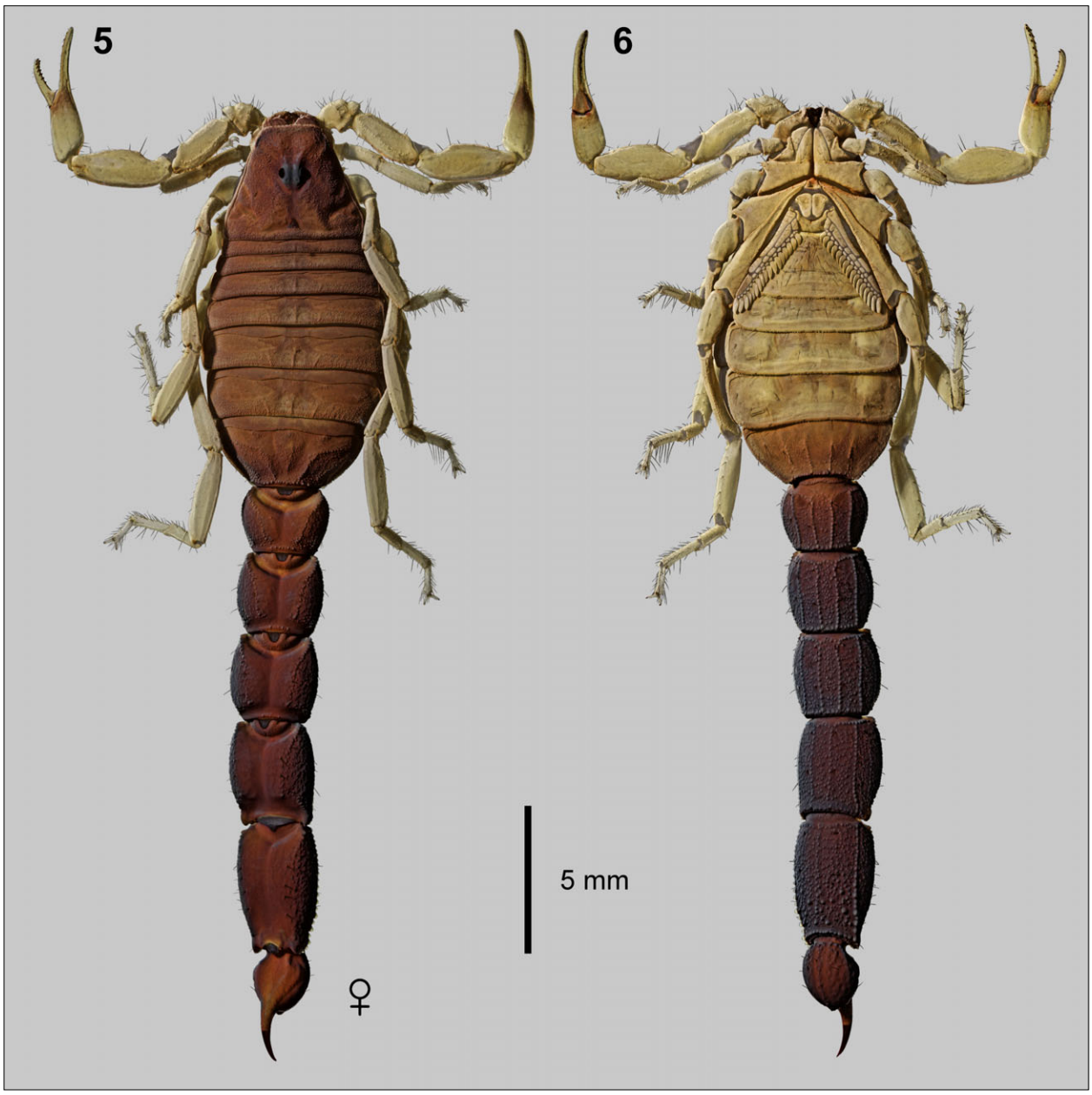

Figures 5–6: Habitus of female *Butheolus gallagheri* Vachon, 1980. **Fig. 5.** Dorsal aspect. **Fig. 6.** Ventral aspect. Same locality data as male in Figs. 1–2. Scale bar: 5 mm.

buthus Hirst, 1911, in which males usually bear much shorter, stouter macrosetae than females (Kovařík & Lowe, 2012).

***Butheolus gallagheri* Vachon, 1980**

(Figs. 1–66, 133–162, 330, 332, 338, Tabs. 1, 3–5)

Butheolus (*Butheolus*) *gallagheri* Vachon, 1980: 253–255, fig. 24, pl. B, C.

Butheolus gallagheri: Vachon & Kinzelbach, 1987: 100; Fet & Lowe, 2000: 88–89; Kovařík, 2003: 137; Kovařík, 2004: 4, 25; Santiago-Blay, Soleglad & Fet, 2004: 8; Fet, Soleglad & Lowe, 2005: 2; Lourenço, 2005: 27–28, fig. 32; Lourenço & Qi, 2006: 93–94, tab. 1; Kamenz & Prendini, 2008: 8, tab. 2, pl. 9; Kovařík & Lowe, 2012: 2, 18–23, figs. 76, 79, 82, 85, 88, 91, 93, 97–98, 102–103; Lourenço & Duhem, 2012: 122; Loria & Prendini, 2014, App. S1: 2, App. S2: 2; Lowe et al., 2014: 117.

Butheolus (*Butheolus*) *gallagheri*: El-Hennawy, 1992: 101, 114; Kovařík, 1998b: 105.

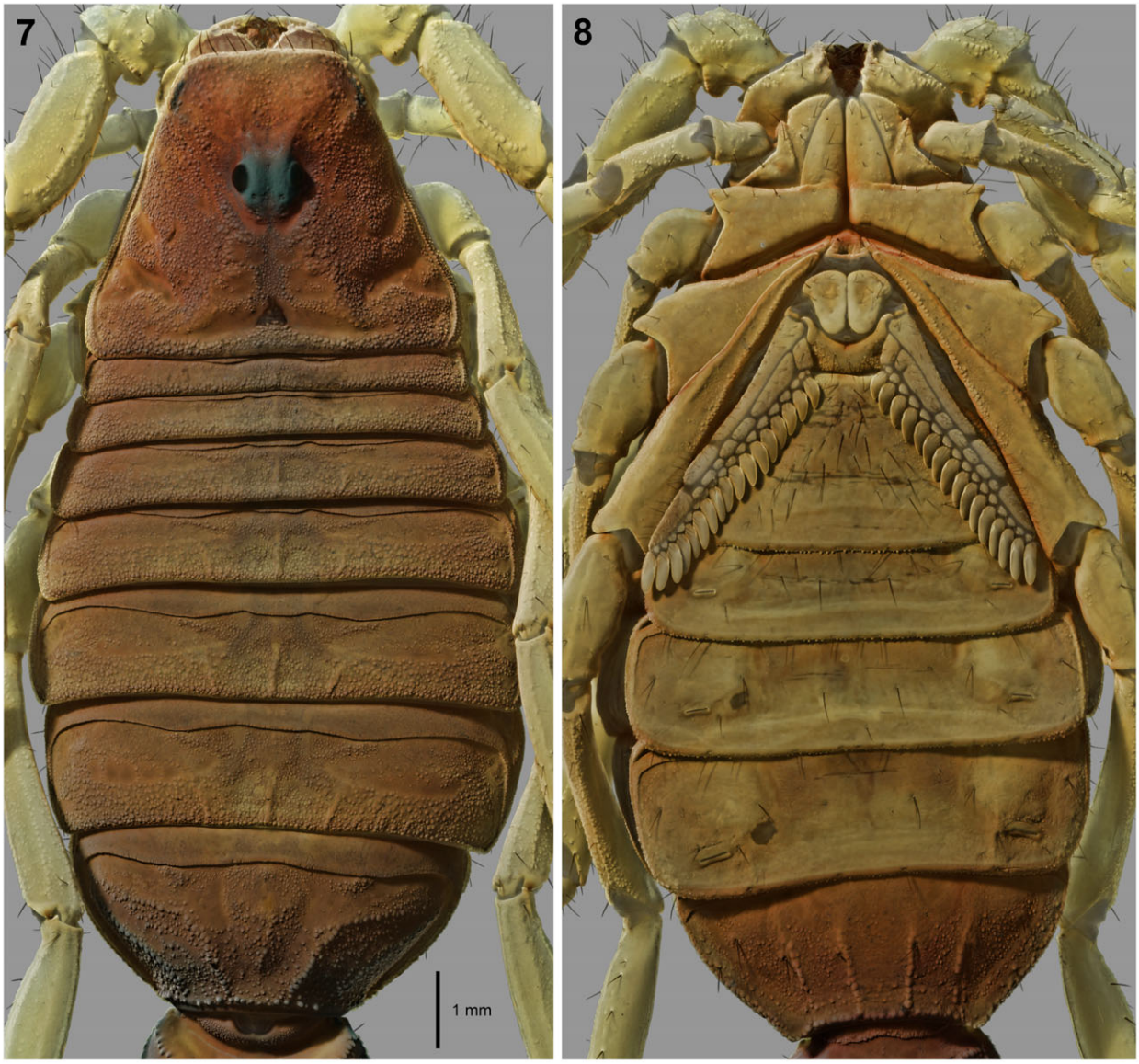

Figures 7–8: Prosoma and mesosoma of adult female *Butheolus gallagheri* Vachon, 1980. **Fig. 7.** Dorsal aspect, carapace and tergites. **Fig. 8.** Ventral aspect, coxosternal area and sternites. Same locality data as male in Figs. 1–2. Scale bar: 1 mm.

TYPE MATERIAL. Holotype ♂, **Oman**, Wadi Rabkut (Raykhut), Jabal Samhan, Dhofar, 17°24'N 55°16'E, 75 rn a.s.l., under rocks on side of wadi, 17–18.X.77, leg. M. D. Gallagher, MDG4738 (MNHN VA 2261) (examined).

OTHER MATERIAL EXAMINED. **Oman:** 1♂, Jabal Samhan, Dhofar, 17°07'N 54°42'E, 1280 m a.s.l., 7.IX. 1989, leg. M.D. Gallagher MDG 8149, (ONHM 1350); 1♂, Khor Rori Beach, UV detection, rock outcrop, archaeological site, 17°02.1'N 54°26.22'E, 0 m a.s.l., 18.X.1993, 20:27 h, leg. G. Lowe, (USNM); 2♀, Khor Rori Beach, UV detection, inland rocky hillock near beach, on rocky slopes, 17°02.21'N 54°26.19'E, 0 m a.s.l., 18.X.1993, 20:32 h, leg. G. Lowe, (ONHM); 8♂, 12♀, 1 juv♀, main road above Khor Rori Beach, UV detection on ground, densely vegetated wadi, E of Taqah; warm and humid with many insects, 17°03.22'N 54°25.33'E, 50 m a.s.l., 18.X.1993, 21:24 h, leg. G. Lowe (BMNH 1♂; FKCP 1♂,1♀; GL 1♂,1♀; MCZ 1♂; NHMB 2♂,10♀; ONHM 1♂,1♀); 2♂, 1♀, Khor Rori Beach, UV detection, densely vegetated wadi, on ground, 17°03.18'N 54°25.51'E, 22 m a.s.l., 24-XII-2001, 02:25-04:45 h, leg. A. Winkler (ZSM); 1♂, Salalah, leg. A. Ullrich (GL).

DIAGNOSIS**.** A member of the genus *Butheolus* differentiated as follows: small scorpions, adults 22–32 mm; base color a uniform dark chocolate brown, with all

Figures 9–32: Pedipalp of *Butheolus gallagheri* Vachon, 1980. **Figs. 9–20.** Male (♂). Dorsal (9–11), external (12–14), ventral (15–17) and internal (18–20) aspect of femur (9, 12, 15, 18), patella (10, 13, 16, 19) and chela (11, 14, 17, 20). **Figs. 21–32.** Female (♀). Dorsal (21–23), external (24–26), ventral (27–29) and internal (30–32) aspect of femur (21, 24, 27, 30), patella (22, 25, 28, 31) and chela (23, 26, 29, 32). Both sexes with same locality data as male in Figs. 1–2. Scale bars: 1 mm.

metasomal segments and telson dark; pedipalps and legs yellow except for fuscosity at base of chela fingers; carapace and tergites uniformly, finely granular; pedipalp patella with dorsomedian carina incomplete, restricted to distal half of segment, weak or obsolete on proximal half; pedipalp chela with carinae weak or obsolete; ventral surface between ventromedian carinae of metasoma I with dense fine granulation in females; ventral and lateral intercarinal surfaces of metasoma II–V with fine granulation; metasoma and telson with sparse, short macrosetae; telson with moderate to small subaculear tubercle, obtuse angle between posterior vesicle surface and aculeus base; pedipalp and metasoma relatively slender: pedipalp femur L/W ♂ 3.00–3.38, ♀ 2.43–2.76; pedipalp patella L/W ♂ 3.20–3.65, ♀ 2.64–2.84; pedipalp chela L/W ♂ 5.16–5.65, ♀ 4.24–4.79; metasoma I L/W ♂ 0.81–0.92, ♀ 0.76–0.81; metasoma IV L/D ♂ 1.44–1.60, ♀ 1.37–1.54, metasoma V L/D ♂

1.96–2.12, ♀ 1.82–2.08, telson L/D ♂ 2.46–2.83, ♀ 2.33–2.56; pectine teeth ♂ 17–21, ♀ 14–17; basitarsus III retrosuperior setae 4–8.

REDESCRIPTION.
Based on 14 ♂, 16 ♀ (including holotype ♂).

Coloration (Figs. 1–32, 51–54, 59–66). Base color a uniform dark brown on dorsal aspect of prosoma. mesosoma and all aspects of metasoma and telson; metasoma darker than mesosoma; carapace slightly lighter in postocular, posterior-median triangular area, tergites with lighter lateral patches in transverse reticulated bands; telson vesicle with pale spots at bases of macrosetae and a pair pale stripes on ventral surface; dorsal aspect of chelicerae dark on fingers and distal margin of manus, yellow-brown reticulated on distal half of manus; legs yellow except for reddish spots on distal external articular condyles; pedipalps yellow except for fuscous patch on distal chela manus at base of pedipalp fingers; ventral aspect of mesosoma yellow except for weak fuscosity on sternite VII.

Carapace (Figs. 1, 3, 5, 7). Strongly trapezoidal, W/L 0.79–0.92, posterior W/ anterior W 1.97–2.38; lateral flanks steeply sloped; median ocular tubercle prominent; postocular area forming triangular posteromedial plateau with shallow transverse posterior marginal furrows; interocular triangle sloped downwards towards anterior margin; anterior margin with 9–11 macrosetae that are longer in females, carapace otherwise devoid of macrosetae; anterolateral margins with 5 pairs of lateral eyes: 3 major ocelli and 1 major or minor posterior ocellus below a granular ridge, 1 minor ocellus above granular ridge; whitish eyespot present below lateral eye cluster; all carinae of carapace obsolete except for superciliary carinae which may extend slightly anterior to median ocular tubercle; entire surface with dense fine granulation except for smooth patches on postocular plateau, posterior transverse and posterior marginal furrows; superciliary carinae may be smooth or weakly granulated, with more granules on posterior slopes; granulation may be coarser on lateral parts of interocular triangle, anterior margin of carapace, and margins of postocular triangular plateau area; males with more densely granulose interocular triangle.

Chelicerae (Figs. 65–66). Dorsal surface of manus smooth, with two short, pale microsetae on apical margin, each with adjacent granules; dorsointernal carina strong, granulate, bearing one long, dark macroseta and one short, pale microseta; fingers robust with dentition typical of genus, movable finger dorsal margin with two large subdistal denticles and two small basal denticles, ventral margin with larger subdistal and smaller basal denticles, fixed finger with large subdistal denticle and proximal bicusp, two denticles on ventral surface; dorsal surface of movable finger smooth, with two pale microsetae.

Coxosternal area (Figs. 2, 4, 6, 8). *Males*. Coxa I finely granulated, endite smooth on anterior half, granulated on posterior half; coxa II densely, finely granulated, endite smooth on anterior third, granulated on posterior two thirds; coxa III densely, finely granulated, granules more coarse along anterior margin; coxa IV densely, finely granulated, anterior margin with band of coarser granules, posterior margin rimmed with linear series of granules; distal anterior surfaces of coxae II–IV smooth; coxae I–III with scattered, mostly anterior macrosetae: coxa I 5–9, II 8–12, III 3–5; coxa IV typically with single macroseta on anterior proximal limit; sternum weakly granulated, subtriangular, with deep posteromedian pit, usually 2 short macrosetae; genital opercula with fine granulation anteriorly, posteriorly smooth, with 2–5 macrosetae, posterolateral margins concave. *Females*. Coxae smooth except for weak granulation on medial endites of coxa I, anterior margins of coxa III–IV, and row of moderate granulation on anterior 2/3 of posterior margin of coxa IV; setation as in males; sternum smooth, with larger median pit; genital opercula smooth, elongate, with 4–8 macrosetae.

Pectines (Figs. 2, 4, 6, 8). Basal piece with concave anterior margin and small median groove and pit, finely granulated in males, smooth anteriorly and finely granulated posteriorly in females, bearing 5–8 macrosetae; pectines with 3 marginal lamellae, 5–7 middle lamellae, extending to proximal 1/4 of trochanter IV in males, distal end of coxa IV in females; teeth longer in males than females; marginal and middle lamellae with moderate cover of short macrosetae; fulcra with 2–4 setae.

Hemispermatophore (Figs. 55–58, 330). Flagelliform, trunk elongate, ca. 4.7 times length of capsule region; flagellum short; sperm hemiduct tripartite, posterior lobe large, laminate, median lobe small, acuminate, anterior lobe of intermediate length, tapered; posterior margin of median lobe overhanging posterior lobe, the two lobes fused along a median lobe carina; basal lobe a prominent, narrow, hook-like projection.

Mesosoma (Figs. 1–8, 332). *Tergites*: pretergites smooth, with sinuous, finely corrugated posterior margins; tergites densely, finely granulated, with smoother transverse lateral strips on tergites IV–VI; tergites I–II without carinae or with trace of weak median carina, III with weak median carina and weak or obsolete lateral carinae, IV–VI weakly tricarinate with median and paired lateral carinae, VII with 5 carinae, the median carina a weak granulated hump; all carinae finely granular, confined to posterior half of tergites, lateral carinae anteriorly divergent; tergite granulation and carination weaker in females than males; all tergites lacking macrosetae; *sternites*: *males*: sternites III–V lacking carinae, medially smooth, laterally shagreened

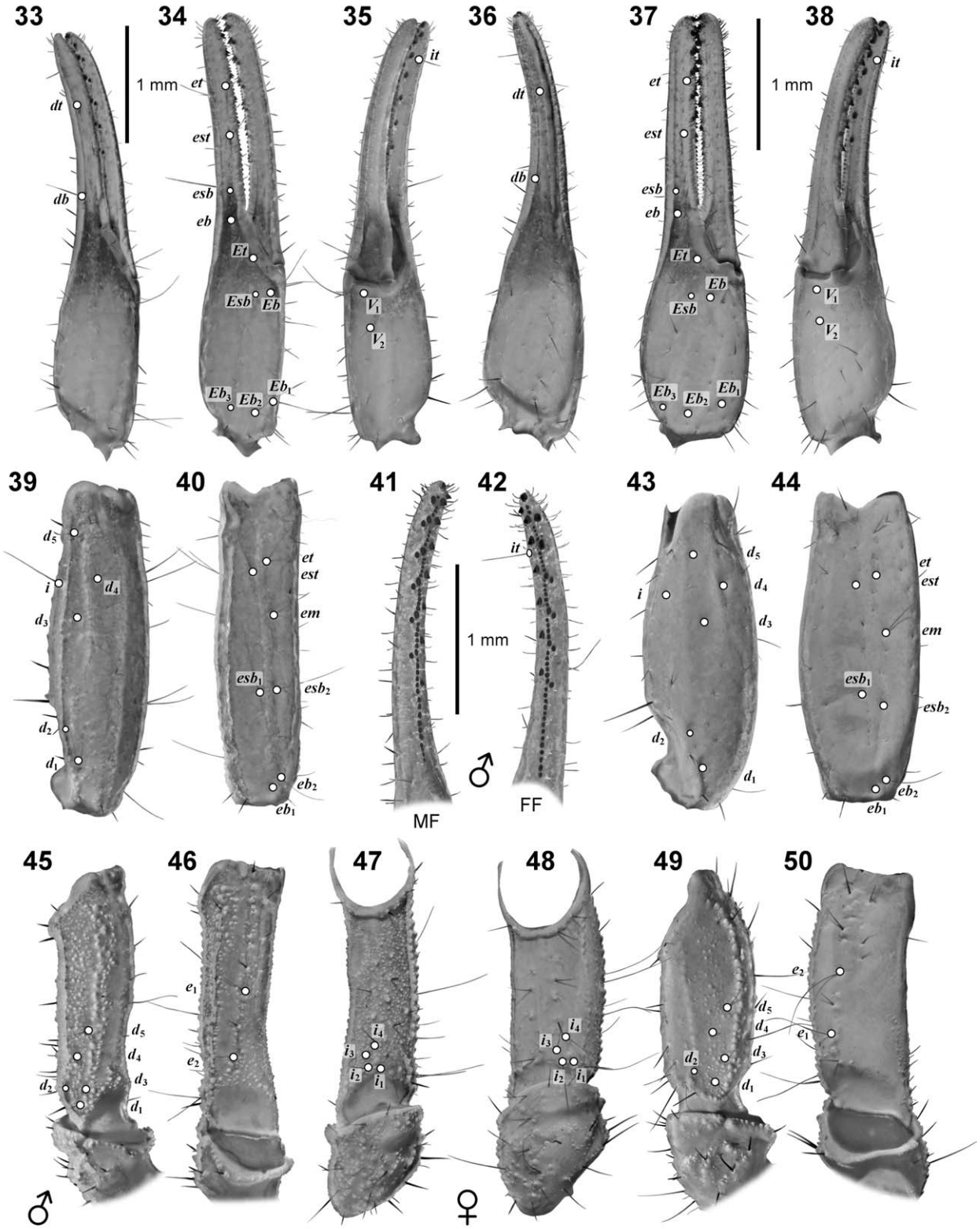

Figures 33–50: Trichobothrial maps and chela finger dentition of *Butheolus gallagheri* Vachon, 1980. Male (♂): dorsal (33), external (34) and ventral (35) aspect of chela; dorsal (39) and external (40) aspect of patella; dorsal (45), external (46) and internal (47) aspect of femur; dentition of movable finger (MF) (41) and fixed finger (FF) (42). Female (♀): dorsal (36), external (37) and ventral (38) aspect of chela; dorsal (43) and external (44) aspect of patella; internal (48), dorsal (49) and external (50) aspect of femur. Same locality data as male in Figs. 1–2. Scale bars: 1 mm (♂, ♂ dentition, ♀).

Figures 51–54: Leg tarsi, tibiae and patellae of male *Butheolus gallagheri* Vachon, 1980. Retrolateral aspect, left leg I tibia, basitarsus and telotarsus (51), left legs II–IV, patella, tibia, basitarsus and telotarsus (52–54 respectively). Same locality data as male in Figs. 1–2. White light illumination. Scale bar: 1 mm.

Figures 55–58: Hemispermatophore of *Butheolus gallagheri* Vachon, 1980. **Fig. 55.** Whole right hemispermatophore, convex aspect. Scale bar: 1 mm. **Figs. 56–58.** Capsule region and flagellum of right hemispermatophore, anterior (56), convex (57) and posterior (58) aspects. In convex view (57), the capsule is compressed to show outlines of lobes. Same locality data as male in Figs. 1–2. White light illumination. Scale bar: 200 µm.

or finely granular; sternite VI with smooth or obsolete inner lateral carinae, weakly granulated outer lateral carinae on posterior half of sternite; sternites IV–VI with wide, posteromedian smooth patch; posterior margins of sternites III–VI with fringe of numerous, small, non-contiguous, closely spaced, digitate denticles; sternite VII densely, finely granular, with granulate median and lateral pairs of carinae confined to posterior 2/3 of sternite, only median pairs extending to posterior margin; all sternites with scattered, sparse macrosetae, sternite VII with 4 stereotypic isolated macrosetae near outer anterior ends of carinae; *females*: sternite III smooth medially, shagreened laterally in areas covered by pectines, sternites IV–VI smooth; carinae absent on sternites III–V, only trace of lateral carinae on VI; posterior marginal denticles of sternites III–VI smaller than in males; sternite VII with two pairs of carinae, weaker than carinae of males, with weaker dense, fine granulation on lateral surfaces; mesosoma much wider in females than males.

Metasoma (Figs. 1–2, 5–6, 59–64). Moderate in length with robust segments, metasoma + telson L/carapace L ♂ 5.3–5.7, ♀ 4.8–5.3; *carination*: segments I–III with 10 complete carinae, IV with 4 complete carinae (dorsosubmedian and dorsolateral carinae visible only on anterior 1/5 of segment), V with 2 carinae (ventrolateral); carinae on segments I–IV uniformly granulate, ventrolateral carinae on V with smaller granules in anterior half, larger granules in posterior half; ventromedian carina on V obsolete, a trace indicated by linear series of granules; lateral anal margin with 2 blunt granules or lobes, ventral anal margin with 10–14 granules; *intercarinal surfaces*: dense, fine granulation on dorsolateral, lateral, ventrolateral and ventral surfaces of all segments; some coarser granules on posterior 1/3 of ventral surface of V; in males, dorsal surfaces sparsely, finely granulated on I–IV and anterior half of V, smooth on posterior slope of IV and posterior half of V in trough accommodating telson; in females, dorsal surfaces smooth except for a few isolated small granules

Figures 59–64: Metasoma and telson of *Butheolus gallagheri* Vachon, 1980. **Figs. 59–61.** Male (♂). Dorsal (59), right lateral (60) and ventral (61) aspects. **Figs. 62–64.** Female (♀). Dorsal (62), right lateral (63) and ventral (64) aspects. Same locality data as male in Figs. 1–2. Scale bars: 2 mm.

(mostly on I–II); *setation*: scattered microsetae and sparse, short macrosetae present on all segments, setae slightly longer in females; dorsal surfaces lack setation, except for metasoma V which may bear 2–4 macrosetae along dorsolateral margins.

Telson (Figs. 1–2, 5–6, 59–64). Vesicle smooth dorsally, strongly granulated laterally and ventrally, ovoid, with steep posterior slope due to development of weak subaculear tubercle; granules on lateral and ventral surfaces arranged in longitudinal bands, separated by smooth lateral and ventrosubmedian troughs; scattered microsetae and short macrosetae on lateral and ventral surfaces; vesicle granulation weaker in female, posterior areas almost smooth, with shallow indentations at setal insertion points; aculeus stout, shorter than vesicle.

Pedipalps (Figs. 9–50). *Males* (Figs. 9–20, 33–35, 39–42, 45–47). *Femur*: L/W 3.00–3.38; dorsointernal carina moderate, with uniform medium-size granules; dorsoexternal carina strong with coarse granules; external carina moderate, nearly smooth with fine granules

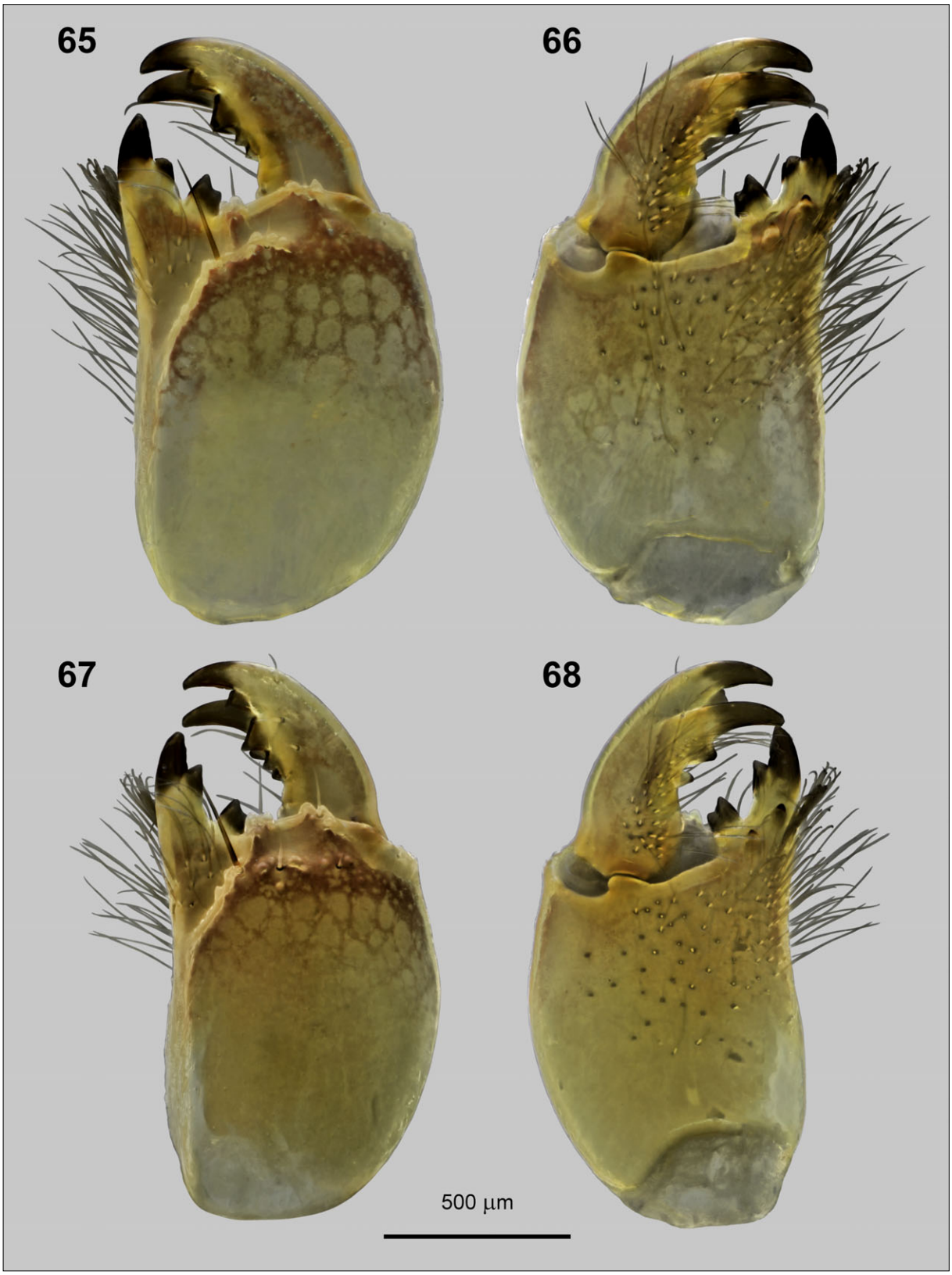

Figures 65–68: Chelicerae of male *Butheolus gallagheri* Vachon, 1980 and *B. harrisoni* sp. n. **Figs. 65–66.** *B. gallagheri*, right chelicera, dorsal (65) and ventral (66) aspect. Same locality data as male in Figs. 1–2. **Figs. 67–68.** *B. harrisoni* sp. n., right chelicera, dorsal (67) and ventral (68) aspect. Paratype male, Oman, Jabal Qara, north slopes, Nejd desert, 17°17.83'N 54°5.11'E, 16.X.1993, leg. G. Lowe. Scale bar: 500 µm.

Measurements (mm)	*Butheolus gallagheri* Vachon, 1980			
	♂ #1	♂ #2	♀ #1	♀ #2
Total L	26.05	27.85	31.80	25.30
Metasoma + Telson L	16.60	18.20	19.88	16.07
Carapace L	3.03	3.46	3.85	3.29
Carapace anterior W	1.57	1.82	2.12	1.71
Carapace posterior W	3.50	3.91	4.79	4.08
Carapace preocular L	1.31	1.46	1.67	1.39
Metasoma I L/W/D	1.96/ 2.22/ 1.84	2.08/ 2.57/ 2.16	2.25/ 2.96/ 2.42	1.92/ 2.45/ 2.04
Metasoma II L/W/D	2.31/ 2.18/ 1.86	2.57/ 2.65/ 2.22	2.69/ 2.92/ 2.38	2.25/ 2.41/ 2.04
Metasoma III L/W/D	2.58/ 2.25/ 2.04	2.76/ 2.71/ 2.38	2.92/ 2.98/ 2.54	2.42/ 2.38/ 2.08
Metasoma IV L/W/D	3.08/ 2.29/ 1.96	3.42/ 2.67/ 2.33	3.50/ 2.90/ 2.54	2.85/ 2.34/ 2.04
Metasoma V L/W/D	3.58/ 2.17/ 1.73	4.18/ 2.42/ 2.13	4.29/ 2.75/ 2.25	3.54/ 2.24/ 1.88
Telson L	3.17	3.50	3.96	3.21
Vesicle L/W/D	1.93/ 1.35/ 1.14	2.25/ 1.62/ 1.39	2.42/ 1.92/ 1.62	1.88/ 1.47/ 1.31
Pedipalp chela L	3.83	4.19	4.58	3.92
Chela movable finger L	2.33	2.55	2.77	2.33
Chela fixed finger L	1.79	1.92	2.11	1.75
Chela manus ventral L/W/D	1.57/ 0.71/ 0.73	1.76/ 0.78/ 0.82	1.89/ 1.08/ 1.16	1.65/ 0.86/ 0.93
Pedipalp femur L/W	2.36/ 0.71	2.54/ 0.85	2.53/ 1.02	2.17/ 0.86
Pedipalp patella L/W	2.93/ 0.90	3.25/ 0.92	3.42/ 1.27	2.83/ 1.06
Pectine length	2.71	3.33	3.29	2.75
Pectine teeth (left/ right)	18/18	19/19	16/17	15/14

Table 1: Measurements of representative adults of *Butheolus gallagheri* Vachon, 1980. Males (♂): Oman, wadi above Khor Rori Beach, E. of Taqah, 17°3.2'N 54°25.33'E, 18.X.1993, leg. G. Lowe. Females (♀): #1, same locality as males; #2, Oman, rocky slopes above Khor Rori Beach, 17°2.21'N 54°26.19'E, 18.X.1993, leg. G. Lowe. Abbreviations: L, length; W, width, D depth.

proximally, larger conical granules distally; ventrointernal carina moderate, with uniform medium-size granules; internal carina weak, with irregular fine and coarse granules; dorsal and internal surfaces with dense, fine granulation, ventral surface with sparse fine granulation or shagreened, external surfaces mostly smooth, with scattered fine granules near carinae; 3–6 accessory macrosetae on distal external surface; *patella*: L/W 3.20–3.65; dorsointernal carina moderate, finely granular; dorsomedian carina moderate, finely granular, continuous only in distal half of segment, residual trace at proximal end of segment indicated by broken granule row; dorsoexternal carina moderate, weakly granular or smooth; external carina weak, broad, smooth; internal carina moderate, finely granulated; other carinae obsolete; dorsal, external and ventral surfaces smooth or slightly roughened, without granulation; internal surface with weak, fine granulation; *chela*: slender, L/W 5.16–5.65, all carinae obsolete, surface smooth with sparse macrosetae and microsetae; 5–7 primary denticle subrows on movable and fixed fingers (including cases of fusion of proximal rows), subrows except proximal typically flanked by internal and external accessory denticles; 5–7 internal or external accessory denticles on movable finger, 4–6 on fixed finger. *Females* (Figs. 21–32, 36–38, 43–44, 48–50). *Femur*: more robust than in males, L/W 2.43–2.76; dorsointernal carina weak to moderate, with uniform medium-size granules; dorsoexternal carina moderate with coarse granules; external carina weak, smooth, with a few distal granules; ventrointernal carina weak, with uniform small granules; internal carina weak, broad, smooth; dorsal surface with

sparse, fine granulation mostly in medial area, ventral surface smooth except for narrow medial band of weak, fine granules in proximal 1/3 of segment, external and internal surfaces smooth; 5–8 accessory macrosetae on distal external surface, including linear series of 3–5 on ventral side of external carina; *patella*: more robust than in males, L/W 2.64–2.84; dorsomedian carina weak, smooth, present only on distal half of segment; dorsointernal, dorsoexternal, external and internal carinae weak, smooth; other carinae obsolete; all intercarinal surfaces smooth; *chela*: more robust than in males, L/W 4.24–4.79, all carinae obsolete, surface smooth with sparse macrosetae and microsetae; finger dentition as in male. *Trichobothriotaxy*: orthobothriotaxic, type Aβ (Vachon, 1974) (Figs. 33–50)

Legs (Figs. 1–2, 5–6, 51–54). Femur and patella I–IV with finely denticulate inferior carinae, other carinae finely granulate; prolateral surfaces of femur I–IV with dense, fine granulation, of patella II–IV with sparse fine granulation, on both segments slightly weaker in females than males; tibia III–IV with spurs; retrolateral tarsal spurs simple, prolateral tarsal spurs basally bifurcate; basitarsi I–III with 4–8 long retrosuperior macrosetae arranged in bristle-combs; ventral surface of telotarsi with dual rows of short, fine macrosetae (occasionally reduced to single row on telotarsus I); tarsal ungues stout.

Measurements. See Table 1.

Variation. Color patterns were stable in the sampled populations. Meristic and morphometric variation are summarized in Tabs. 3–5, and Figs. 133–162.

DISTRIBUTION. Known only from coastal sites around Jabal Samhan or Jabal Qara, in the Dhofar Province of Oman (Fig. 338).

ECOLOGY. Most examined material was collected from low elevations (< 100 m a.s.l.), but one record was at 1,280 m a.s.l. on the plateau atop the Jabal Samhan escarpment. The species occurs in mesic or humid environments along the coast, in densely vegetated rocky wadis with gravel and sandy soil. Scorpions that occurred together with *B. gallagheri* were: *Hottentotta salei* (Vachon, 1980) and *Leiurus haenggii* Lowe et al., 2014.

Butheolus harrisoni, sp. n.

(Figs. 67–162, 333, 338, Tabs. 2–5)

http://zoobank.org/urn:lsid:zoobank.org:act:CCE68C77-AC8B-4D80-AECD-5EF8297554F

Butheolus gallagheri: Wood, 1993: 17.

TYPE MATERIAL. Holotype ♂, **Oman**, Jabal Qara, Salalah-Thumrait road, UV detection, arid rocky wadi, edge of Nejd Desert, 17°17.26'N 54°05.36'E, 800 m a.s.l., 17.X.1993, 20:53 h, leg. G. Lowe (NHMB).

PARATYPES. **Oman:** 3♂, 6♀, 1 juv♂, same locality as holotype (NHMB 3♂, 4♀; ONHM 1♂, 2♀); 1♂, Jabal Qara, 6.IX.1989, leg. M.D. Gallagher MDG 8146.2 (ONHM 1351); 6♂, 7♀, 1 juv♂, 1 juv♀, Jabal Qara; north slopes, Nejd, UV detection, rocky wadi & rocky slopes, 17°17.83'N 54°05.11'E, 800 m a.s.l., 16.X.1993, 22:38 h, leg. G. Lowe (BMNH 1♂; MNHN 1♂; NHMB 3♂, 6♀; USNM 1♂, 1♀); 1♀, Jabal Qara, north slopes, Nejd Desert, UV detection, vegetated wadi bottom, chirping crickets, 17°17.01'N 54°05.81'E, 520 m a.s.l., 16.X.1993, 23:39 h, leg. G. Lowe (MCZ); 1♀, Jabal Qara, Salalah-Thumrait road, UV detection, grassy/ rocky plateau with low hills and slopes, just south of police checkpoint, 17°15.98'N 54°04.88'E, 850 m a.s.l., 17.X.1993, 20:04 h, leg. G. Lowe (MNHN); 4♂, 2♀, 2 juv♂, 1 juv♀, Jabal Qara, Salalah-Thumrait road, UV detection, wide rocky wadi, nr edge of wadi and rocky flats, 17°17.58'N 54°04.97'E, 800 m a.s.l., 17.X.1993, 21:45 h, leg. G. Lowe (NHMB); 1♀, Jabal Qara, Nejd Desert, road to Ayun, UV detection, edge of wadi, major wadi below Ayun, fine silt and gravel in middle of wadi, rocky slopes and large rock formations on edges, day to dusk (few scorpions), 17°13.4'N 53°54.36'E, 600 m a.s.l., 20.X.1993, 18:36 h, leg. G. Lowe (BMNH); 1♂, 2♀, 3 juv♂, 1 juv♀, Jabal Qamr, wadi between steep winding roads, UV detection, on gravel in wide wadi with boulders/ rounded rocks, 16°52.3'N 53°43.28'E, 40 m a.s.l., 27.IX.1995, 23:25 h, leg. G. Lowe, M.D. Gallagher (GL); 7♂, 2♀, 1 juv♂, E of Jabal Qamr, along coastal wadi, UV detection on slope and gravel at base of slope, vegetated slopes with rocks, soil suitable for burrowing, 16°53.71'N 53°48.75'E, 15 m a.s.l., 28.IX. 1995, 00:30 h, leg. G. Lowe, M.D. Gallagher (ONHM); 1 subadult♂, Jabal Qamar, 2 km E of Ardit (Loc. F/10), windswept plateau with small rocky wadis, under rocks on slope, 16°50.7'N 53°23.69'E, 1060 m a.s.l., 1.I.1999, 11:00–16:30 h, leg. A. Winkler, B. Winkler (ZSM); 1♀, Wadi Uyun (Loc. F/12), sand alluvium under big bush under stone, 17°14.39'N 53°53.99'E, 400 m a.s.l., 2.I.1999, 16:30 h, leg. A. Winkler (ZSM); 1♀, Wadi Uyun (Loc. F/12), sand alluvium, under big bush under stone, 17°14.39'N 53°53.99'E, 400 m a.s.l., 3.I.1999, 10:00–12:00 h, leg. A. Winkler (ZSM); 1 juv♀, Jabal Qamar, 2 km E of Ardit (Loc. F/15II), UV detection, windswept plateau with rocky wadis, between small shrubs, 16°50.7'N 53°23.69'E, 1060 m a.s.l., 31.I.2000, 16:00–21:00 h, leg. B. Winkler (ZSM); 1 juv♂, Jabal Qamar, 3 km E of Ardit (Loc. F/13), UV detection, windswept plateau with rocky wadis, under small stone, 16°50.71'N 53°23.72'E, 1076 m a.s.l., 19.XII.2001, 18:00–20:30 h, leg. A. Winkler (ZSM); 1♂, 2♀, Jabal Qamar, 3 km E of Ardit (Loc. F/14), UV detection, windswept plateau with rocky wadis, under small stone,

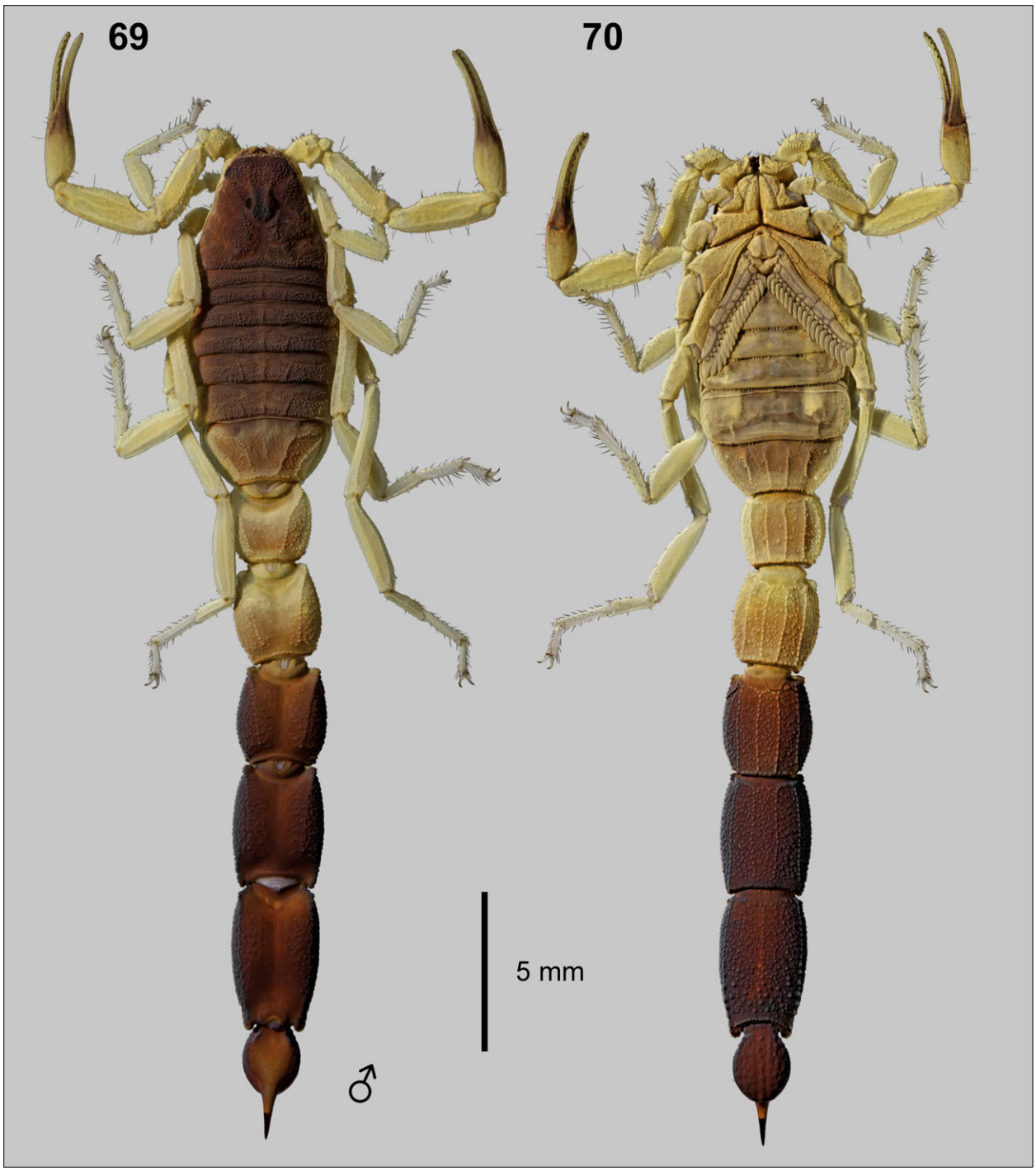

Figures 69–70: Habitus of male *Butheolus harrisoni* sp. n. **Fig. 69.** Dorsal aspect. **Fig. 70.** Ventral aspect. Holotype male (♂), Oman, Jabal Qara, Salalah-Thumrait road, 17°17.26'N 54°5.36'E, 17.X.1993, leg. G. Lowe. Scale bar: 5 mm.

16°50.87'N 53°23.77'E, 1067 m a.s.l., 19.XII.2001, 21:00–22:15 h, leg. A. Winkler (ZSM).

DIAGNOSIS**.** A member of the genus *Butheolus* differentiated as follows: small scorpions, adults 25–35 mm; bicolored, carapace and mesosoma moderate to dark brown but usually lighter on posterior tergites, metasomal segments IV–V and telson dark brown, metasoma I–II lighter brown to yellow, pedipalps and legs yellow except for fuscosity at base of chela fingers; carapace and tergites with mixture of fine and coarse granulation; pedipalp patella with dorsomedian carina

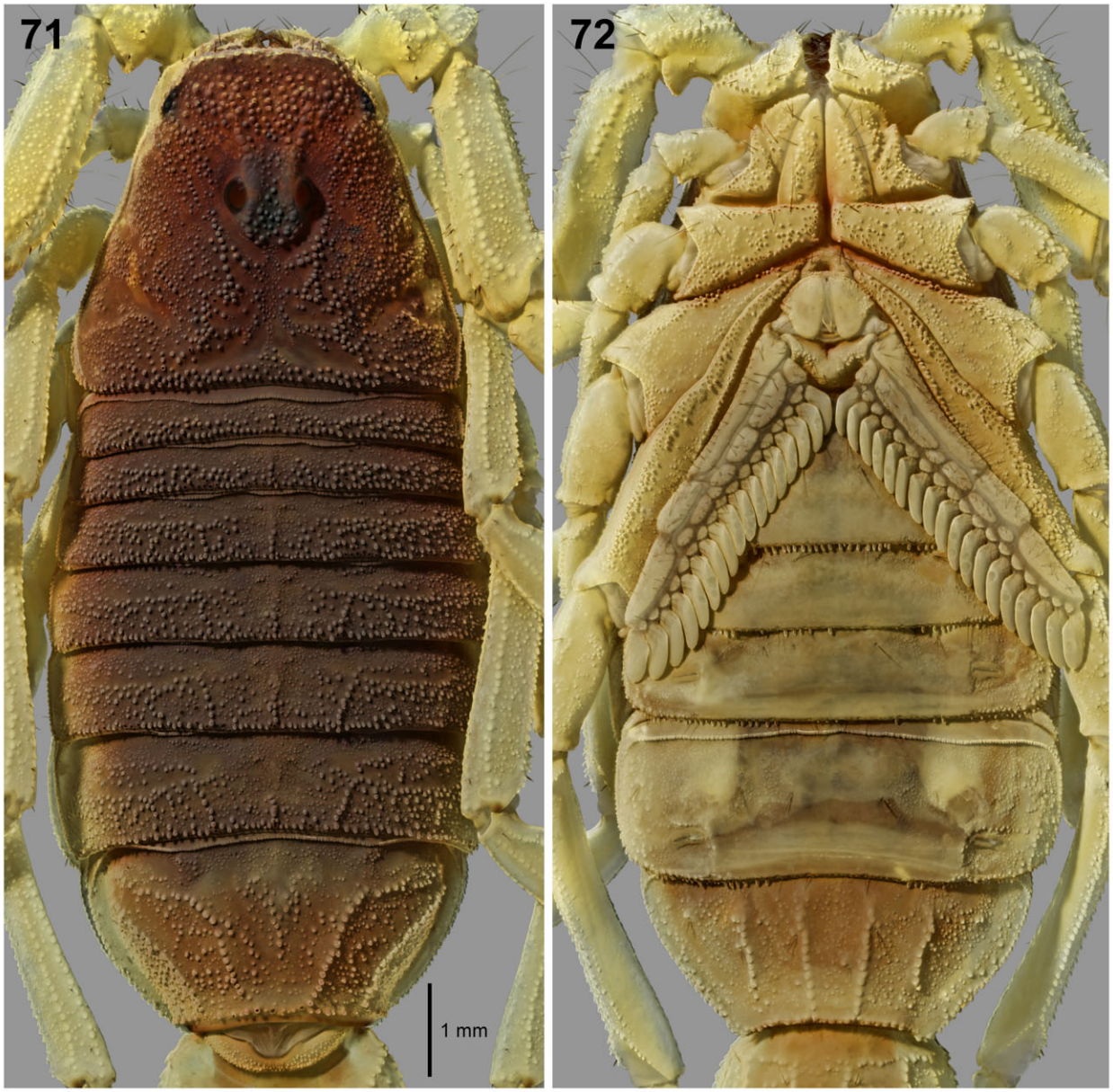

Figures 71–72: Prosoma and mesosoma of male *Butheolus harrisoni* sp. n. **Fig. 71.** Dorsal aspect, carapace and tergites. **Fig. 72.** Ventral aspect, coxosternal area and sternites. Holotype male. Scale bar: 1 mm.

complete; pedipalp chela with carinae weak or obsolete; ventral surface between ventromedian carinae of metasoma I with sparse, fine granulation or smooth in females; ventral and lateral intercarinal surfaces of metasoma II–V with moderately coarse granulation; metasoma and telson with sparse, short macrosetae; telson with subaculear tubercle small or absent, obtuse angle between posterior vesicle surface and aculeus base; pedipalp and metasoma moderately stout; pedipalp femur L/W ♂ 2.72–3.23, ♀ 2.29–2.47; pedipalp patella L/W ♂ 2.84–3.46, ♀ 2.33–2.64; pedipalp chela L/W ♂ 4.90–5.48, ♀ 4.07–4.67; metasoma I L/W ♂ 0.81–0.91, ♀ 0.74–0.83; metasoma IV L/D ♂ 1.43–1.69, ♀ 1.37–1.54, metasoma V L/D ♂ 1.92–2.28, ♀ 1.86–2.10, telson L/D ♂ 2.33–2.73, ♀ 2.27–2.51; pectine teeth ♂ 17–21, ♀ 14–17; basitarsus III retrosuperior setae 6–10.

COMPARISONS. Most similar to *B. gallagheri*, from which it differs in the following characters: pale color of metasoma I–II, coarser granulation on carapace and tergites, complete dorsomedian carina on pedipalp patella, subaculear tubercle on telson vesicle small or indistinct; on average, higher numbers of setae in basitarsal bristlecombs (Figs. 148–149), more robust pedipalp femur and

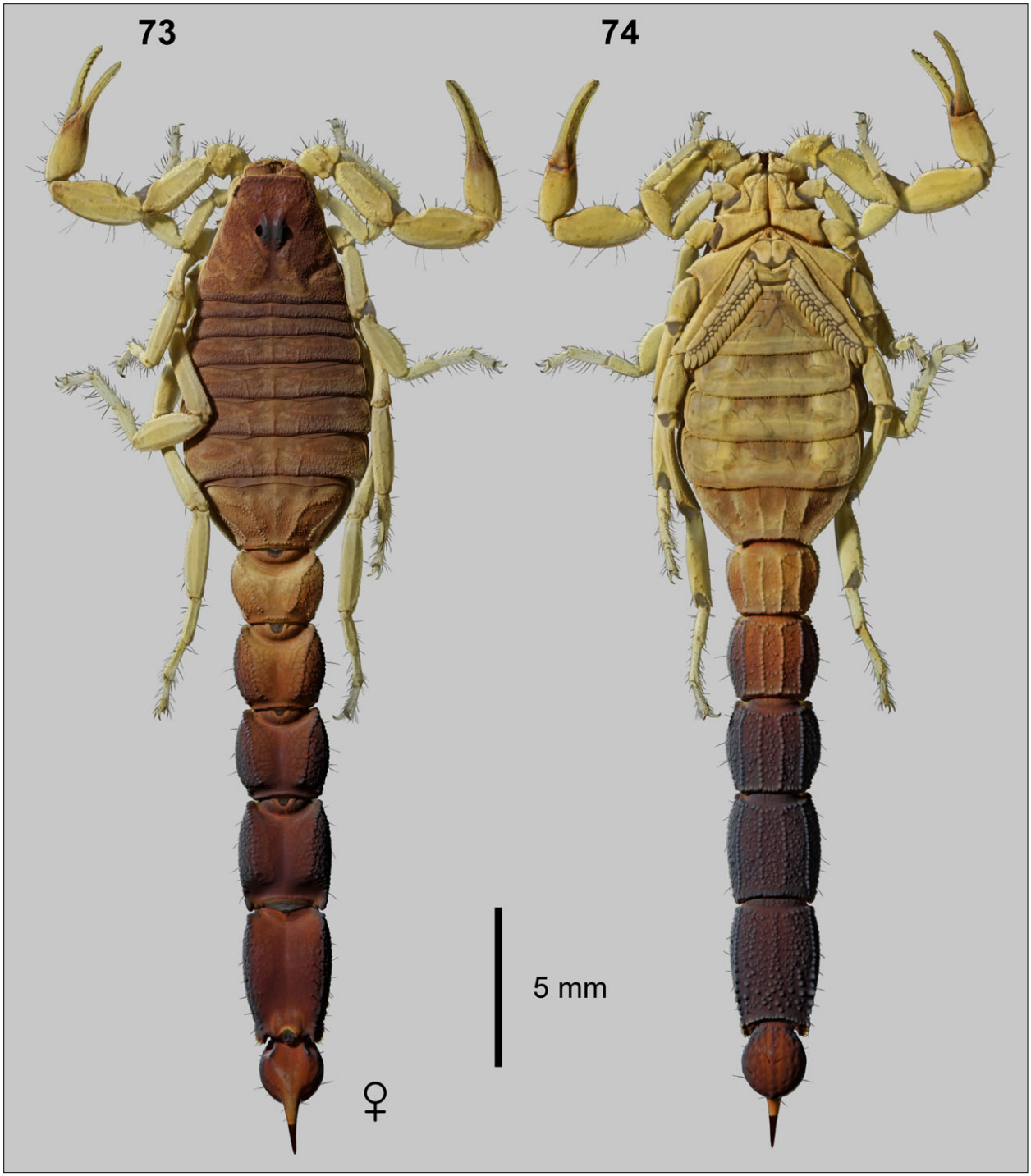

Figures 73–74: Habitus of female *Butheolus harrisoni* sp. n. **Fig. 73.** Dorsal aspect. **Fig. 74.** Ventral aspect. Paratype female, same locality data as male in Figs. 67–68. Scale bar: 5 mm.

patella (Figs. 151, 157), wider and deeper pedipalp chela manus (Fig. 136) relative to carapace.

ETYMOLOGY. A patronym in honor of Ian D. Harrison, who collected and contributed much material in support of studies on the scorpion fauna of Oman.

DESCRIPTION.
Based on holotype ♂, 32 ♂ and 29 ♀ paratypes.

Coloration (Figs. 69–100, 119–122, 127–132). Bicolored or with variable fuscous pattern; carapace and tergites vary from dark brown to light yellowish-brown,

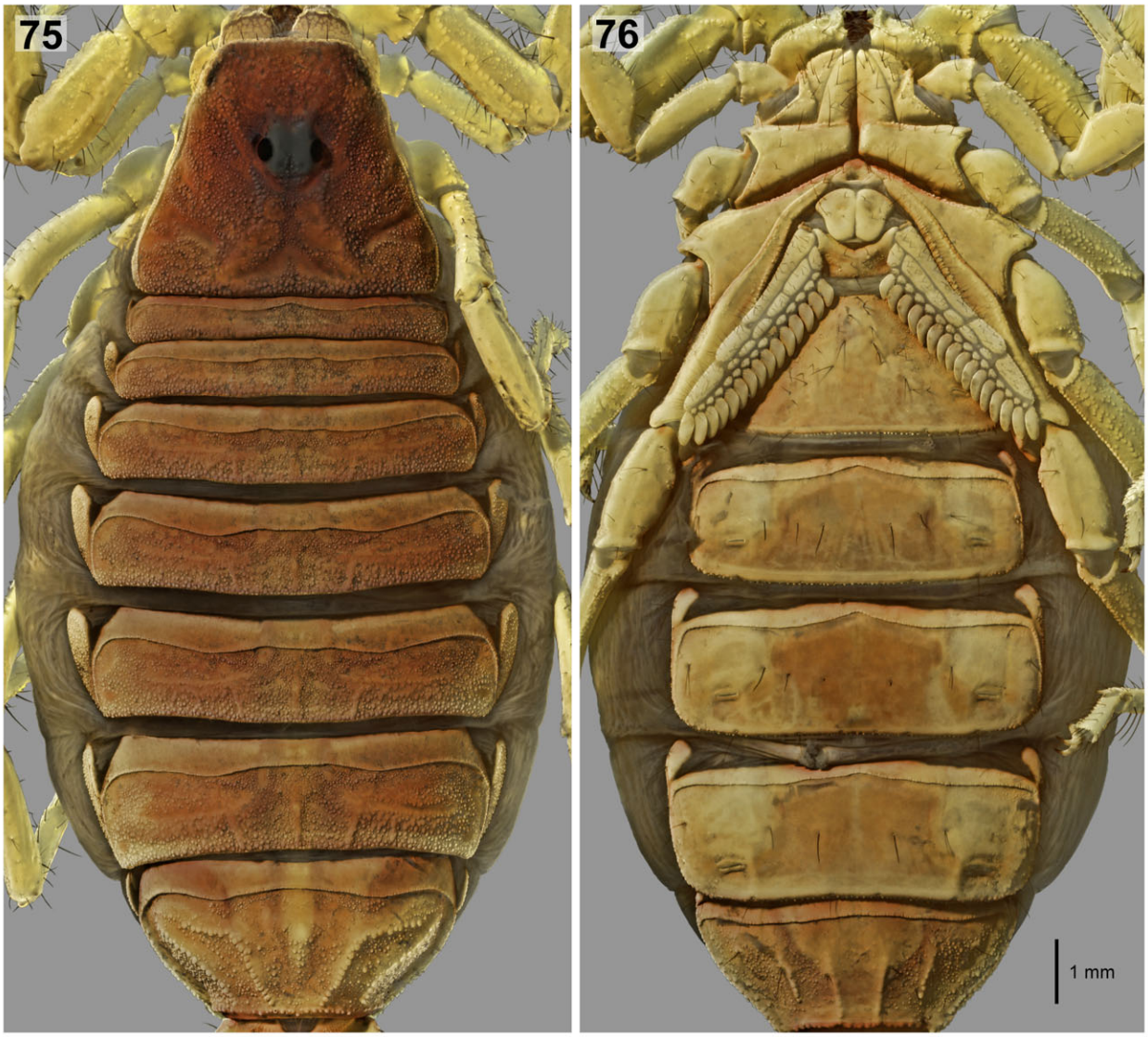

Figures 75–76: Prosoma and mesosoma of adult female *Butheolus harrisoni* sp. n. **Fig. 75.** Dorsal aspect, carapace and tergites. **Fig. 76.** Ventral aspect, coxosternal area and sternites. Paratype female, same locality data as male in Figs. 67–68. Scale bar: 1 mm.

tergite VII may be lighter than others; metasomal segments I–II range from yellow to light brown, IV–V dark brown, III more variable, ranging from bright yellow to a dark brown matching IV–V; telson dark reddish brown, not as dark as metasoma IV–V, vesicle with pale spots at bases of macrosetae and a pair of pale stripes on ventral surface; carapace slightly lighter in postocular, posterior-median triangular area, tergites with lighter lateral patches in transverse reticulated bands; dorsal aspect of chelicerae dark on fingers and distal margin of manus, yellow-brown reticulated on distal quarter of manus; legs yellow except for reddish spots on distal external articular condyles; pedipalps yellow except for fuscous patch on distal chela manus at base of pedipalp fingers, and dorsal femur and patella may occasionally have weak fuscous markings that leave pale spots at the bases of trichobothria; coxosternal area and ventral surface of mesosoma yellow, sternite VII may be light brownish-yellow.

Carapace (Figs. 69, 71, 73, 75). Strongly trapezoidal, W/L 0.78–0.97, posterior W/ anterior W 2.00–2.46; lateral flanks steeply sloped; median ocular tubercle prominent; postocular area forming triangular posteromedial plateau with shallow transverse posterior marginal furrows; interocular triangle sloped downwards towards anterior margin; anterior margin with 8–10 macrosetae that are longer in females, carapace otherwise devoid of macrosetae; anterolateral margins with 5

Figures 77–100: Pedipalp of *Butheolus harrisoni* sp. n. **Figs. 77–88.** Holotype male (♂). Dorsal (77–79), external (80–82), ventral (83–85) and internal (86–88) aspect of femur (77, 80, 83, 86), patella (78, 81, 84, 87) and chela (79, 82, 85, 88). **Figs. 89–100.** Paratype female (♀), same locality data as male in Figs. 67–68. Dorsal (89–91), external (92–94), ventral (95–97) and internal (98–100) aspect of femur (89, 92, 95, 98), patella (90, 93, 96, 99) and chela (91, 94, 97, 100). Scale bars: 1 mm.

pairs of lateral eyes: 3 major ocelli and 1 major or minor posterior ocellus below granular ridge, 1 minor ocellus above granular ridge; whitish eyespot present below lateral eye cluster; all carinae of carapace obsolete except for superciliary carinae which may extend slightly anterior to median ocular tubercle; entire surface with dense fine to coarse granulation except for smooth patches on postocular plateau, posterior transverse and posterior marginal furrows; granulation fine on lateral flanks, coarse on interocular triangle, moderately coarse on posterior margin of carapace and borders of postocular triangular plateau; granulation weaker in females than males; superciliary carinae of females smooth, of males smooth above, granulated anteriorly and posteriorly.

Chelicerae (Figs. 67–68). Dorsal surface of manus smooth, with two short, pale microsetae on apical margin, each with adjacent granules; dorsointernal car-

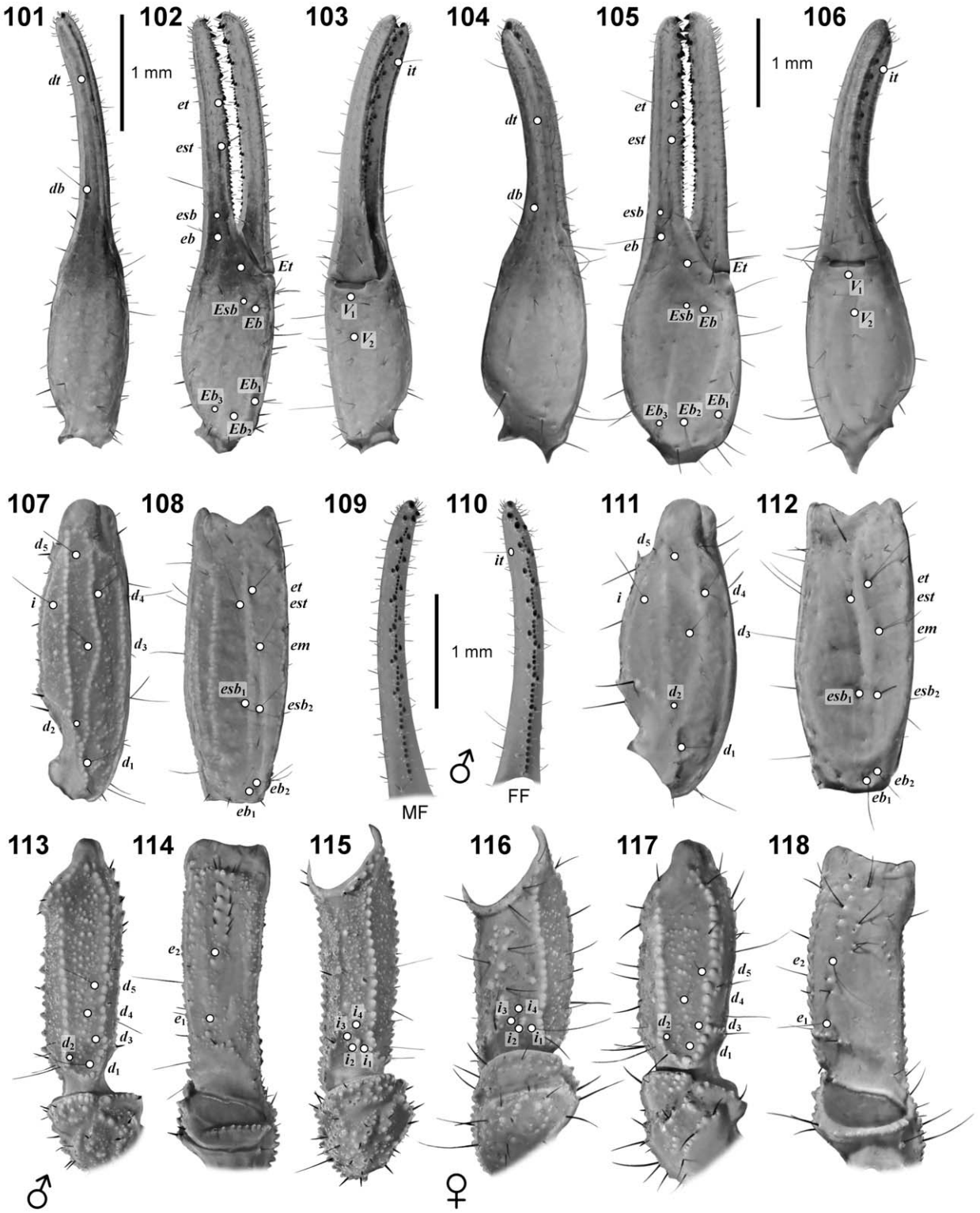

Figures 101–118: Trichobothrial maps and chela finger dentition of *Butheolus harrisoni* sp. n. Holotype male (♂): dorsal (101), external (102) and ventral (103) aspect of chela; dorsal (107) and external (108) aspect of patella; dorsal (113), external (114) and internal (115) aspect of femur; dentition of movable finger (MF) (109) and fixed finger (FF) (110). Paratype female (♀), same locality data as male in Figs. 67–68: dorsal (104), external (105) and ventral (106) aspect of chela; dorsal (111) and external (112) aspect of patella; internal (116), dorsal (117) and external (118) aspect of femur. Scale bars: 1 mm (♂, ♂ dentition, ♀).

Figures 119–122: Leg tarsi and tibiae of male *Butheolus harrisoni* sp. n. Holotype male. Retrolateral aspect, left leg I (119), II (120), III (121), IV (122) tibia, basitarsus and telotarsus. White light illumination. Scale bar: 1 mm.

ina strong, granulate, bearing one long, dark macroseta and one short, pale microseta; fingers robust with dentition typical of genus, movable finger dorsal margin with two large subdistal denticles and two small basal denticles, ventral margin with larger subdistal and smaller basal denticles, fixed finger with large subdistal denticle and proximal bicusp, two denticles on ventral surface; dorsal surface of movable finger smooth, with 2–3 pale microsetae.

Coxosternal area (Figs. 70, 72, 74, 76). *Males*. Coxa I coarsely granulated, endite smooth on anterior half, granulated on posterior half; coxa II coarsely, irreg-

Figures 123–126: Hemispermatophore of *Butheolus harrisoni* sp. n. **Fig. 123.** Whole right hemispermatophore, convex aspect. Scale bar: 1 mm. **Figs. 124–126.** Capsule region of right hemispermatophore, anterior (124), convex (125) and posterior (126) aspects. In convex view (125), the capsule is compressed to show outlines of lobes. Paratype male, same locality data as male in Figs. 67–68. White light illumination. Scale bar: 200 µm.

ularly granulated, endite with granules concentrated along midline, surface smooth on medial and lateral margins; coxa III irregularly, coarsely granulated, granules concentrated along anterior margin; coxa IV with numerous coarse granules in anterior marginal band and posterior marginal row, central smooth strip in narrow anterior half of coxa, finely granulated in broad posterior half; distal anterior surface of coxae II–IV with reduced granulation or smooth; coxae I–III with scattered, mostly anterior macrosetae: coxa I 7–11, II 12–18, III 4–8; coxa IV typically with single macroseta on anterior proximal limit; sternum weakly granulated, subtriangular, with deep posteromedian pit, usually 2 macrosetae; genital opercula with fine granulation near anterior margins, otherwise smooth, with 3–7 macrosetae, posterolateral margins concave. *Females*. Coxa I with weak coarse granulation, smooth on anterior part of endites; coxa II with very weak granulation, almost smooth; coxa III smooth except for anterior marginal granulation; coxa IV smooth except for anterior and posterior marginal fine granulation; sternum smooth, with larger median pit; genital opercula smooth, elongate; setation as in male, but with longer setae.

Pectines (Figs. 70, 72, 74, 76). Basal piece with concave anterior margin and small median groove and pit, coarsely granulated in males, smooth anteriorly and finely shagreened posteriorly in females, bearing 2–8 macrosetae; pectines with 3 marginal lamellae, 5–7 middle lamellae, extending to proximal 1/5–1/3 of trochanter IV in males, distal end of coxa IV in females; teeth longer in males than females; marginal and middle lamellae with moderate cover of short macrosetae; fulcra with 2–4 setae.

Hemispermatophore (Figs. 123–126). Flagelliform, trunk elongate, ca. 6 times length of capsule region; flagellum short with thicker pars recta and thinner pars reflecta; sperm hemiduct tripartite, posterior lobe large, laminate, median lobe small, acuminate, anterior lobe of intermediate length, tapered; posterior margin of median lobe overhanging posterior lobe, the two lobes fused along a median lobe carina; basal lobe a prominent, narrow, hook-like projection.

Mesosoma (Figs. 69–76, 333). *Tergites*: pretergites smooth, with sinuous, finely corrugated posterior margins; tergites densely, finely granulated, with smoother transverse lateral strips on tergites IV–VI; tergites I–II without carinae or with trace of weak median carina, III with weak median carina and weak or obsolete lateral carinae, IV–VI weakly tricarinate with median and paired lateral carinae, VII with 5 carinae, the median

carina weak; all carinae finely granular, confined to posterior half of tergites, lateral carinae anteriorly divergent; tergite granulation and carination weaker in females than males; all tergites lacking macrosetae; *sternites*: *males*: sternites III–V lacking carinae, medially smooth or shagreened, laterally shagreened or finely granular; sternite VI with smooth or obsolete inner lateral carinae, smooth or weakly granulated outer lateral carinae on posterior half of sternite; sternites IV–VI with wide, posteromedian smooth patch; posterior margins of sternites III–VI with fringe of numerous, small, non-contiguous, closely spaced, digitate denticles; sternite VII densely, finely granular, with granulate median and lateral pairs of carinae confined to posterior 3/4–4/5 of sternite, only median pairs extending to posterior margin; all sternites with scattered, sparse macrosetae, sternite VII with 4 stereotypic isolated macrosetae on mid- to anterior external sides of carinae; *females*: sternite III smooth medially, shagreened laterally in areas covered by pectines, sternites IV–VI smooth; carinae absent on sternites III–V, only smooth traces of outer lateral carinae on VI; posterior marginal denticles of sternites III–VI smaller than in males; sternite VII with two pairs of weakly granular or almost smooth carinae, weaker than carinae of males, with weaker dense, fine granulation or shagreened on median and lateral surfaces; mesosoma much wider in females than males.

Metasoma (Figs. 69–70, 73–74, 127–132). Moderate in length with robust segments, metasoma + telson L/ carapace L ♂ 4.8–5.8, ♀ 4.7–5.5; *carination*: segments I–III with 10 complete carinae, IV with 4 complete carinae (dorsosubmedian and dorsolateral carinae usually visible only on anterior 1/2 of segment), V with 2 carinae (ventrolateral) strongly developed, dorsolateral carinae may be weakly developed and only visible in anterior part of segment; carinae on segments I–IV uniformly granulate, ventrolateral carinae on V with smaller granules in anterior half, larger granules in posterior half; ventromedian carina on V obsolete, a trace indicated by linear series of granules; females with coarser granulation of carinae than males, with segment I having weaker granulation on ventrolateral and ventral carinae; lateral anal margin with 2 blunt granules or lobes, ventral anal margin with 13–18 granules; *intercarinal surfaces*: segment I with dense, fine granulation on lateral surfaces, weakly shagreened on ventrolateral and ventral surfaces; II–V with dense, fine granulation on lateral, ventrolateral and ventral surfaces, V with some coarser granules on posterior 1/3 of ventral surface; dorsal surfaces sparsely, finely granulated on I–IV and anterior half of V, smooth on posterior slope of IV and posterior half of V in trough accommodating telson; in females, granulation less dense and coarser on all surfaces, segments I–II may have ventrolateral and ventral surfaces sparsely granulated or smooth; dorsal surfaces in female smooth except for few isolated small granules, usually on segments I–II; *setation*: scattered microsetae and sparse, short macrosetae present on all segments, macrosetae slightly longer in females; dorsal surfaces lack setation, except for metasoma V which may bear 2–4 macrosetae along dorsolateral margins.

Telson (Figs. 69–70, 73–74, 127–132). Vesicle smooth dorsally, rugose and weakly granulated laterally and ventrally with small granules more apparent on anterior-ventral surface, ovoid with gentle posterior slope; subaculear tubercle very weak or indistinct; smooth lateral and ventrosubmedian longitudinal troughs weak; scattered microsetae and short macrosetae on lateral and ventral surfaces; rugose surfaces arise from development of shallow indentations at setal insertion points; aculeus stout, shorter than vesicle.

Pedipalps (Figs. 77–118). *Males* (Figs. 77–88, 101–103, 107–110, 113–115). *Femur*: L/W 2.72–3.23; dorsointernal, dorsoexternal and ventrointernal carinae strong, with uniform coarse granulation; external carina strong, weakly granular, with fine granules proximally, larger granules distally; internal carina moderate with medium to coarse granules; dorsal surface with fine and coarse granulation, internal surface densely finely granulated or shagreened, external surfaces weakly granulated or shagreened, nearly smooth in parts, ventral surface with sparse mix of medium and fine granules; 7–12 accessory macrosetae on distal external surface; *patella*: L/W 2.84–3.46; dorsointernal carina strong, granular; dorsomedian carina strong, granular, complete; dorsoexternal carina moderate, weakly granular; external carina moderate, smooth; ventroexternal and ventromedian carinae weak or obsolete, indicated by rows of fine granules; ventrointernal carina weak, indicated by coarse granules; internal carina moderate, finely granulated; dorsal, external and internal surfaces with sparse fine granulation or sparsely shagreened; ventral surface with very sparse fine granulation, or smooth; *chela*: slender, L/W 4.90–5.48, carinae obsolete with only weak, smooth traces of digital, exterior secondary and exterior marginal carinae discernible at base of manus; surface smooth with sparse macrosetae and microsetae; 5–8 primary denticle subrows on movable finger, 5–7 on fixed finger (including cases of fusion of proximal rows), subrows except proximal typically flanked by internal and external accessory denticles; 4–8 internal or external accessory denticles on movable finger, 4–7 on fixed finger. *Females* (Figs. 89–100, 104–106, 111–112, 116–118). *Femur*: more robust than in males, L/W 2.29–2.47; dorsointernal and dorsoexternal carinae moderate, with uniform medium to coarse granules; external carina weak, smooth, distal half with sparse, coarse granules; ventrointernal carina moderate with uniform coarse granules; internal carina weak with irregular large granules; dorsal surface with moderate cover of mixed fine granules or microgranules, internal and ventral sur-

Figures 127–132: Metasoma and telson of *Butheolus harrisoni* sp. n. **Figs. 127–129.** Holotype male (♂). Dorsal (127), right lateral (128) and ventral (129) aspects. **Figs. 130–132.** Paratype female (♀), same locality data as male in Figs. 67–68. Dorsal (130), right lateral (131) and ventral (132) aspects. Scale bars: 2 mm.

faces almost smooth with sparse weak, fine granules or weakly shagreened, external surfaces smooth; 6–9 accessory macrosetae on distal external surface, including linear series of 4–6 on ventral side of external carina; *patella*: more robust than in males, L/W 2.33–2.64; dorsomedian carina complete; dorsointernal, dorsomedian and dorsoexternal carinae weak, smooth, other carinae obsolete; all intercarinal surfaces smooth; *chela*: more robust than in males, L/W 4.07–4.67, all carinae obsolete, surface smooth with sparse macrosetae and microsetae; finger dentition similar to males, 6–8 primary denticle subrows on movable finger, 6–7 on fixed finger, 5–8 internal or external accessory denticles on movable finger, 5–7 on fixed finger. *Trichobothriotaxy*: orthobothriotaxic, type Aβ (Vachon, 1974) (Figs. 101–118).

Legs (69–70, 73–74, 119–122). *Males*: Femur and patella I–IV with strongly serrate-denticulate inferior carinae, other carinae denticulate-granulate; prolateral surfaces of femur I–IV with dense, fine granulation, of patella I–IV weakly shagreened, nearly smooth; *females*: femur and patella I–IV with weakly serrate-crenulate

Measurements (mm)	*Butheolus harrisoni* sp. n.			
	♂ holotype	♂ paratype	♀ paratype #1	♀ paratype #2
Total L	30.50	30.00	32.54	31.42
Metasoma + Telson L	20.17	17.30	19.46	19.20
Carapace L	3.56	3.25	4.08	3.83
Carapace anterior W	1.83	1.67	2.20	2.04
Carapace posterior W	4.08	3.75	4.60	4.52
Carapace preocular L	1.52	1.37	1.78	1.78
Metasoma I L/W/D	2.41/ 2.71/ 2.25	2.06/ 2.45/ 2.04	2.38/ 2.92/ 2.46	2.35/ 2.90/ 2.38
Metasoma II L/W/D	2.92/ 2.75/ 2.38	2.45/ 2.41/ 2.04	2.79/ 2.92/ 2.50	2.83/ 2.83/ 2.43
Metasoma III L/W/D	3.02/ 2.83/ 2.34	2.65/ 2.46/ 2.08	3.00/ 3.00/ 2.51	2.92/ 2.86/ 2.46
Metasoma IV L/W/D	3.83/ 2.88/ 2.33	3.17/ 2.42/ 2.04	3.71/ 3.04/ 2.42	3.58/ 2.83/ 2.44
Metasoma V L/W/D	4.38/ 2.76/ 2.13	3.73/ 2.31/ 1.83	4.46/ 2.85/ 2.17	4.25/ 2.68/ 2.17
Telson L	3.67	3.33	3.92	3.92
Vesicle L/W/D	2.35/ 1.82/ 1.51	2.08/ 1.53/ 1.35	2.38/ 1.96/ 1.64	2.42/ 1.95/ 1.67
Pedipalp chela L	4.92	4.23	4.98	4.79
Chela movable finger L	3.13	2.58	3.08	2.93
Chela fixed finger L	2.46	2.04	2.33	2.25
Chela manus ventral L/W/D	2.00/ 0.94/ 1.02	1.67/ 0.83/ 0.86	2.04/ 1.14/ 1.22	2.06/ 1.14/ 1.22
Pedipalp femur L/W	2.83/ 0.92	2.38/ 0.86	2.58/ 1.10	2.50/ 1.06
Pedipalp patella L/W	3.53/ 1.10	2.98/ 1.00	3.35/ 1.35	3.35/ 1.35
Pectine length	3.42	3.33	3.08	3.23
Pectine teeth (left/ right)	17/17	20/19	15/17	16/16

Table 2: Measurements of representative adults of *Butheolus harrisoni* sp. n. Males (♂): holotype ♂: Oman, Jabal Qara, Salalah-Thumrait road, 17°17.26'N 54°5.36' E, 17.X.1993, leg. G. Lowe; paratype ♂: Oman, E. of Jabal Qamr, coastal wadi, 16°53.71'N 53°48.75'E, 28.IX.1995, leg. G. Lowe, M.D. Gallagher. Females (♀): paratype ♀ #1, same locality as holotype; paratype ♀ #2, Oman, Jabal Qara, north slopes, 17°17.83'N 54°5.11'E, 16.X.1993, leg. G. Lowe. Abbreviations: L, length; W, width, D depth.

inferior carinae, other carinae weakly granulate; prolateral surfaces of femur I–IV mostly smooth, sparsely shagreened or granulate on proximal parts, of patella I–IV nearly smooth; in both sexes, tibia III–IV with spurs; retrolateral tarsal spurs simple, prolateral tarsal spurs basally bifurcate; basitarsi I–III with 4–10 long retrosuperior macrosetae arranged in bristle-combs; ventral surface of telotarsi with dual rows of short, fine macrosetae (occasionally reduced to single row on telotarsus I); tarsal ungues stout.

Measurements. See Table 2.

Variation. Color patterns were variable. The carapace and tergites ranged from a lighter dusky brown to darker brown. Metasoma III color ranged from light brown to dark brown in Jabal Qara specimens, and from yellow to light brown in Jabal Qamr specimens. At a single collection site in Jabal Qara, examples of both light and dark brown metasoma III were observed. Meristic and morphometric variation are summarized in Tabs. 3–5, and Figs. 133–162.

DISTRIBUTION. Recorded from inland sites in Jabal Qara mountains and coastal sites around Jabal Qamr, in the Dhofar Province of Oman (Fig. 338).

ECOLOGY. The species occurs in mesic environments along the coast as a characteristic faunal element of lush woodland or grassland zones of south facing slopes of the Jabal Qara (Sale, 1980). Collections were made in wadi bottoms among small shrubs. However, it can tolerate more xeric conditions, as there are records from semi-arid scrub zones of northern Jabal Qara near the

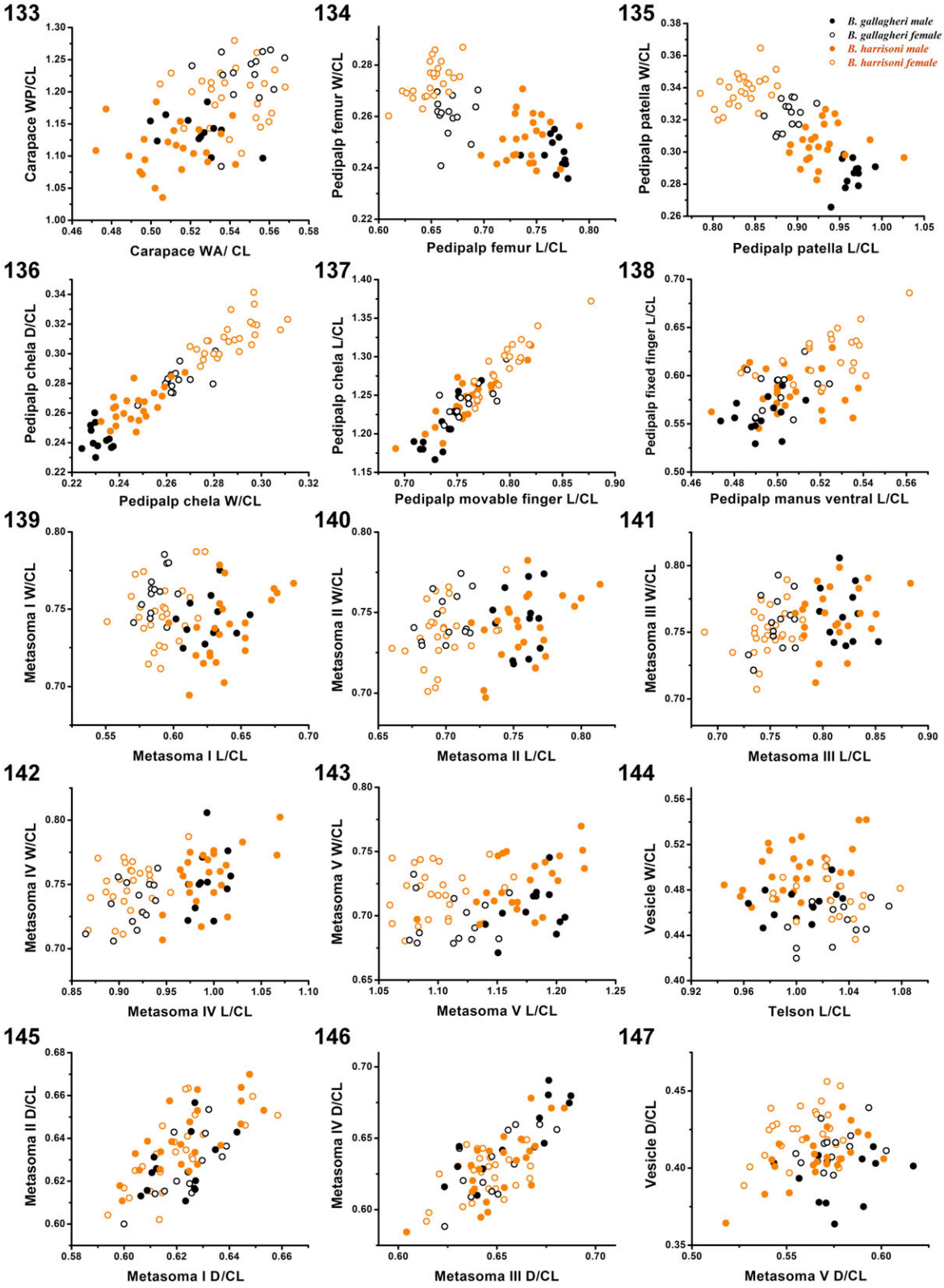

Figures 133–147: Scatter plots showing variation in morphometric ratios of *Butheolus gallagheri* Vachon, 1980 and *B. harrisoni* sp. n. Selected measurements normalized to carapace length (CL). Each symbol represents one specimen. *B. gallagheri*: black symbols; *B. harrisoni*: orange symbols. Males: filled circles, females: open circles. Abbreviations: L, length; W, width, WA anterior width, WP posterior width, D depth.

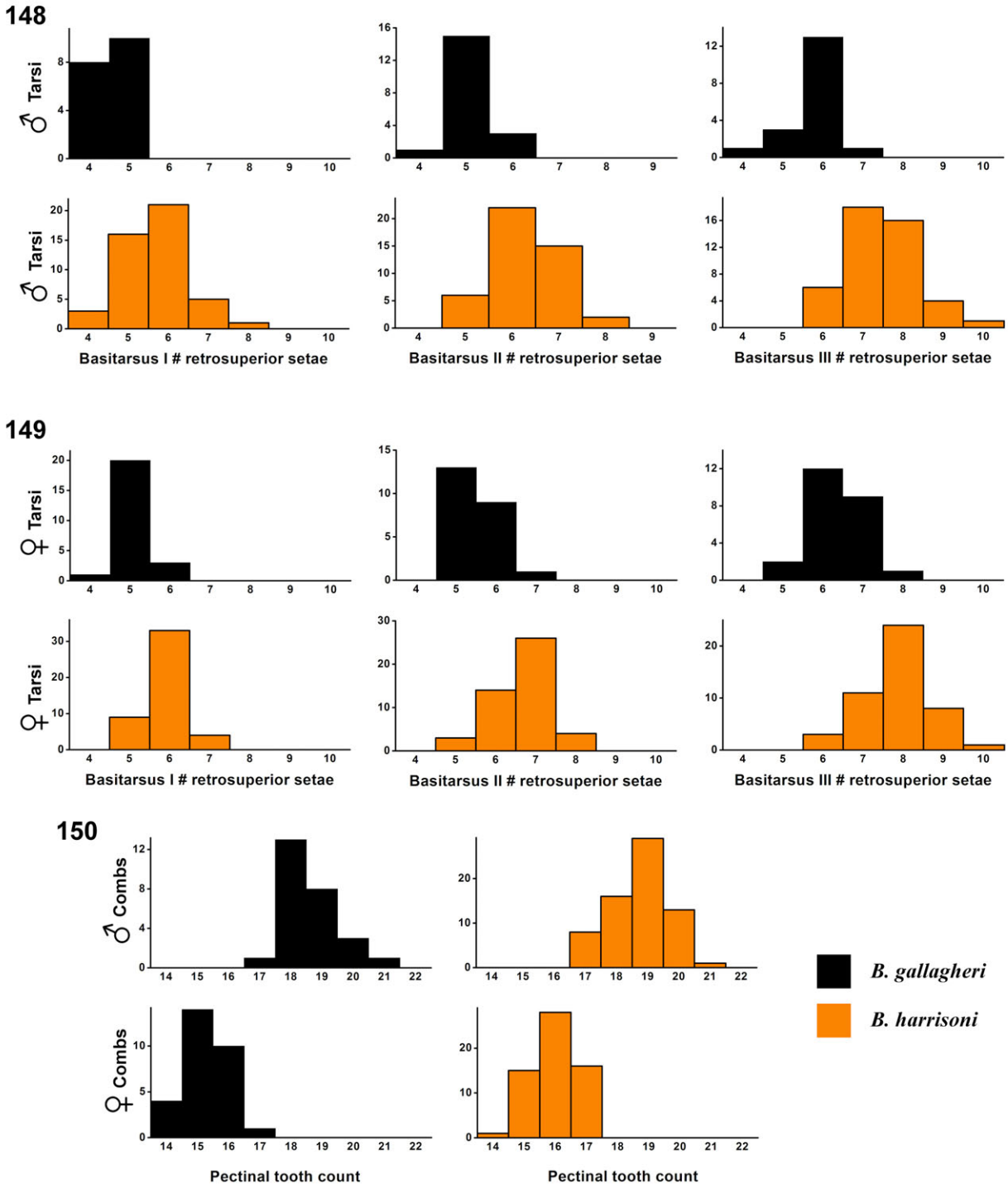

Figures 148–150: Histograms showing variation in meristic counts of basitarsal setation and pectine teeth for *Butheolus gallagheri* Vachon, 1980 and *B. harrisoni* sp. n. **Figs. 148–149.** Distributions of number of retrosuperior macrosetae ("bristle-comb" setae) on basitarsi I–III for males (148) and females (149). **Fig. 150.** Distributions of number of pectine teeth in male (♂) and female (♀) combs. In all plots: *B. gallagheri*, black bars; *B. harrisoni*, orange bars. Ordinates are numbers of tarsi or combs, pooling data from left and right appendages of all specimens examined.

edge of the Nejd Desert, and from the plateau of Jabal Qamr. Recorded elevation range was 15–1,076 m a.s.l. The substrate preference was rocky or gravelly wadis, and some were found by day in shallow scrapes under rocks. Scorpions that occurred together with *B. harrisoni* **sp. n.** were: *Compsobuthus acutecarinatus* (Simon, 1882), *Hottentotta salei* (Vachon, 1980), *Leiurus haenggii* Lowe et al., 2014, *Nebo whitei* Vachon, 1980,

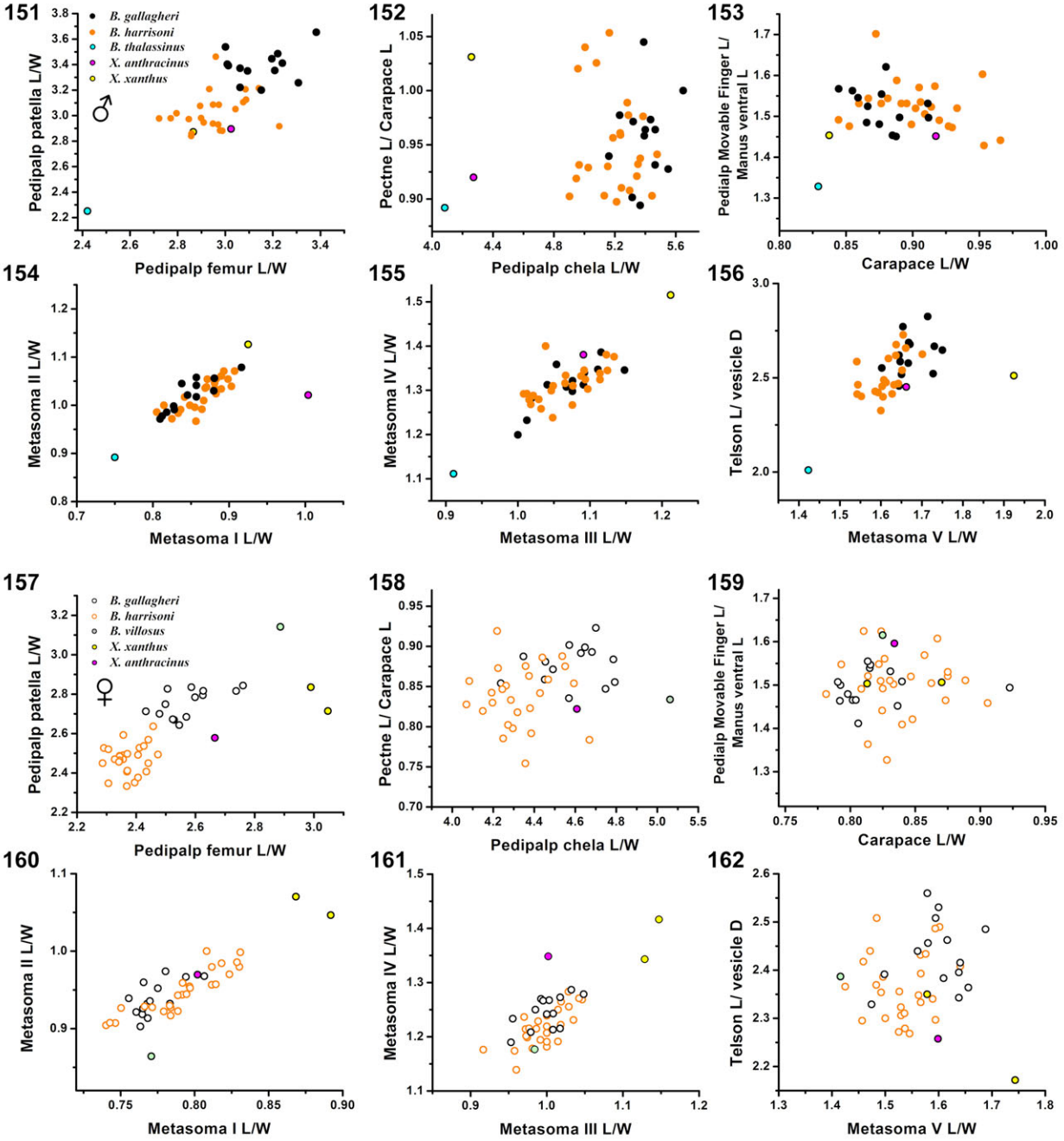

Figures 151–162: Scatter plots showing variation in morphometric ratios of species of *Butheolus* and *Xenobuthus* gen. n. **Figs. 151–156.** Selected ratios of males (♂). *B. gallagheri*: black filled symbols; *B. harrisoni*: orange filled symbols; *B. thalassinus*: cyan circles; *X. anthracinus*: magenta circles; *X. xanthus*: yellow circles. **Figs. 157–162.** Selected ratios of females (♀). *B. gallagheri*: black open symbols; *B. harrisoni*: orange open symbols; *B. villosus*: light green circles; *X. anthracinus*: magenta circles; *X. xanthus*: yellow circles. Abbreviations: L, length; W, width (carapace W = posterior width), D depth.

Microbuthus kristensenorum Lowe, 2010, and *Xenobuthus xanthus* **sp.n.**. The two similar species, *B. harrisoni* and *B. gallagheri*, have so far not been recorded together at the same site (UV detection sampling at 14 separate sites for *B. harrisoni*, 3 for *B. gallagheri*). The lack of overlap may reflect spatial partitioning according to local environmental factors and competitive exclusion in preferred habitats of each species.

Butheolus thalassinus Simon, 1882

(Figs. 151–156, 163–178, 338, Tab. 6)

Butheolus thalassinus Simon, 1882: 248–249, pl. VIII, fig. 20;

Butheolus thalassinus: Simon, 1889: Simon, 1890: 122; Kraepelin, 1891: 75; Kraepelin, 1895: 5; Pocock, 1895: 295, 316; Laurie, 1896: 122; Kraepelin, 1899: 37; Kraepelin, 1903: 565; Birula, 1910: 171;

Meristic count		*Butheolus gallagheri* Vachon, 1980		*Butheolus harrisoni* sp. n.		*Xenobuthus* gen. n. *xanthus* sp. n.	
		♂	♀	♂	♀	♂	♀
Pectine teeth		17–21 (26) 18.62 ± 0.90	14–17 (29) 15.28 ± 0.75	17–21 (67) 18.75 ± 0.96	14–17 (60) 15.98 ± 0.77	18–21 (8) 19.63 ± 1.06	18–20 (10) 19.50 ± 0.85
Pedipalp chela movable finger	denticle subrows	5–7 (24) 6.04 ± 0.36	6–7 (28) 6.29 ± 0.46	5–8 (50) 6.86 ± 0.45	6–8 (53) 6.85 ± 0.53	9 (4) 9.00 ± 0.00	8–10 (10) 9.20 ± 0.63
	external accessory denticles	5–7 (24) 5.83 ± 0.48	5–6 (24) 5.71 ± 0.46	4–7 (48) 6.40 ± 0.71	5–8 (49) 6.51 ± 0.62	7–9 (4) 8.00 ± 0.82	8–9 (10) 8.70 ± 0.48
	internal accessory denticles	5–6 (20) 5.70 ± 0.47	6–7 (24) 6.13 ± 0.34	5–8 (48) 7.00 ± 0.46	6–8 (49) 7.02 ± 0.38	6–9 (4) 7.75 ± 1.26	8–9 (10) 8.80 ± 0.42
	primary denticles	31–39 (22) 34.41 ± 2.09	33–39 (26) 35.92 ± 1.72	29–42 (50) 35.68 ± 2.87	29–42 (52) 35.83 ± 2.90	43–51 (4) 47.25 ± 3.86	45–55 (10) 50.30 ± 3.43
Pedipalp chela fixed finger	denticle subrows	5–7 (20) 6.20 ± 0.52	5–7 (27) 6.11 ± 0.51	5–7 (50) 6.44 ± 0.54	6–7 (54) 6.37 ± 0.49	5–8 (4) 7.25 ± 1.50	8–9 (10) 8.60 ± 0.52
	external accessory denticles	4–5 (20) 4.60 ± 0.50	4–5 (23) 4.61 ± 0.50	4–7 (48) 5.69 ± 0.59	5–7 (50) 5.72 ± 0.61	3–8 (4) 6.25 ± 2.22	7–9 (10) 7.90 ± 0.57
	internal accessory denticles	5–6 (20) 5.10 ± 0.31	4–6 (23) 5.04 ± 0.37	5–7 (48) 6.08 ± 0.45	5–7 (50) 6.12 ± 0.44	4–8 (4) 6.50 ± 1.73	8 (10) 8.00 ± 0.00
	primary denticles	29–39 (22) 32.64 ± 2.32	28–36 (25) 32.68 ± 2.30	28–36 (50) 33.06 ± 2.03	28–39 (54) 32.57 ± 2.50	31–52 (4) 41.50 ± 8.66	42–53 (10) 47.60 ± 3.92
Basitarsus I setae		4–5 (18) 4.56 ± 0.51	4–6 (24) 5.08 ± 0.41	4–8 (46) 5.67 ± 0.84	5–7 (46) 5.89 ± 0.53	7 (2) 7.00 ± 0.00	7–8 (4) 7.50 ± 0.58
Basitarsus II setae		4–6 (19) 5.11 ± 0.46	5–7 (23) 5.48 ± 0.59	5–8 (45) 6.29 ± 0.76	5–8 (47) 6.66 ± 0.73	9–10 (2) 9.50 ± 0.71	9–12 (4) 10.25 ± 1.26
Basitarsus III setae		4–7 (18) 5.78 ± 0.65	5–8 (24) 6.38 ± 0.71	6–10 (45) 7.47 ± 0.92	6–10 (47) 7.85 ± 0.86	12 (2) 12.00 ± 0.00	10–14 (4) 12.00 ± 1.83

Table 3: Summary statistics showing variation of meristic counts from *Butheolus gallagheri* Vachon, 1980, *B. harrisoni* sp. n. and *Xenobuthus* gen. n. *xanthus* sp. n. Numbers in each table cell are: range = minimum – maximum (N = sample size), mean ± SD. Pedipalp finger denticle subrows and accessory denticle counts exclude the most distal denticle group that includes the enlarged terminal tooth and sub-terminal denticles. A subrow is defined as having 2 or more small primary denticles. Primary denticle counts include small denticles in subrows, but exclude the enlarged denticle at the proximal end of each subrow (when present). Basitarsus setal counts represent the retrosuperior series of long macrosetae ("bristle-combs") on legs I–III. Sample size N represents total number of appendages (including left and right appendages, so N is approximately twice the number of individuals).

Borelli, 1915: 461–462; Birula, 1917a: 215, 230; Birula, 1937: 101; Kästner, 1941: 231; Vachon, 1966: 210; Stahnke, 1972: 129; Sissom, 1994: 7–8, figs. 9–13; Kovařík, 1998b: 105; Fet & Lowe, 2000: 89; Kovařík, 2004: 4, 25; Fet, Soleglad & Lowe, 2005: 2; Lourenço, 2005: 27, fig. 33; Hendrixson, 2006: 56, 61; Acosta et al., 2008: 493; El-Hennawy, 2009: 121; El-Hennawy, 2014: 45; Kovařík & Lowe, 2012: 1–2, 4, 18–23, figs. 7–8, 75, 78, 81, 84, 87, 90, 99, 104; Lowe et al., 2014: 117.

Butheolus (*Butheolus*) *thalassinus*: Vachon, 1980: 255; El-Hennawy, 1992: 101, 114.

TYPE MATERIAL. Syntypes, **Yemen**, Aden, MCSN (not examined).

MATERIAL EXAMINED. **Yemen:** 2 ♀, Shaik Ottiman, 9.II.1895 (BMNH); 1 ♂ Ta'izz, 3800 ft a.s.l., 10.I.1951, leg. H. Hoogstraal, under rock on Euphorbia Aloe Hill (WDS).

DIAGNOSIS**.** A member of the genus *Butheolus* differentiated as follows: base color deep chocolate brown, with all metasomal segments and telson dark; pedipalps and legs yellow or brownish-yellow; carapace and ter-

Morphometric ratio	*Butheolus gallagheri* Vachon, 1980		*Butheolus harrisoni* sp. n.	
	13 ♂	14 ♀	24 ♂	26 ♀
Carapace L/W	0.84–0.91 0.88 ± 0.02	0.79–0.92 0.82 ± 0.03	0.84–0.97 0.90 ± 0.03	0.78–0.91 0.84 ± 0.03
Carapace posterior W/ anterior W	1.97–2.31 2.18 ± 0.09	2.02–2.38 2.23 ± 0.09	2.00–2.46 2.17 ± 0.11	2.02–2.41 2.21 ± 0.11
Pectine L/Carapace L	0.89–1.04 0.96 ± 0.04	0.84–0.92 0.88 ± 0.02	0.90–1.05 0.95 ± 0.05	0.75–0.92 0.84 ± 0.04
Pedipalp chela L/W	5.16–5.65 5.40 ± 0.13	4.24–4.79 4.58 ± 0.17	4.90–5.48 5.20 ± 0.17	4.07–4.67 4.33 ± 0.15
Pedipalp chela manus L/W	2.05–2.26 2.17 ± 0.06	1.72–1.96 1.87 ± 0.07	1.95–2.29 2.10 ± 0.08	1.56–1.85 1.76 ± 0.07
Pedipalp chela manus W/D	0.88–1.00 0.96 ± 0.04	0.90–1.00 0.94 ± 0.02	0.87–1.00 0.94 ± 0.03	0.87–0.97 0.92 ± 0.03
Chela movable finger L/ manus ventral L	1.45–1.62 1.52 ± 0.05	1.41–1.55 1.49 ± 0.04	1.43–1.70 1.53 ± 0.06	1.33–1.62 1.50 ± 0.07
Chela fixed finger L/ manus ventral L	1.09–1.25 1.17 ± 0.05	1.06–1.19 1.14 ± 0.04	1.11–1.34 1.19 ± 0.05	1.04–1.26 1.16 ± 0.06
Pedipalp femur L/W	3.00–3.38 3.15 ± 0.12	2.43–2.76 2.57 ± 0.09	2.72–3.23 2.95 ± 0.12	2.29–2.47 2.37 ± 0.05
Pedipalp patella L/W	3.20–3.65 3.39 ± 0.13	2.64–2.84 2.75 ± 0.07	2.84–3.46 3.04 ± 0.15	2.33–2.64 2.47 ± 0.07
Metasoma I L/W	0.81–0.92 0.85 ± 0.03	0.76–0.81 0.77 ± 0.01	0.81–0.91 0.87 ± 0.03	0.74–0.83 0.79 ± 0.03
Metasoma II L/W	0.97–1.08 1.02 ± 0.03	0.90–0.97 0.94 ± 0.02	0.97–1.07 1.02 ± 0.03	0.90–1.00 0.95 ± 0.03
Metasoma III L/W	1.00–1.15 1.07 ± 0.04	0.95–1.05 1.00 ± 0.03	1.01–1.13 1.07 ± 0.04	0.92–1.05 1.00 ± 0.03
Metasoma IV L/W	1.20–1.39 1.31 ± 0.05	1.19–1.29 1.25 ± 0.03	1.24–1.40 1.31 ± 0.04	1.14–1.28 1.22 ± 0.04
Metasoma V L/W	1.60–1.75 1.67 ± 0.04	1.47–1.69 1.60 ± 0.06	1.54–1.70 1.61 ± 0.04	1.42–1.64 1.53 ± 0.05
Metasoma I L/D	0.95–1.07 1.00 ± 0.04	0.92–0.96 0.94 ± 0.01	0.96–1.12 1.02 ± 0.03	0.90–1.00 0.95 ± 0.03
Metasoma II L/D	1.14–1.41 1.22 ± 0.07	1.07–1.17 1.12 ± 0.03	1.12–1.26 1.18 ± 0.04	1.04–1.17 1.10 ± 0.03
Metasoma III L/D	1.16–1.30 1.24 ± 0.05	1.09–1.23 1.16 ± 0.04	1.14–1.36 1.24 ± 0.05	1.11–1.24 1.16 ± 0.03
Metasoma IV L/D	1.44–1.60 1.52 ± 0.06	1.37–1.54 1.45 ± 0.05	1.43–1.69 1.57 ± 0.06	1.37–1.54 1.46 ± 0.05
Metasoma V L/D	1.96–2.12 2.04 ± 0.05	1.82–2.08 1.94 ± 0.06	1.92–2.28 2.07 ± 0.07	1.85–2.10 1.97 ± 0.07
Telson L/D	2.46–2.83 2.62 ± 0.10	2.33–2.56 2.43 ± 0.07	2.33–2.73 (21) 2.51 ± 0.11	2.27–2.51 2.37 ± 0.07

Table 4: Summary statistics showing variation of selected morphometric ratios from *Butheolus gallagheri* Vachon, 1980 and *B. harrisoni* sp. n. Numbers in each table cell are: range = minimum – maximum (N = sample size, where different from column header), mean ± SD. Abbreviations: L, length; W, width, D depth.

gites coarsely granulated; pedipalp patella with dorsomedian carina complete; pedipalp chela with strong dorsal secondary and external secondary carinae, moderate to strong dorsal marginal, digital, external, ventroexternal and ventrointernal carinae; ventral surface between ventromedian carinae of metasoma I with dense coarse and fine granulation; ventral and lateral intercarinal surfaces of metasoma II–V with moderately

Variable normalized to Carapace L	*Butheolus gallagheri* Vachon, 1980		*Butheolus harrisoni* sp. n.	
	12 ♂	14 ♀	23 ♂	26 ♀
Carapace anterior W	0.50–0.56, 0.52 ± 0.02	0.52–0.57, 0.55 ± 0.01	0.47–0.54, 0.51 ± 0.02	0.51–0.57, 0.54 ± 0.02
Carapace posterior W	1.10–1.18, 1.14 ± 0.03	1.08–1.27, 1.22 ± 0.05	1.04–1.18, 1.11 ± 0.04	1.10–1.28, 1.19 ± 0.04
Metasoma I L	0.60–0.66, 0.63 ± 0.02	0.57–0.60, 0.59 ± 0.01	0.60–0.69, 0.64 ± 0.02	0.55–0.62, 0.59 ± 0.02
Metasoma I W	0.73–0.78, 0.74 ± 0.01	0.74–0.79, 0.76 ± 0.02	0.70–0.78, 0.74 ± 0.02	0.71–0.79, 0.75 ± 0.02
Metasoma I D	0.61–0.64, 0.62 ± 0.01	0.60–0.64, 0.63 ± 0.01	0.600.65, 0.62 ± 0.02	0.59–0.66, 0.62 ± 0.02
Metasoma II L	0.74–0.77, 0.76 ± 0.01	0.68–0.72, 0.70 ± 0.01	0.72–0.81, 0.76 ± 0.02	0.66–0.75, 0.70 ± 0.02
Metasoma II W	0.72–0.77, 0.75 ± 0.02	0.73–0.77, 0.75 ± 0.02	0.70–0.78, 0.74 ± 0.02	0.70–0.78, 0.74 ± 0.02
Metasoma II D	0.61–0.66, 0.63 ± 0.01	0.60–0.65, 0.63 ± 0.01	0.61–0.67, 0.64 ± 0.02	0.60–0.66, 0.64 ± 0.02
Metasoma III L	0.80–0.85, 0.82 ± 0.02	0.73–0.77, 0.76 ± 0.01	0.77–0.88, 0.81 ± 0.03	0.69–0.78, 0.75 ± 0.02
Metasoma III W	0.74–0.81, 0.76 ± 0.02	0.72–0.80, 0.76 ± 0.02	0.71–0.80, 0.76 ± 0.02	0.71–0.79, 0.75 ± 0.02
Metasoma III D	0.62–0.69, 0.66 ± 0.02	0.62–0.68, 0.65 ± 0.02	0.60–0.68, 0.65 ± 0.02	0.61–0.67, 0.64 ± 0.01
Metasoma IV L	0.97–1.02, 1.00 ± 0.02	0.87–0.94, 0.92 ± 0.02	0.95–1.07, 1.00 ± 0.03	0.87–0.97, 0.91 ± 0.02
Metasoma IV W	0.72–0.81, 0.75 ± 0.02	0.71–0.76, 0.74 ± 0.02	0.71–0.80, 0.76 ± 0.02	0.71–0.79, 0.75 ± 0.02
Metasoma IV D	0.61–0.69, 0.65 ± 0.03	0.59–0.66, 0.63 ± 0.02	0.58–0.68, 0.63 ± 0.03	0.59–0.65, 0.63 ± 0.02
Metasoma V L	1.14–1.21, 1.18 ± 0.02	1.08–1.16, 1.11 ± 0.03	1.08–1.22, 1.17 ± 0.03	1.06–1.16, 1.10 ± 0.03
Metasoma V W	0.67–0.75, 0.71 ± 0.02	0.68–0.73, 0.70 ± 0.02	0.69–0.77, 0.73 ± 0.02	0.68–0.75, 0.72 ± 0.02
Metasoma V D	0.54–0.62, 0.58 ± 0.02	0.54–0.62, 0.58 ± 0.02	0.52–0.60, 0.57 ± 0.02	0.53–0.58, 0.56 ± 0.02
Telson L	0.99–1.07, 1.03 ± 0.03	0.96–1.04, 1.01 ± 0.02	0.98–1.08, 1.03 ± 0.03*	0.95–1.05, 1.00 ± 0.03
Telson vesicle D	0.36–0.41, 0.39 ± 0.02	0.40–0.44, 0.41 ± 0.01	0.36–0.44, 0.41 ± 0.02	0.39–0.46, 0.42 ± 0.02
Telson vesicle W	0.42–0.47, 0.45 ± 0.02	0.45–0.50, 0.47 ± 0.02	0.44–0.51, 0.47 ± 0.02	0.47–0.54, 0.50 ± 0.02
Pedipalp chela L	1.21–1.30, 1.24 ± 0.02	1.17–1.27, 1.21 ± 0.03	1.23–1.37, 1.29 ± 0.03	1.18–1.32, 1.24 ± 0.03
Pedipalp manus ventral L	0.49–0.52, 0.50 ± 0.01	0.47–0.51, 0.43 ± 0.01	0.48–0.56, 0.52 ± 0.02	0.47–0.54, 0.51 ± 0.02
Chela movable finger L	0.73–0.80, 0.76 ± 0.02	0.71–0.77, 0.74 ± 0.02	0.77–0.88, 0.80 ± 0.03	0.69–0.82, 0.76 ± 0.03
Pedipalp chela W	0.22–0.24, 0.23 ± 0.004	0.25–0.28, 0.26 ± 0.01	0.23–0.27, 0.25 ± 0.01	0.27–0.31, 0.29 ± 0.01
Pedipalp chela D	0.23–0.26, 0.24 ± 0.01	0.27–0.30, 0.28 ± 0.01	0.25–0.29, 0.27 ± 0.01	0.29–0.34, 0.31 ± 0.01
Chela fixed finger L	0.55–0.63, 0.58 ± 0.02	0.53–0.60, 0.56 ± 0.02	0.58–0.69, 0.62 ± 0.03	0.55–0.63, 0.59 ± 0.02
Pedipalp femur L	0.74–0.78, 0.77 ± 0.01	0.66–0.69, 0.67 ± 0.01	0.70–0.79, 0.74 ± 0.02	0.61–0.68, 0.65 ± 0.02
Pedipalp femur W	0.24–0.26, 0.25 ± 0.01	0.24–0.27, 0.26 ± 0.01	0.24–0.27, 0.25 ± 0.01	0.26–0.29, 0.27 ± 0.01
Pedipalp patella L	0.94–0.99, 0.97 ± 0.01	0.86–0.92, 0.89 ± 0.02	0.89–1.03, 0.93 ± 0.03	0.79–0.88, 0.84 ± 0.02
Pedipalp patella W	0.27–0.30, 0.29 ± 0.01	0.31–0.33, 0.32 ± 0.01	0.28–0.33, 0.31 ± 0.01	0.32–0.37, 0.34 ± 0.01

Table 5: Summary statistics showing variation of measurements normalized to carapace length for *Butheolus gallagheri* Vachon, 1980 and *B. harrisoni* sp. n. Numbers in each table cell are: range = minimum – maximum, mean ± SD. Samples sizes of cells listed in column headers, unless otherwise indicated (* N=20 for *B. harrisoni* ♂ telson L). Abbreviations: L, length; W, width, D depth.

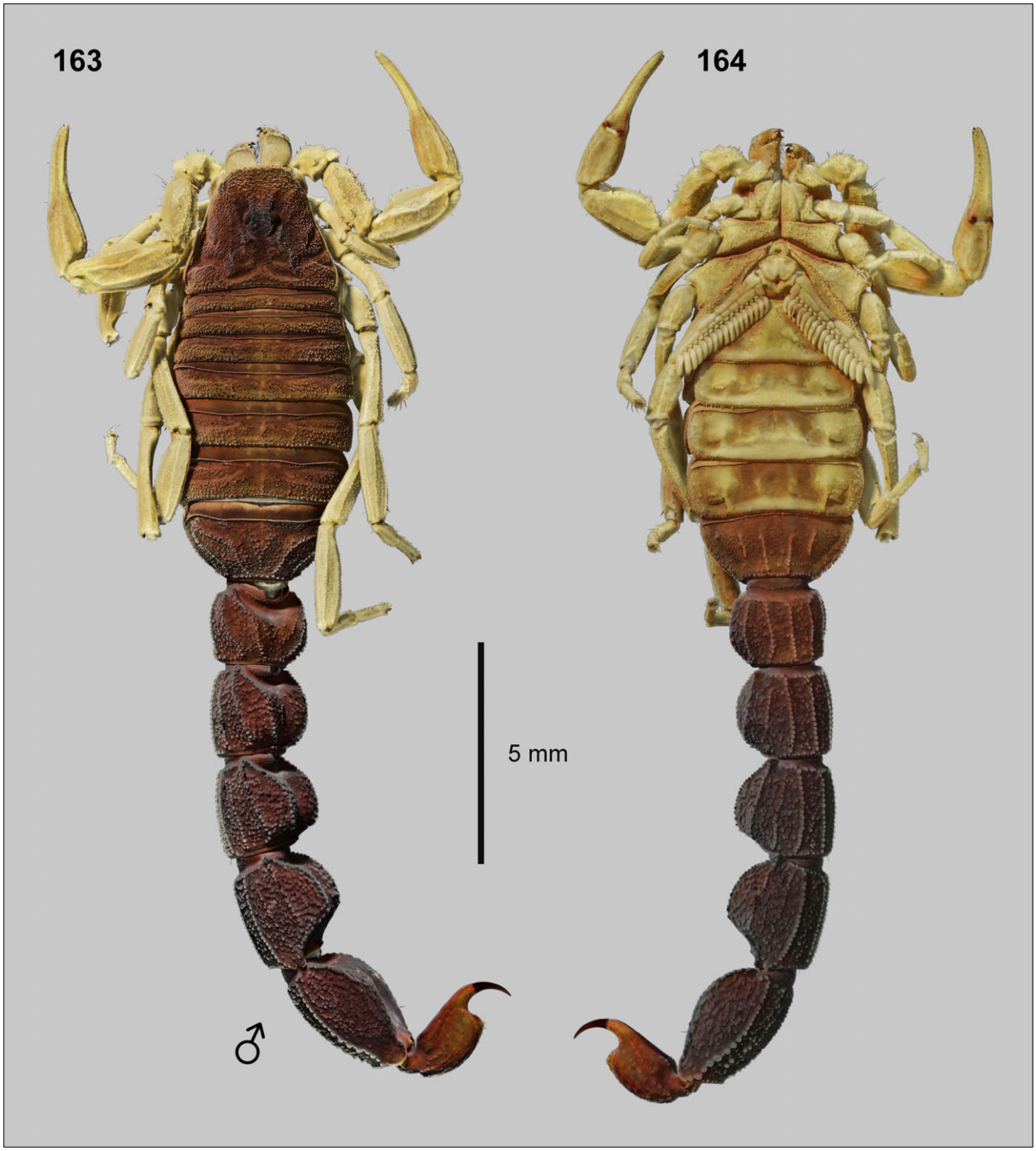

Figures 163–164: Habitus of male *Butheolus thalassinus* Simon, 1882. **Fig. 163.** Dorsal aspect. **Fig. 164.** Ventral aspect. Yemen, Ta'izz, 1158 m a.s.l., under rock on Euphorbia-Aloe hill, 10. I. 1951, H. Hoogstraal (cf. Sissom, 1994: 7–8, figs. 8–13). Scale bar: 5 mm.

coarse granulation; metasoma and telson with sparse, short macrosetae; telson with large, broad subaculear tubercle, acute angle between posterior vesicle surface and aculeus base; pedipalp and metasoma stout; pedipalp femur L/W ♂ 2.42; pedipalp patella L/W ♂ 2.25; pedipalp chela L/W ♂ 4.08; metasoma I L/W ♂ 0.75; metasoma IV L/D ♂ 1.24, metasoma V L/D ♂ 1.68, telson L/D ♂ 2.01; pectine teeth ♂ 17–18, ♀ 14–16.

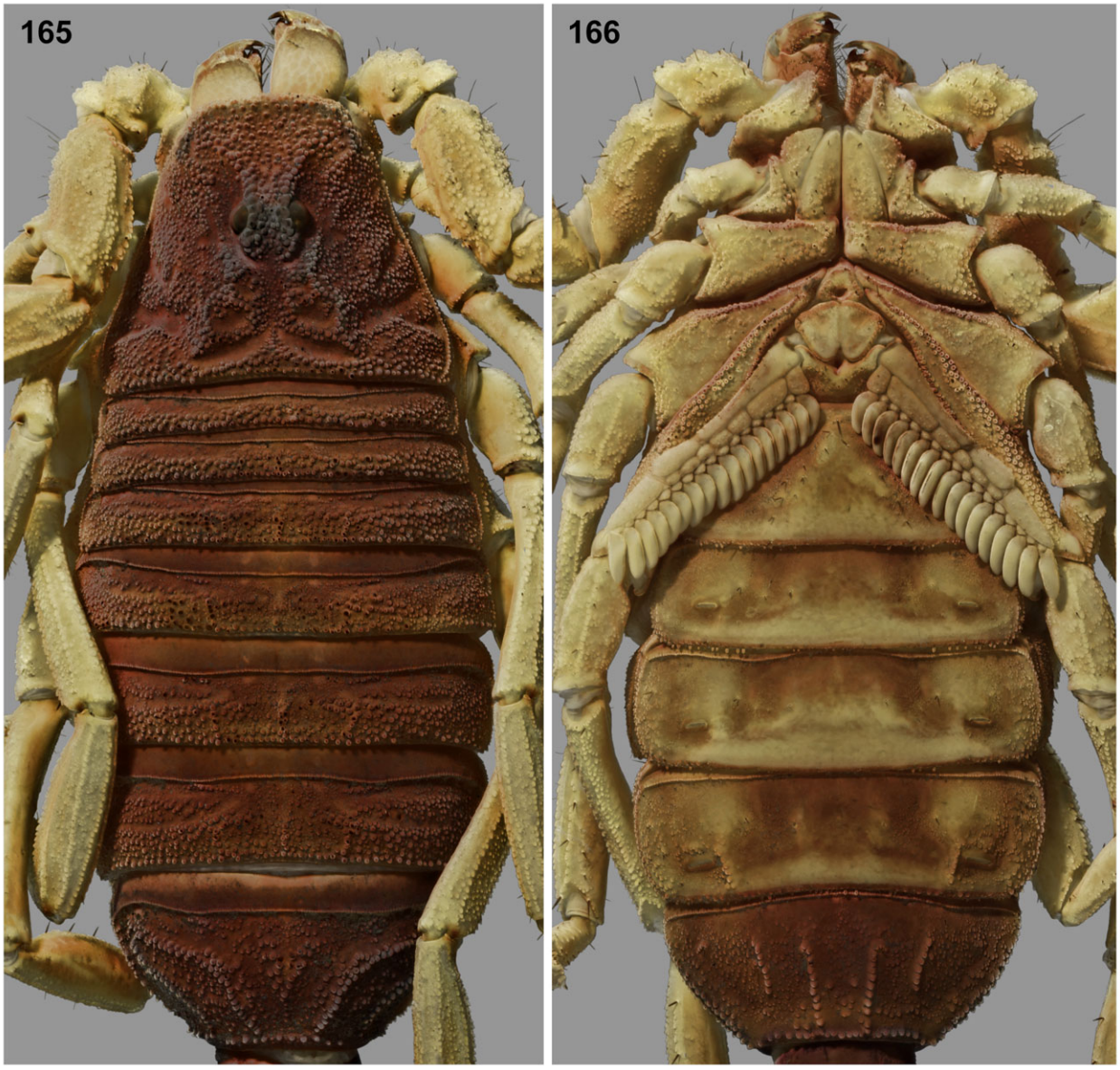

Figures 165–166: Prosoma and mesosoma of male *Butheolus thalassinus* Simon, 1882. **Fig. 165.** Dorsal aspect, carapace and tergites. **Fig. 166.** Ventral aspect, coxosternal area and sternites. Same male as in Figs. 163–164. Scale bar: 1 mm.

***Butheolus villosus* Hendrixson, 2006**

(Figs. 157–162, 179–193, 338, Tab. 6)

Butheolus villosus Hendrixson, 2006: 51–53, 59–61, figs. 6, 9, pl. 7, Tab.1.

Butheolus villosus: El-Hennawy, 2009: 121; Kovařík & Lowe, 2012: 2, 23; El-Hennawy, 2014: 45.

TYPE MATERIAL. Holotype ♀, **Saudi Arabia:** Khashm Dhibi, 28.II.1980, leg. A. Barkham (NHMB 0618) (examined).

DIAGNOSIS**.** A member of the genus *Butheolus* differentiated as follows: base color of prosoma and mesosoma light brown with carapace and tergite VII a darker brown, all metasomal segments dark brown; pedipalps and legs brownish yellow, except for pale, straw colored tarsi; carapace and tergites with mixture of fine and coarse granulation; pedipalp patella with dorsomedian carina complete; pedipalp chela with carinae weak or obsolete; surface between ventromedian carinae of metasoma I with sparse, coarse granulation in females; ventral and lateral intercarinal surfaces of metasoma II–V with moderately coarse granulation;

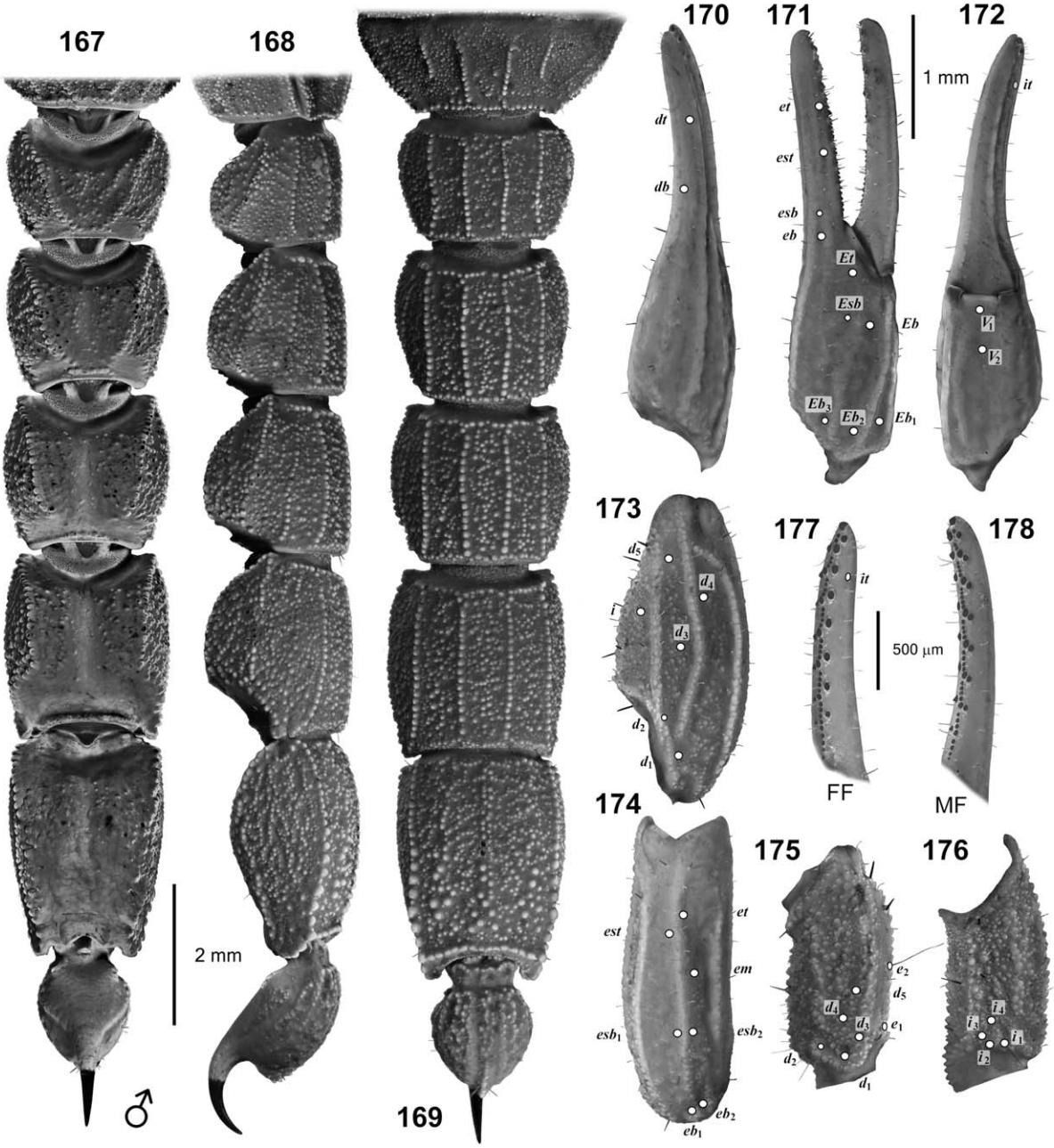

Figures 167–178: Metasoma, telson, pedipalp and trichobothrial map of *Butheolus thalassinus* Simon, 1882. Male, same as in Figs. 163–164. UV fluorescence. **Figs. 167–169.** Metasoma and telson. Dorsal (167), right lateral (168) and ventral (169) aspects. Scale bar: 2 mm. **Figs. 170–176.** Pedipalp and trichobothria. Dorsal (170), external (171) and ventral (172) aspect of chela; dorsal (173) and external (174) aspect of patella; dorsal (175) and internal (176) aspect of femur. Scale bar: 1 mm. **Figs. 177–178.** Dentition of fixed finger (FF) (177) and movable finger (MF) (178). Scale bar: 500 µm.

metasoma and telson with dense cover of medium to long macrosetae; telson without subaculear tubercle, obtuse angle between posterior vesicle surface and aculeus base; pedipalp and metasoma relatively slender; pedipalp femur L/W ♀ 2.89; pedipalp patella L/W ♀ 3.14; pedipalp chela L/W ♀ 5.06; metasoma I L/W ♀ 0.77; metasoma IV L/D ♀ 1.43, metasoma V L/D ♀ 1.82, telson L/D ♀ 2.39; pectine teeth ♀ 18; basitarsus III retrosuperior setae 11–12. Known only from the holotype female. Male unknown.

REMARKS. The numerous long setae in the basitarsal bristle-combs and the long, slender tarsal ungues (Figs. 190–193) are typical psammophilous adaptations (Navi-

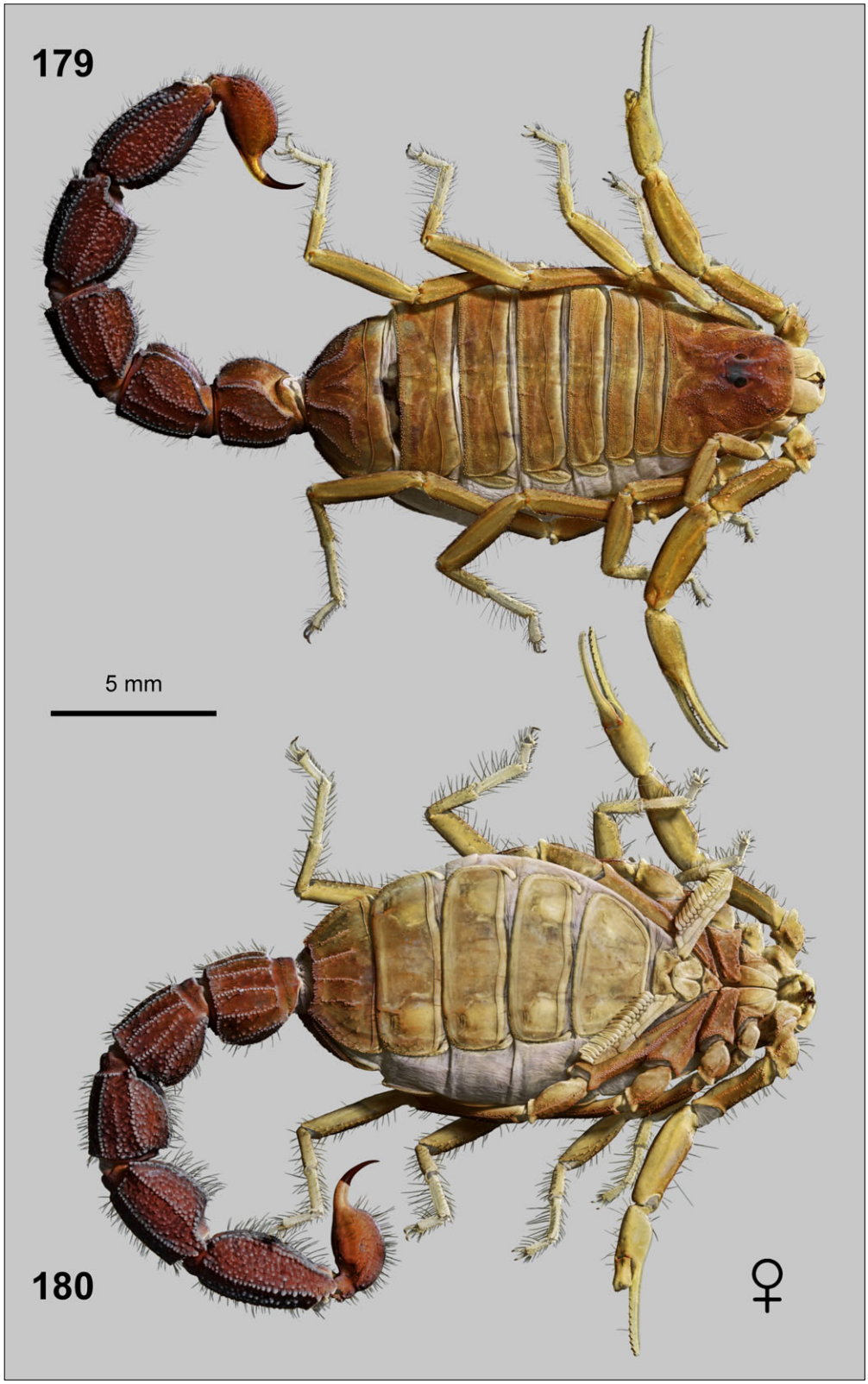

Figures 179–180: Habitus of *Butheolus villosus* Hendrixson, 2006. Holotype female (♀). **Fig. 179.** Dorsal aspect. **Fig. 180.** Ventral aspect. Khashm Dhibi, Saudi Arabia, 28.II.1980, leg. A. Barkham, NHMB 0618 (cf. Hendrixson, 2006: 59–61, pl. 7, fig. 9). Scale bar: 5 mm.

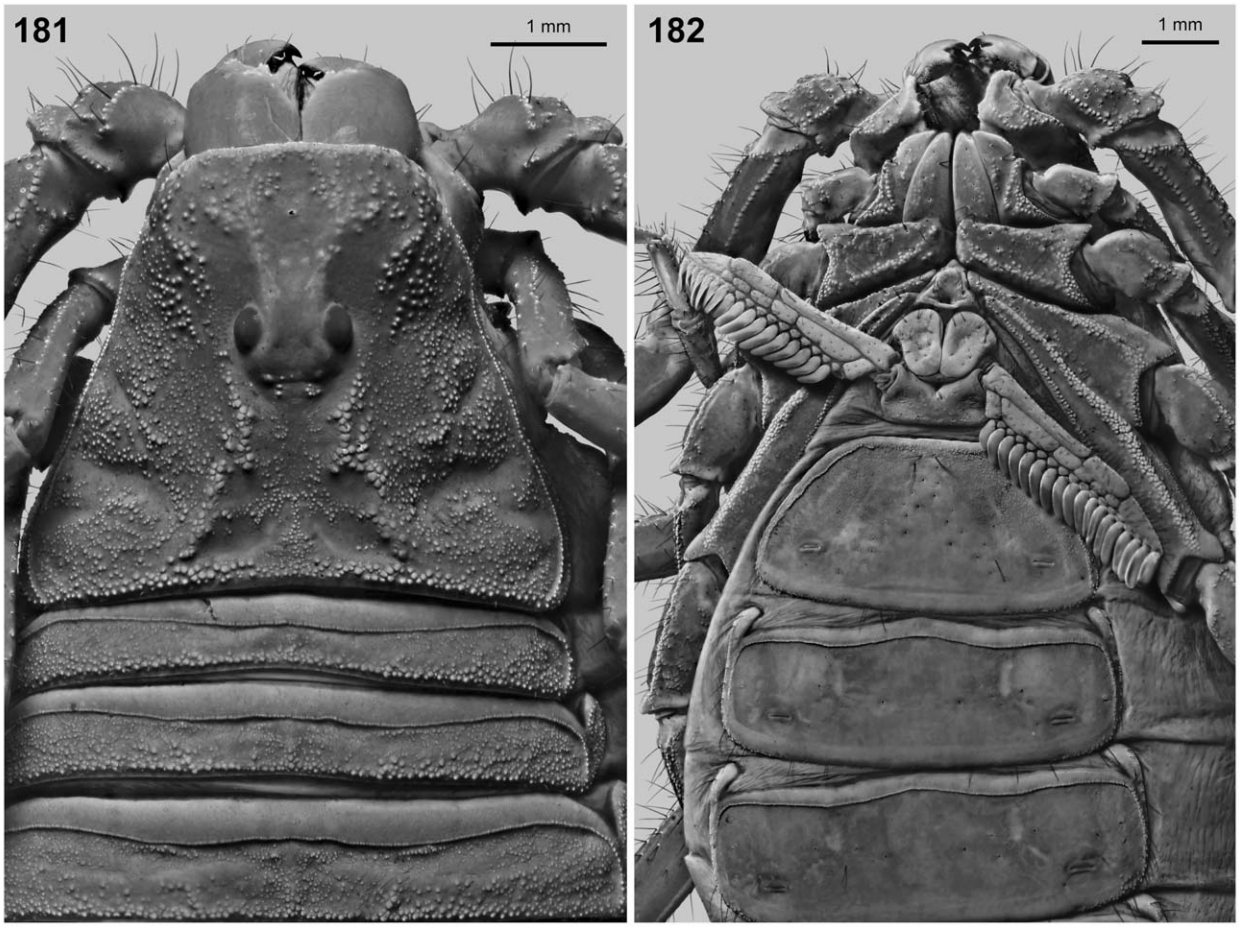

Figures 181–182: Prosoma and anterior mesosoma of female *Butheolus villosus* Hendrixson, 2006. Holotype female. **Fig. 181.** Dorsal aspect, carapace and tergites I–III. **Fig. 182.** Ventral aspect, coxosternal area and sternites III–V. UV fluorescence. Scale bars: 1 mm.

dpour & Lowe, 2009). On the pedipalp fixed finger, trichobothrium *dt* is located slightly distal to *et*, contrary to fig. 9e of Hendrixson (2006: 61) which shows *dt* midway between *est* and *et*.

Genus ***Xenobuthus*, gen. nov.**

http://zoobank.org/urn:lsid:zoobank.org:act:CC2E0A92-2CDF-4D3B-A4A0-66974E8A567D

DIAGNOSIS**.** Small to medium-sized buthids (Kovařík, 2009; Sissom, 1990), adults 35–50 mm in length; carapace strongly trapezoidal, ratio of posterior W/ anterior W 2.1–2.4, preocular area inclined downwards towards anterior margin, surface granular, without distinct carinae; tergites granular, tergites I–III lacking carinae or with weak median carina, IV–VI weakly tricarinate with median and paired lateral carinae; tergite VII with broad median carina, two pairs of lateral carinae; posterior margins of sternites III–VI armed with fringe of non-contiguous digitate denticles that are larger in males; metasoma segments nearly uniform in width and depth, robust with smooth or granulated carinae, sparsely or moderately granular on lateral and ventral intercarinal surfaces; metasoma I–III with 10 carinae, IV with 6 or 8 carinae, V with 3 or 5 carinae; ventrolateral carinae on metasoma V without enlarged lobate dentition; telson with bulbous vesicle, without subaculear tubercle, aculeus shorter than vesicle; pectines with fulcra; hemispermatophore with flagellum separated from a 3-lobed sperm hemiduct, basal lobe a broad, low, axially oriented, curved scoop; chelicerae with characteristic buthid pattern of dentition (Vachon, 1963), two denticles on ventral aspect of fixed finger; pedipalps orthobothriotaxic, type Aβ (Vachon 1974, 1975), patella with d_3 internal to dorsomedian carina, manus with V_2 not strongly displaced internally, V_1–V_2 axis nearly collinear with long axis of chela, chela fixed finger with *db* on proximal half of finger between *esb* and *est*, *it* near tip; pedipalps short, chelae small with carinae reduced or obsolete, dentate margins of fingers armed with 8–10 non-imbricated linear subrows of primary denticles; subrows flanked by mid-row internal and proximal ex-

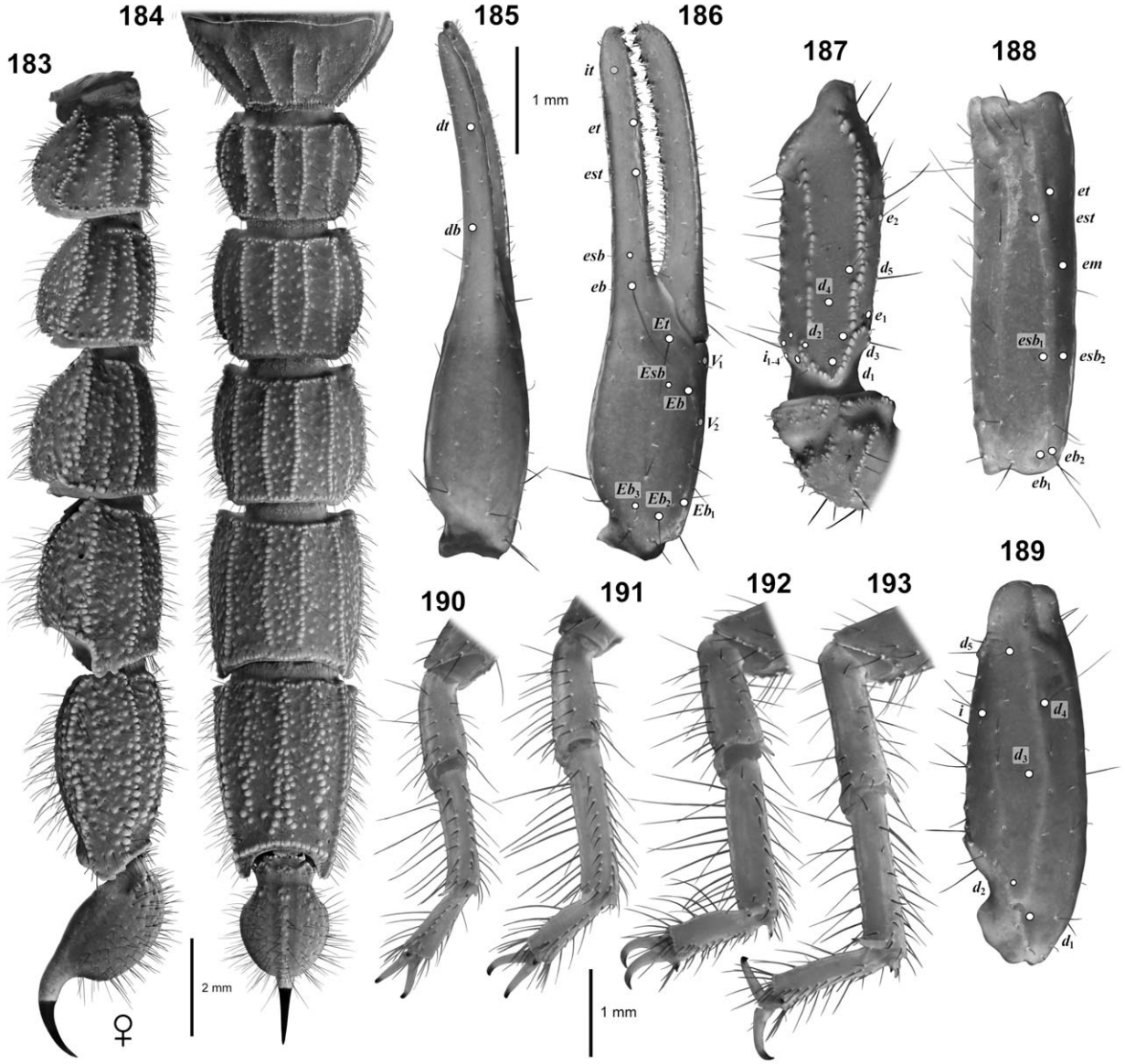

Figures 183–193: Metasoma, telson, pedipalp, trichobothrial map and leg tarsi of *Butheolus villosus* Hendrixson, 2006. Holotype female. UV fluorescence. **Figs. 183–184.** Metasoma and telson. Right lateral (183) and ventral (184) aspects. Scale bar: 2 mm. **Figs. 185–189.** Pedipalp and trichobothria. Dorsal (185) and external (186) aspect of chela; dorsal (187) aspect of femur; external (188) and dorsal (189) aspect of patella. Scale bar: 1 mm. **Figs. 190–193.** Tarsi and tibia of left leg I (190), II (191), III (192) and IV (193), retrolateral aspect. Scale bar: 1 mm.

ternal accessory denticles; movable finger with 3 enlarged subdistal denticles; males without recess or scalloping of dentate margins at base of pedipalp fingers, with chela manus wider than females; tergites lacking macrosetae; tibial spurs present on legs III–IV; basitarsi I–III with regular series of long macrosetae on retrosuperior, retroinferior and inferior margins; ventral surfaces of telotarsi with paired rows of macrosetae, often reduced to single row on legs I–III; prolateral and retrolateral tarsal spurs present on all legs; size of macrosetae on carapace, pedipalps, legs and metasoma not sexually dimorphic.

ETYMOLOGY. Prefix from Greek ξένος (xénos) meaning alien or strange, i.e. a strange buthid that resembles *Butheolus* in some features but differs from it in others.

TYPE SPECIES. *Buthus anthracinus* Pocock, 1895 [=*Xenobuthus anthracinus* (Pocock, 1895), **comb. n.**], designated here.

Measurements (mm)	*Butheolus thalassinus* Simon, 1882	*Butheolus villosus* Hendrixson, 2006
	♂	♀ holotype
Total L	24.00	34.80
Metasoma + Telson L	14.60	19.50
Carapace L	2.79	3.91
Carapace anterior W	1.59	2.07
Carapace posterior W	3.37	4.74
Carapace preocular L	1.20	1.56
Metasoma I L/W/D	1.71/ 2.29/ 1.88	2.32/ 3.01 / 2.46
Metasoma II L/W/D	2.02/ 2.27/ 1.96	2.67/ 3.09/ 2.46
Metasoma III L/W/D	2.13/ 2.33/ 2.06	3.10/ 3.15/ 2.64
Metasoma IV L/W/D	2.58/ 2.33/ 2.08	3.73/ 3.17/ 2.60
Metasoma V L/W/D	3.08/ 2.17/ 1.83	4.12/ 2.91/ 2.27
Telson L	2.67	4.01
Vesicle L/W/D	1.83/ 1.16/ 1.33	2.51/ 1.83/ 1.68
Pedipalp chela L	3.46	4.86
Chela movable finger L	2.07	3.02
Chela fixed finger L	1.53	2.36
Chela manus ventral L/W/D	1.56/ 0.85/ 0.90	1.87/ 0.96/ 1.08
Pedipalp femur L/W	1.88/ 0.78	2.80/ 0.97
Pedipalp patella L/W	2.49/ 1.11	3.55/ 1.13
Pectine length	2.49	3.26
Pectine teeth (left/ right)	17/ 17	18/ 18

Table 6: Measurements of adult male *Butheolus thalassinus* Simon, 1882 and adult female *B. villosus* Hendrixson, 2006. *B. thalassinus* (♂): Yemen, Ta'izz, 1158 m, under rock on Euphorbia-Aloe hill, 10. I. 1951, H. Hoogstraal (c.f. Sissom, 1994: 7–8). *B. villosus* (holotype ♀): Khashm Dhibi, Saudi Arabia, 28.II.1980, leg. A. Barkham, NHMB 0618 (c.f. Hendrixson, 2006: 59–61). Abbreviations: L, length; W, width, D depth.

***Xenobuthus anthracinus* (Pocock, 1895), comb. n.**
(Figs. 151–162, 194–259, 326–327, 331, 334, 338, Tab. 7)

Buthus anthracinus Pocock, 1895: 294–295, 315, pl. IX, figs. 1, 1a.

Buthus anthracinus: Kraepelin, 1899: 18; Simon, 1910: 77; Táborský, 1934: 40; Birula, 1937: 101; Weidner, 1959: 99; Pérez, 1974: 43; Lamoral & Reynders, 1975: 504; Sissom, 1994: 36.

Buthus (*Hottentotta*?) *antracinus*: Birula, 1910: 171; Birula, 1937: 101.

Buthus (*Hottentotta*?) *anthracinus*: Birula, 1917a: 230.

Butheolus anthracinus: Fet & Lowe, 2000: 88; Kovařík, 2003: 137; Kovařík, 2004: 3, 25; Fet, Soleglad &

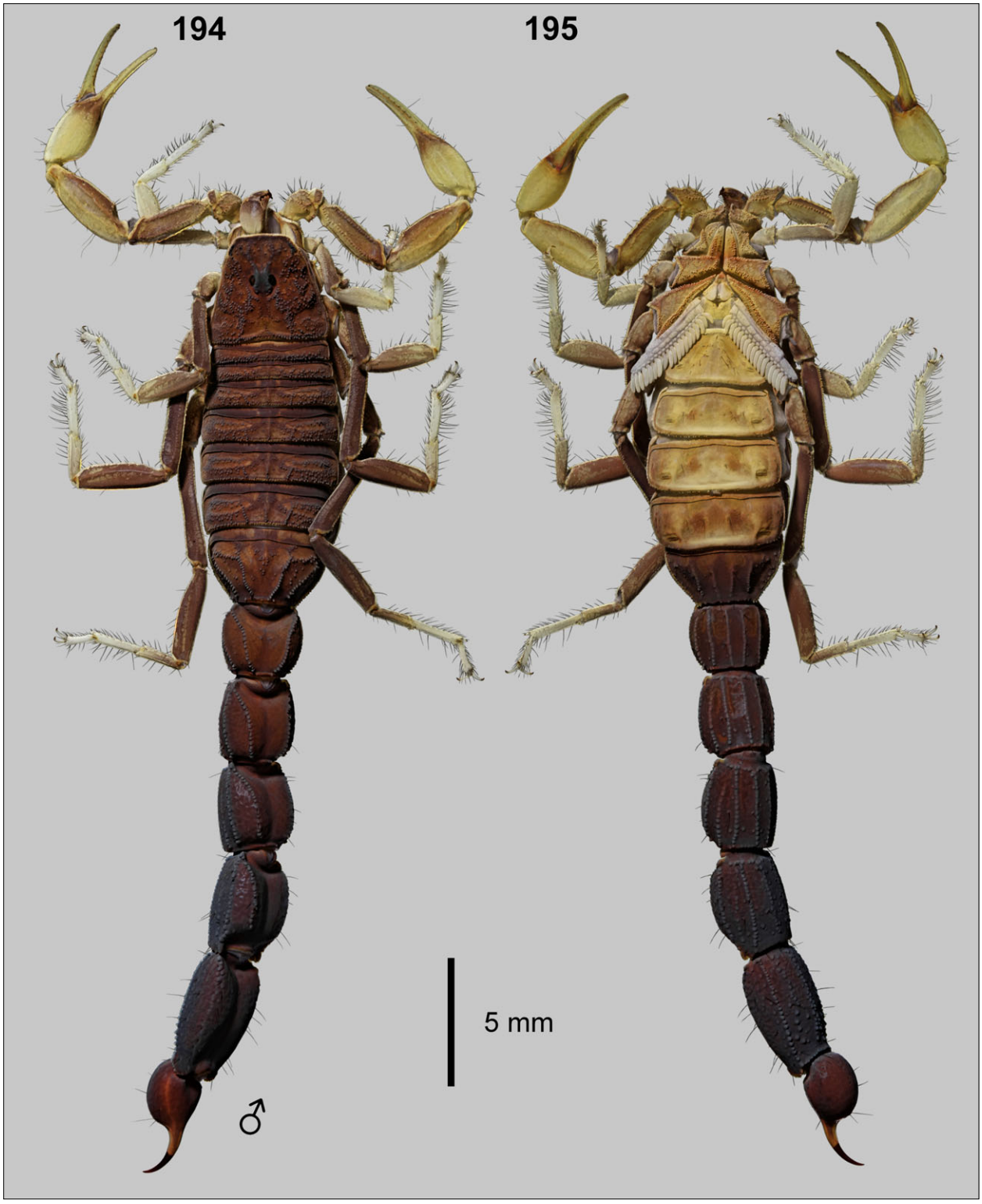

Figures 194–195: Habitus of male *Xenobuthus* gen. n. *anthracinus* (Pocock, 1895). **Fig. 194.** Dorsal aspect. **Fig. 195.** Ventral aspect. Same locality data as male in Table 7. Scale bar: 5 mm.

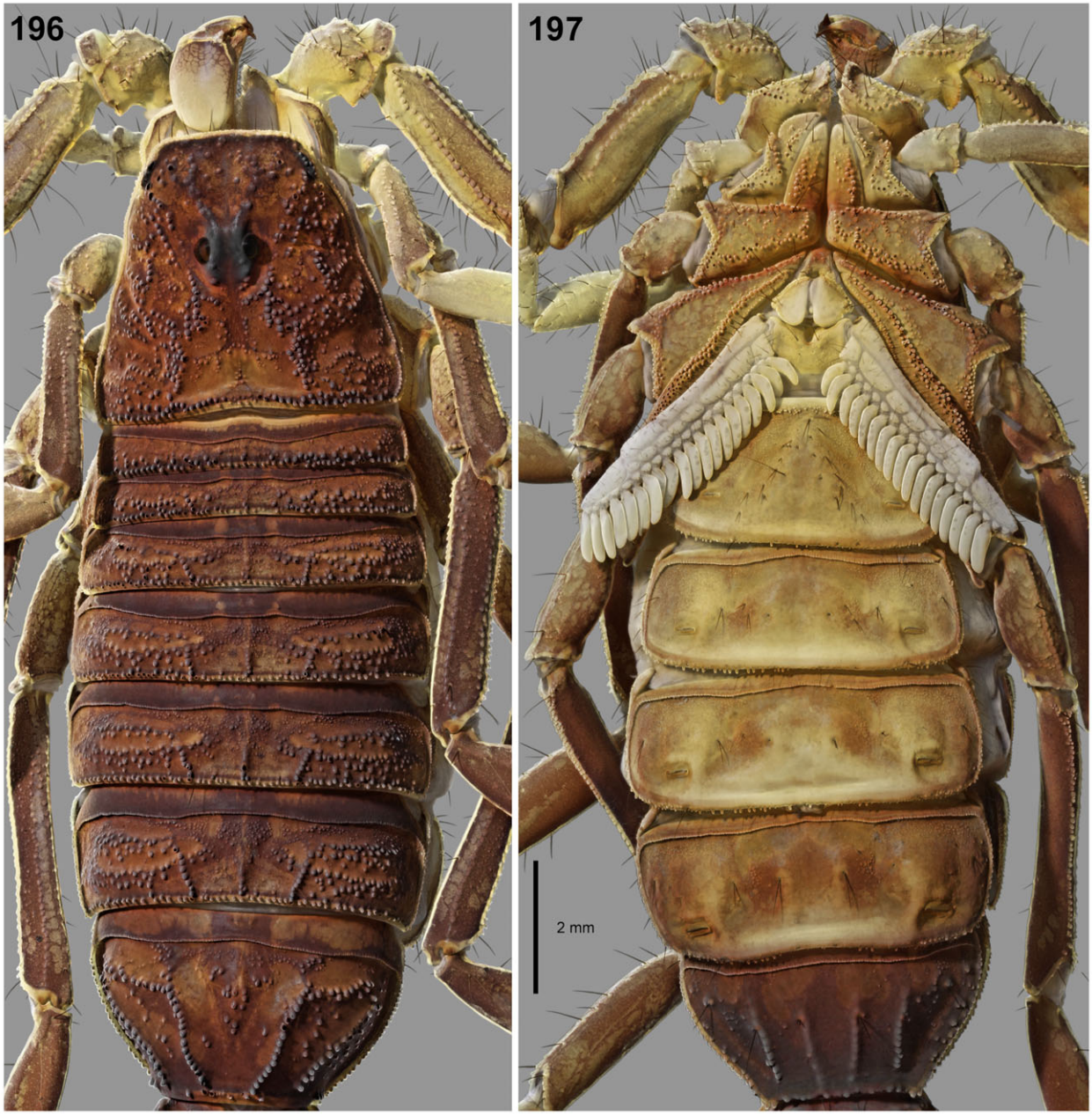

Figures 196–197: Prosoma and mesosoma of male *Xenobuthus* gen. n. *anthracinus* (Pocock, 1895). **Fig. 196.** Dorsal aspect, carapace and tergites. **Fig. 197.** Ventral aspect, coxosternal area and sternites. Same locality data as male in Table 7. Scale bar: 2 mm.

Lowe, 2005: 2; Hendrixson, 2006: 51–53, 56–59. figs. 6, 8, pl. 6, Tab. 1; Lourenço & Qi, 2006: 93–94, tab. 1; El-Hennawy, 2009: 121; Kovařík & Lowe, 2012: 2, 20, 22–23, fig. 94; Lowe et al., 2014: 117.

TYPE MATERIAL. Lectotype ♀, Yemen, Hadramaut (ZMUH) (not examined). The syntypes of Pocock in BMNH were not found, and a lectotype was designated by Kovařík (2004: 3).

MATERIAL EXAMINED. **Oman:** 1♀, S of Thumrait, Nejd Desert, UV detection, edge of small vegetated wadi, open plain, fine silty soil, rock outcrops, 17°30.76' N 54°02.76'E, 580 m a.s.l., 16.X.1993, 19:28 h, leg. G. Lowe, (NHMB); 1♂, S of Thumrait; Nejd Desert, UV detection, silty plain, edge of small vegetated wadi, fine

Figures 198–199: Habitus of female *Xenobuthus* gen. n. *anthracinus* (Pocock, 1895). **Fig. 198.** Dorsal aspect. **Fig. 199.** Ventral aspect. Same locality data as female in Table 7. Scale bar: 5 mm.

Figures 200–201: Prosoma and mesosoma of female *Xenobuthus* gen. n. *anthracinus* (Pocock, 1895). **Fig. 200.** Dorsal aspect, carapace and tergites. **Fig. 201.** Ventral aspect, coxosternal area and sternites. Same locality data as female in Table 7. Scale bar: 2 mm.

silty soil, open plain, rock outcrops, 17°30.77'N 54°02. 82'E, 600 m a.s.l., 19.X.1993, 23:02 h, leg. G. Lowe, (NHMB). **Saudi Arabia:** 1♀ (adult or subadult?), Khamis Mushayt, 18°18'N 42°44'E, ca. 2,000 m a.s.l., leg. Digby Lickfold (AMNH).

DIAGNOSIS**.** A member of the genus *Xenobuthus* differentiated as follows: small to medium-sized scorpions, adults 35–50 mm; base color a uniform dark, reddish brown, almost black, all metasomal segments dark brown to black; pedipalp femur and patella light to dark brown, chela with yellow fingers, fuscosity on manus at base of fingers; legs darker brown on femur and patella, lighter on tibia, pale straw color on tarsi; carapace and tergites with moderately dense, fine granulation; metasoma IV with lateral median carinae distinct; metasoma V with ventromedian carina posteriorly bifurcate, males with ventral intercarinal surface granular on posterior 1/4 of segment; posterior metasomal segments relatively stout in male: metasoma III L/W ♂ 1.09; metasoma IV L/W ♂ 1.38; metasoma V L/W ♂ 1.66, L/D 2.17; pectine teeth 17–22.

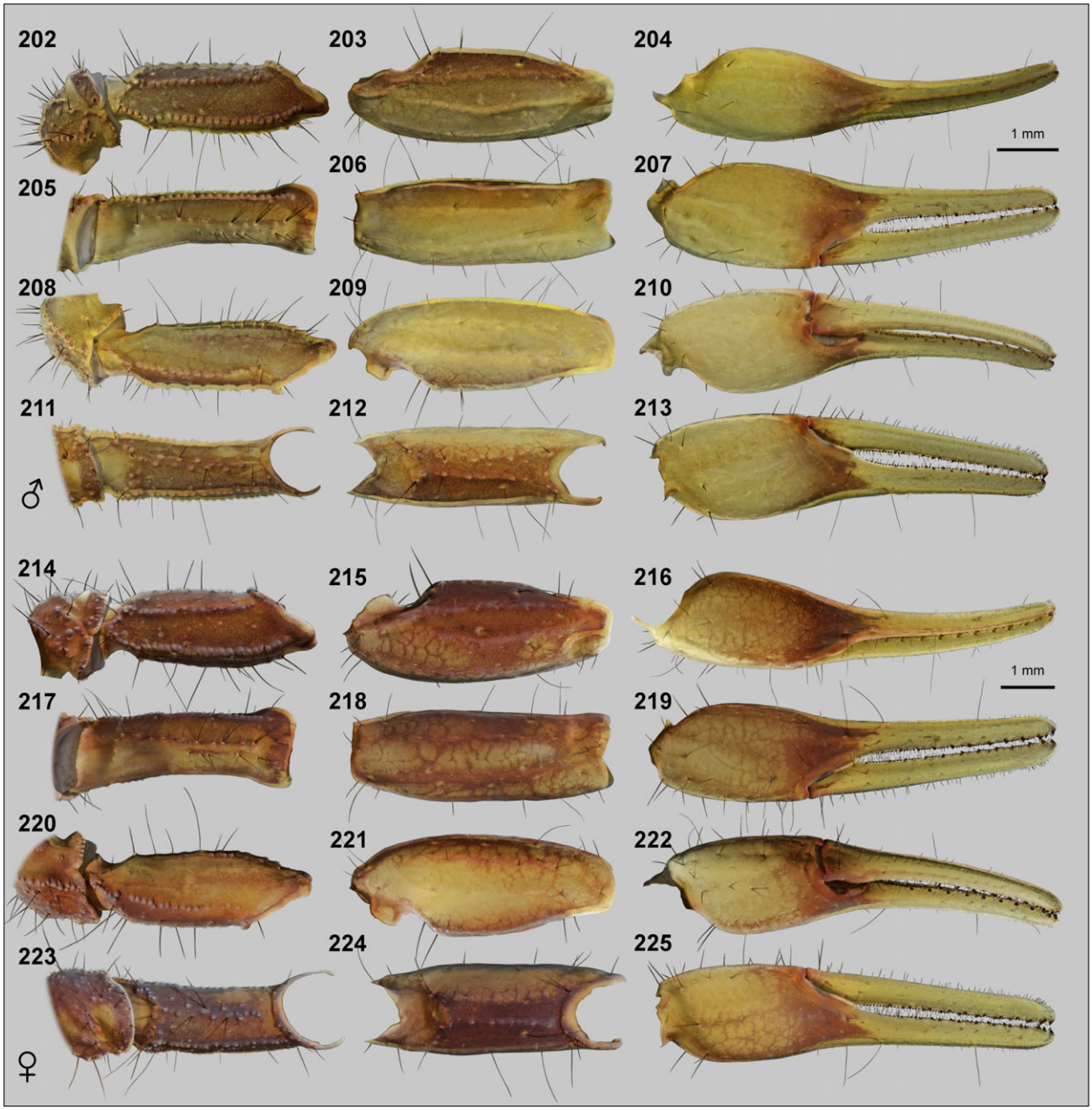

Figures 202–225: Pedipalp of *Xenobuthus* gen. n. *anthracinus* (Pocock, 1895). **Figs. 202–213.** Male (♂). Dorsal (202–204), external (205–207), ventral (208–210) and internal (211–213) aspect of femur (202, 205, 208, 211), patella (203, 206, 209, 212) and chela (204, 207, 210, 213). **Figs. 214–225.** Female (♀). Dorsal (214–216), external (217–219), ventral (220–222) and internal (223–225) aspect of femur (214, 217, 220, 223), patella (215, 218, 221, 224) and chela (216, 219, 222, 225). Both sexes with same locality data as in Table 7. Scale bars: 1 mm.

REDESCRIPTION.
Based on 1 ♂, 1 ♀ from Dhofar, Oman.

Coloration (Figs. 194–225, 244–247, 252–259). Base color dark brown, nearly black, on dorsal aspect of prosoma. mesosoma and all aspects of metasoma and telson; tergites with lighter lateral patches in transverse reticulated bands; telson vesicle with lighter spots at bases of macrosetae, lighter lateral stripes, and a pair of lighter sub-median stripes on ventral surface; dorsal aspect of chelicerae dark on proximal fingers and distal margin of manus, yellow-dark brown reticulated on distal half of manus; legs dark brown on trochanter, femur and patella except for lighter spots on distal patella and lighter patella I; leg tibia I pale whitish-yellow, tibia II–IV light brown; leg tarsi pale whitish-yellow; pedipalps

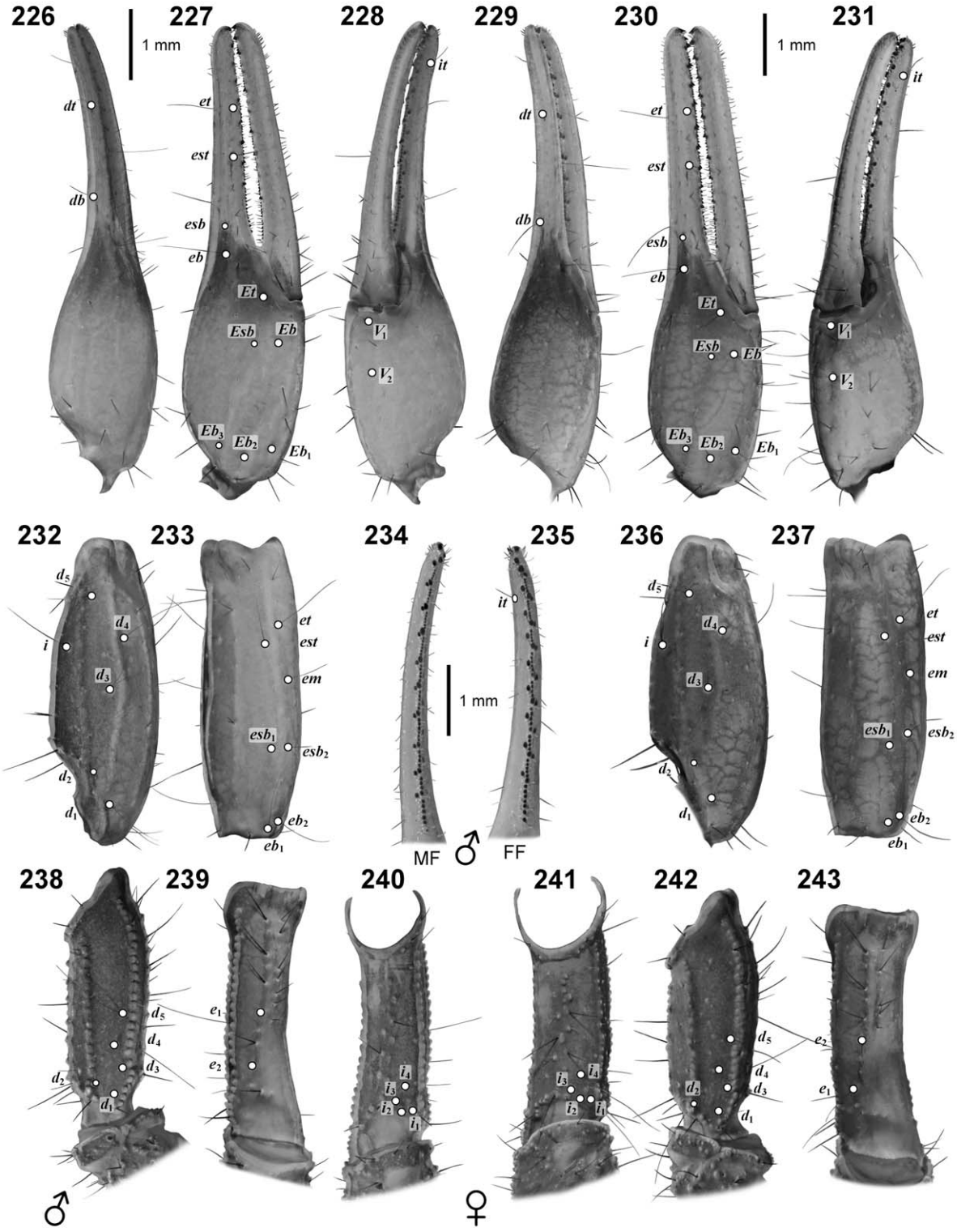

Figures 226–243: Trichobothrial maps and chela finger dentition of *Xenobuthus* gen. n. *anthracinus* (Pocock, 1895). Male (♂): dorsal (226), external (227) and ventrointernal (228) aspect of chela; dorsal (232) and external (233) aspect of patella; dorsal (238), external (239) and internal (240) aspect of femur; dentition of movable finger (MF) (234) and fixed finger (FF) (235). Female (♀): dorsal (229), external (230) and ventrointernal (231) aspect of chela; dorsal (236) and external (237) aspect of patella; internal (241), dorsal (242) and external (243) aspect of femur. Both sexes with same locality data as in Table 7. Scale bars: 1 mm (♂, ♂ dentition, ♀).

light to dark brown on trochanter, femur and patella, chela manus light brown or yellow, with dark distal band at base of fingers, chela fingers yellow; ventral aspect of mesosoma a lighter shade of brown, except for dark brown sternite VII.

Carapace (Figs. 194, 196, 198, 200, 326–327). Strongly trapezoidal, W/L 1.09–1.20, posterior W/ anterior W 2.14–2.24; lateral flanks steeply sloped; median ocular tubercle prominent; postocular area forming triangular posteromedial plateau with shallow depressions; interocular triangle gently sloped downwards towards anterior margin, less so in female; anterior margin with 10 (♂), or 12 (♀) macrosetae, carapace otherwise devoid of macrosetae; anterolateral margins with 6 pairs of lateral eyes: 3 major ocelli and 1 minor ocellus below granular ridge, and 2 minor ocelli above granular ridge; whitish eyespot present below lateral eye cluster; all carinae of carapace obsolete except for superciliary carinae which may extend slightly anterior to median ocular tubercle; central median and posterior median carinae indicated by granule rows along edges of postocular plateau; surface with sparse to moderate irregular coarse granulation, with locally smooth areas in postocular plateau, posterior transverse and posterior marginal furrows, and most of interocular triangle; superciliary carinae smooth, with a few coarse granules on posterior slopes; granulation of female carapace similar to male, slightly weaker.

Chelicerae (Figs. 258–259). Dorsal surface of manus smooth, with two short, pale microsetae on apical margin, each with adjacent granules; dorsointernal carina strong, granulate, bearing one long, dark macroseta and one short, pale microseta; fingers robust, movable finger dorsal margin with two large subdistal denticles and two small basal denticles, ventral margin with larger subdistal and smaller basal denticles, fixed finger with large subdistal denticle and proximal bicusp, two denticles on ventral surface; dorsal surface of movable finger smooth, with three pale microsetae.

Coxosternal area (Figs. 195, 197, 199, 201). *Male*. Coxa I finely granulated, endite smooth on anterior margin, sparsely granulated on posterior areas; coxa II with fine granules concentrated along margins, central surfaces sparsely granulated mostly smooth, endite smooth on anterior quarter and medial margin, granulated elsewhere; coxa III with strong peg-like granulation concentrated along anterior and distal margins, posterior margin weakly granular in proximal half, central area of sclerite smooth; coxa IV with dense band of strong peg-like granulation along anterior margin, rimmed with row of similar granules along proximal half of posterior margin, central surface smooth or very weakly shagreened; coxae I–III with scattered, mostly anterior macrosetae: coxa I 5–6, II 6–9, III 5; coxa IV with single macroseta on anterior proximal limit; sternum weakly granulated, subtriangular, with deep posteromedian pit, bearing 2 short macrosetae; genital opercula with fine granulation on anterior margin, otherwise smooth, with 4–5 macrosetae, posterolateral margins weakly concave. *Female*. Coxa I strongly granulated, similar to male; coxa II granulation weaker than male, granules strong only on distal and anterior margins, endites almost smooth; coxa III smooth except for narrow strip of granules along proximal 3/4 of anterior margin; coxa IV with granulation similar to male but slightly weaker, strong granulation on anterior and proximal posterior margins; coxal macrosetae: I 4–6, II 8, III 5–6, IV 1; sternum similar to male, granulate with larger median pit, 2 setae; genital opercula smooth except for weak granulation along outer anterior margin, 3–5 macrosetae.

Pectines (Figs. 195, 197, 199, 201). Basal piece with anterior margin concave, with deep median pit or groove; surface in male nearly flat, weakly shagreened, bearing 5 setae, in female strongly biconcave posteriorly, granulated in depressions and along posterior margin, bearing 7 setae; pectines with 3 marginal lamellae, 7–8 middle lamellae, extending to distal end of coxa IV in male, falling short of distal end in female; marginal and middle lamellae with moderate cover of short macrosetae; fulcra with 1–4 fine macrosetae (mostly 3–4); teeth of similar length in both sexes, tooth counts: ♂ 19/20, ♀ 19/19.

Hemispermatophore (Figs. 248–251, 331). Flagelliform, trunk elongate, ca. 6.4 times length of capsule region; flagellum with short pars recta bearing anterior marginal lamella, longer pars reflecta gradually tapering to cylindrical hyaline filament; sperm hemiduct tripartite, posterior lobe large, laminate, median lobe small, acuminate, anterior lobe of intermediate length; posterior margin of median lobe overhanging posterior lobe, the two lobes fused along median lobe carina; basal lobe a low, broad, axially oriented, curved scoop, with posterior-facing concavity, proximally angled in posterior direction, distally confluent with median lobe carina.

Mesosoma (Figs. 194–201, 334). *Tergites*: pretergites smooth, with weak, fine corrugations on posterior margins; tergites I–VI with lateral areas of coarse granulation in central and posterior parts, broken by smooth transverse patches, anterior lateral and medial areas heavily shagreened, posterior margins of sclerites rimmed by regular rows of granules; tergite I without distinct carinae, II with weak traces of median or median plus paired lateral carinae; tergites III–VI tricarinate with anteriorly divergent, granulate carinae which become stronger on more posterior tergites; granulation and carination pattern of female similar to male but much weaker; tergite VII with 5 carinae, median carina a weak granulated hump, lateral carinae strongly granular, inner lateral carinae anteriorly divergent, intercarinal areas with sparse or moderate density of coarse granules, smoother in male; all tergites lacking macrosetae;

Figures 244–247: Leg tarsi and tibiae of male *Xenobuthus* gen. n. *anthracinus* (Pocock, 1895). Retrolateral aspect, left leg I (244), II (245), III (246), IV (247) tibia, basitarsus and telotarsus. Same locality data as male in Table 7. White light illumination. Scale bar: 1 mm.

sternites: *male*: sternites III–V lacking carinae, medially smooth, weakly shagreened anterolaterally, III densely shagreened on surface covered by pectines; sternites IV–VI with weak, smooth remnants of outer lateral carinae near posterior margins adjacent to spiracles, VI with weak, smooth remnants of inner lateral carinae; sternites IV–VI with wide, posteromedian smooth patch; posterior margins of sternites III–VI with fringe of small,

Figures 248–251: Hemispermatophore of *Xenobuthus* gen. n. *anthracinus* (Pocock, 1895). **Figs. 248–250.** Capsule region of right hemispermatophore, anterior (284), convex (249) and posterior (250) aspects. Scale bar: 200 μm. In convex view (249), the capsule is compressed to show outlines of lobes. **Fig. 251.** Whole left hemispermatophore, convex aspect. Same locality data as male in Table 7. White light illumination. Scale bar: 1 mm.

non-contiguous, digitate denticles; sternite VII smooth except for sparse fine granulation on outer lateral areas, median carinae weakly granulose, nearly smooth, lateral carinae strongly granulose; carinae confined to posterior 2/3 of sternite, only median pairs extending to posterior margin; non-marginal macrosetae: III 20 along edges of pectinal contact area, IV 10, V 7, VI 6, VII 6 including 4 stereotypic isolated macrosetae near outer anterior ends of carinae; *female*: sternite III smooth except for finely shagreened areas on surface covered by pectines; sternites IV–VI smooth except for very weakly shagreened anterior edges adjacent to pre-sternite borders; sternite VII smooth medially and anteriorly, sparsely granulate on mediolateral and lateral intercarinal surfaces; carinae obsolete on sternite III, reduced to smooth posterior wrinkles on medial sides of spiracles on IV–VI; posterior marginal denticles of sternites III–VI much smaller than in male; sternite VII with two pairs of well-developed smooth or weakly granular carinae, sparse granulation on mediolateral and lateral surfaces; non-marginal macrosetae: III 26, IV 12, V 6, VI 7, VII 6; mesosoma wider in female than male.

Metasoma (Figs. 194–195, 198–199, 252–257). Length about equal to prosoma and mesosoma, metasoma + telson L/ carapace L ♂ 5.33, ♀ 5.27; segments moderately robust; *carination*: segments I–IV with 10 complete carinae, IV with lateral median carinae weaker than I–II but distinct; segment V with 7 carinae in male, 5 carinae in female (ventrosubmedian carinae indistinct); carinae on segments I–IV uniformly granulate, except

Figures 252–257: Metasoma and telson of *Xenobuthus* gen. n. *anthracinus* (Pocock, 1895). **Figs. 252–254.** Male (♂). Dorsal (252), right lateral (253) and ventral (254) aspects. **Figs. 255–257.** Female (♀). Dorsal (255), right lateral (256) and ventral (257) aspects. Both sexes with same locality data as in Table 7. Scale bars: 2 mm.

for nearly smooth ventromedian and ventrolateral carinae on metasoma I of female; ventrolateral carinae on V with granules gradually increasing in size, from finer anteriorly to coarser posteriorly; segment V with ventromedian carina marked by series of coarse granules, bifurcating in posterior half, ventrosubmedian carinae of male marked by series of coarse granules in anterior half, breaking up in posterior half, of female indistinct with coarse granules occupying broader longitudinal strips; lateral anal margin with 2 blunt granules or lobes, ventral anal margin with 17 (♂) or 20 (♀) granules; *intercarinal surfaces*: lateral and ventral aspects of segments I–IV mostly smooth with sparse fine granulation or isolated granules, except for denser fine granulation on ventral aspect of female metasoma VI; dorsolateral and lateral surfaces of segments II–VI rugose in female, weakly rugose in male; segment V of male with sparse granulation on lateral and ventral surfaces, of female with sparse granulation on lateral surface, denser granulation on ventral surface, lateral surface rugose in female, weakly so in male; dorsal surfaces of all segments smooth in both sexes; *setation*: all segments equipped with scattered long, curved, golden macrosetae on all aspects, most located near or

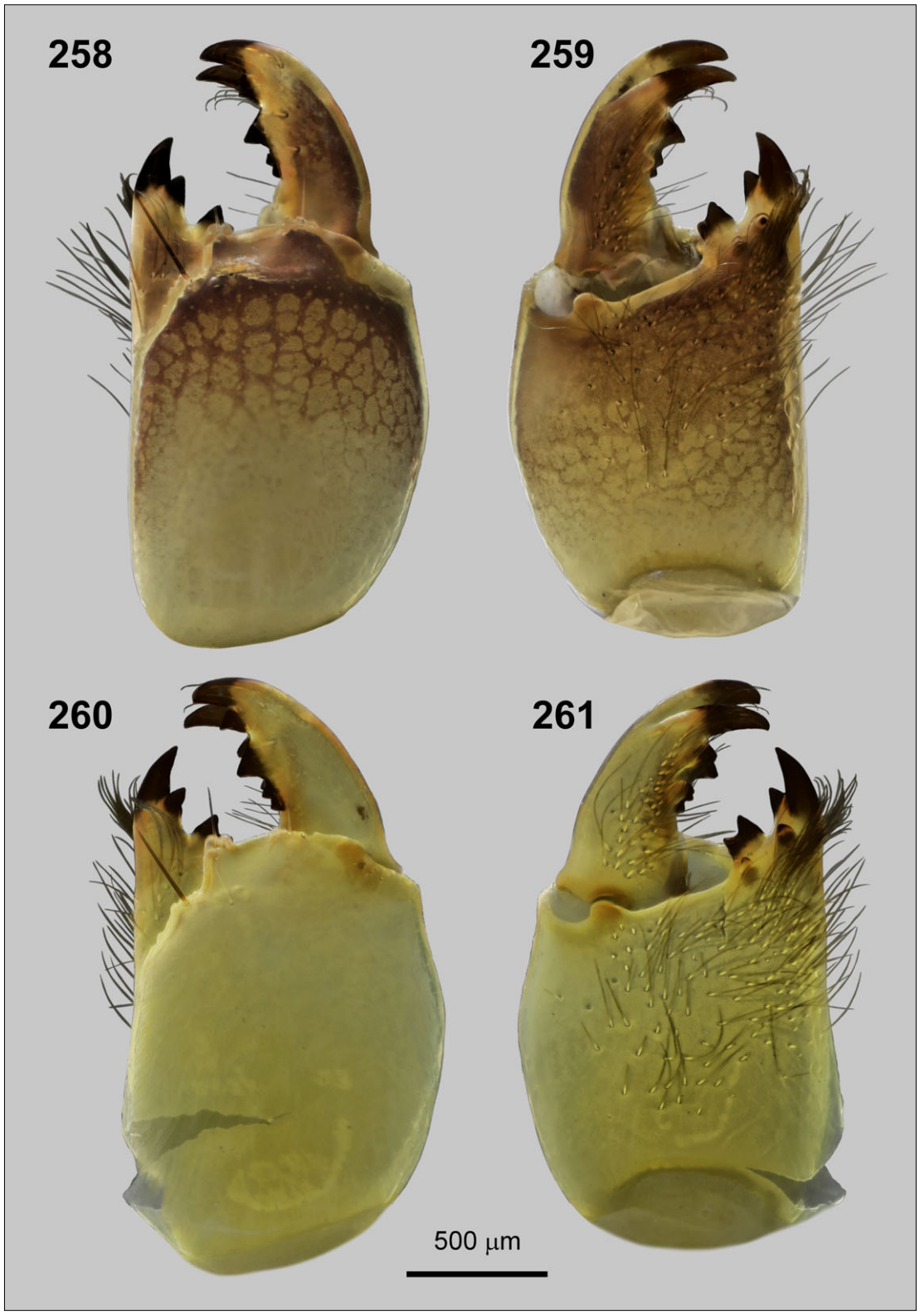

Figures 258–261: Chelicerae of male *Xenobuthus* gen. n. *anthracinus* (Pocock, 1895) and *X. xanthus* sp. n. **Figs. 258–259.** *X. anthracinus*, right chelicera, dorsal (258) and ventral (259) aspect. Same locality data as male in Table 7. **Figs. 260–261.** *X. xanthus* sp. n., right chelicera, dorsal (260) and ventral (261) aspect. Holotype male. Scale bar: 500 µm.

on carinae, setae of similar length in both sexes; metasoma V with 5–6 macrosetae along dorsolateral margins.

Telson (Figs. 194–195, 198–199, 252–257). Vesicle smooth dorsally and laterally, mostly smooth ventrally except for a few granules at anterior end; small indentations at setal insertion points; bulbous, with steep posterior slope, subaculear tubercle absent, but a slight ridge indicates trace of tubercle; several long macrosetae on lateral and ventral surfaces; aculeus slightly shorter than vesicle.

Pedipalps (Figs. 202–243). *Male* (Figs. 202–213, 226–228, 232–235, 238–240). *Femur*: L/W 3.02; dorsointernal and dorsoexternal carinae strong, ventrointernal carina moderate, all with regular coarse granulation; external carina strong, nearly smooth with isolated coarse granules associated with setal insertion points; internal carina moderate, with isolated medium to coarse granules; dorsal surface faintly shagreened, nearly smooth, other surfaces smooth; 8–10 accessory macrosetae on distal external surface; *patella*: L/W 2.90; internal, dorsointernal and dorsomedian carinae moderate, weakly granulated, nearly smooth; dorsoexternal carina weak, smooth; external carina moderate, smooth; other carinae obsolete, ventromedian and ventroexternal carinae barely visible as smooth traces of thickened integument; intercarinal surfaces smooth; *chela*: slender, L/W 4.27, all carinae obsolete, surface smooth with sparse macrosetae and microsetae; 9–10 primary denticle subrows on movable fingers, 8 on fixed fingers, total count of non-enlarged primary denticles on movable fingers 45/48, on fixed fingers 45/46; denticle subrows except proximal flanked by internal and external accessory denticles, 8–9 internal or external accessory denticles on movable finger, 7–8 on fixed finger. *Female* (Figs. 214–225, 229–231, 236–237, 241–243). *Femur*: more robust than male, L/W 2.67; carination and surface texture similar to male; 9–11 accessory macrosetae on distal external surface; *patella*: more robust than male, L/W 2.56; dorsointernal and dorsomedian carinae smooth, internal carina with weaker granulation than male, other carinae similar to male; intercarinal surfaces smooth; *chela*: more slender than male, L/W 4.61, all carinae obsolete, surface smooth with sparse macrosetae and microsetae; 9–10 primary denticle subrows on movable fingers, 8 on fixed fingers, total count of non-enlarged primary denticles on movable fingers 52/53, on fixed fingers 41/58; 9 internal or external accessory denticles on movable fingers, 8–9 on fixed finger. *Trichobothriotaxy*: orthobothriotaxic, type Aβ (Vachon, 1974) (Figs. 226–243)

Legs (Figs. 194–195, 198–199, 244–247). Inferior carinae finely denticulate on femur I–III, finely crenulate on femur IV; other carinae on femora finely granulate; prolateral surfaces of femora sparsely shagreened; patella II–IV with weakly denticulate inferior carinae, other carinae smooth, prolateral surfaces smooth; tibia III–IV with spurs; retrolateral tarsal spurs simple, prolateral tarsal spurs basally bifurcate; basitarsi I/II/III with 8/11/12–13 long retrosuperior macrosetae arranged in bristle-combs; ventral surface of telotarsi with dual rows of long, fine macrosetae, but dual row condition may be confined to only basal portion on basitarsi I–III, leaving a single file of setae in distal portion (cf. Pocock, 1895: 295); tarsal ungues moderately long.

Measurements. See Table 7.

Variation. A second, smaller female (35 mm, subadult?) from Khamis Mushayt, Saudi Arabia (AMNH) was examined, and did not differ significantly in key diagnostic characters from the larger adult female (48 mm) from Dhofar described here (see also description of that specimen in Hendrixson, 2006). The specimens examined match very well the excellent original description and plates of Pocock (1895), for material collected from the Hadramaut in Yemen. Pocock noted variation in fuscous markings on proximal leg segments, and on carinae of pedipalp femur and patella. The lectotype female (ZMUH, photograph examined) appears to be an immature or juvenile instar (27 mm). It has more slender pedipalp segments, which is typical of immature *Xenobuthus* (e.g. in juvenile *X. xanthus* **sp. n.**, cf. Figs. 266 vs. 270).

DISTRIBUTION. The distribution apparently covers the mountainous plateau region of the southwestern Arabian Peninsula, ranging from Asir highlands of Khamis Mushayt (Saudi Arabia), through the Hadramaut of Yemen, to the Nejd Desert in Dhofar, Oman. A similar range of distribution is seen in other scorpions that inhabit the mountain ranges tracking the west to southwest coast of the Arabian Plate, e.g. *Leiurus haenggii* Lowe et al., 2014, and *Microbuthus kristensenorum* Lowe, 2010.

ECOLOGY. The male and female described here were both collected from the edge of a small sandy wadi in the arid Nejd Desert region (580 m a.s.l.), north of the Jabal Qara mountains in Dhofar. Scorpions that occurred together with *X. anthracinus* were: *Compsobuthus acutecarinatus* (Simon, 1882), *Hottentotta salei* (Vachon, 1980) and *Leiurus macroctenus* Lowe et al., 2014.

Xenobuthus xanthus sp. n.

(Figs. 151–162, 260–325, 328–329, 335, 338, Tabs. 3, 7)

http://zoobank.org/urn:lsid:zoobank.org:act:6BA2FD27-C501-4025-B258-2B7FB1F912D0

Butheolus anthracinus: Lowe, 2010a: 23.

HOLOTYPE. Holotype♂, Jabal Zulul, escarpment above Ash Shuwaymiyah, UV detection, on ground, silt and gravel, rocky bowl surrounded by rocky cliffs and

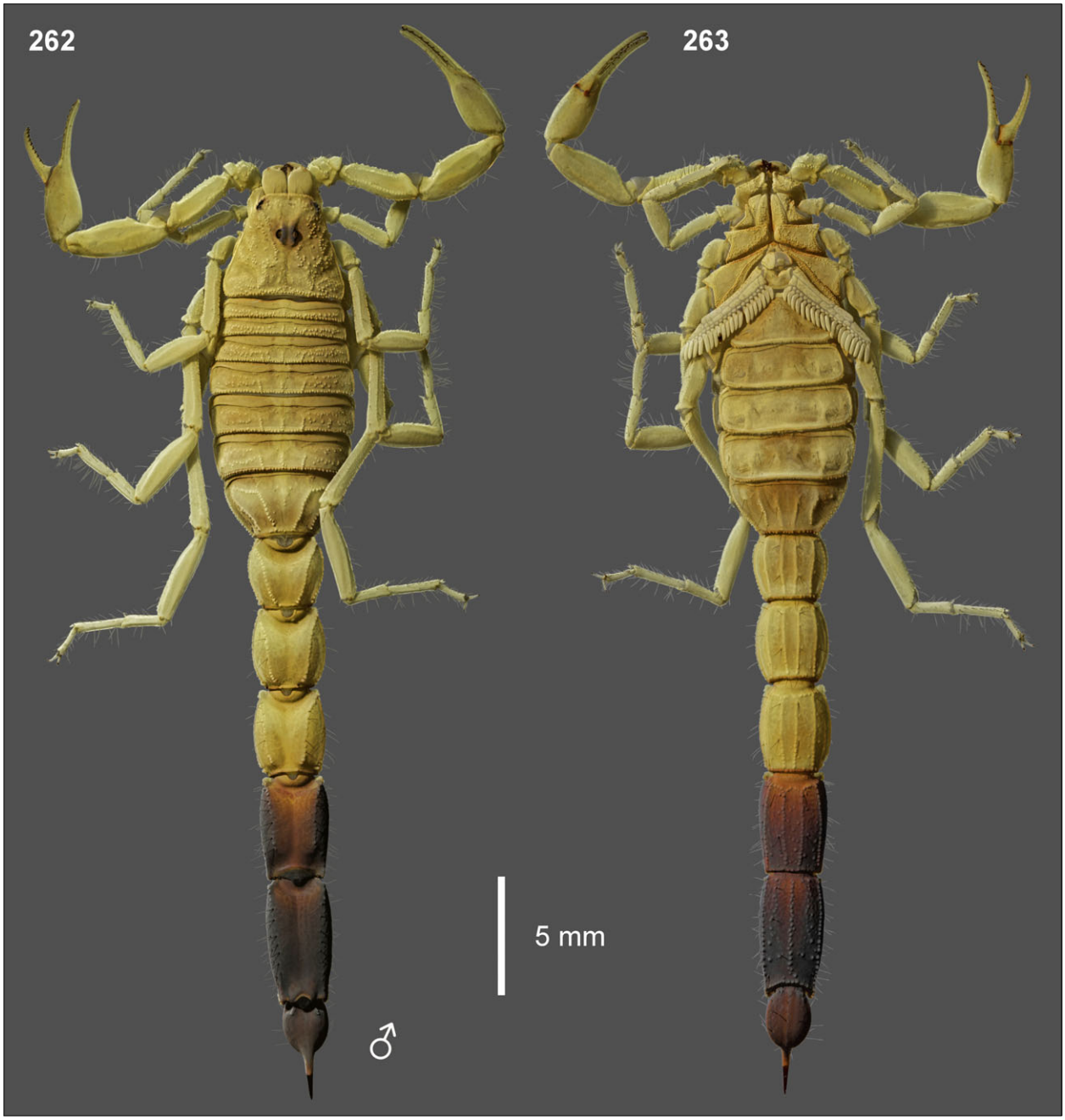

Figures 262–263: Habitus of male *Xenobuthus* gen. n. *xanthus* sp. n. **Fig. 262.** Dorsal aspect. **Fig. 263.** Ventral aspect. Holotype male (♂). Scale bar: 5 mm.

slopes, partly disturbed by earthmoving equipment, 17° 57.12'N 55°39.28'E, 215 m a.s.l., 26.IX.1995, 00:45 h, leg. G. Lowe, M.D. Gallagher (NHMB).

PARATYPES. 2 juv♂, same locality as holotype; 1 subadult♀, Jabal Qara, north slopes, Nejd Desert, UV detection, rocky wadi and rocky slopes, 17°17.83'N 54°05.11'E, 800 m a.s.l., 16.X.1993, 22:38 h, leg. G. Lowe (MNHN); 1♀, Wadi Ara, Jabal Samhan, under rocks at base of cliff, 17°16'N 54°57'E, 1050 m a.s.l., 2 Feb 1994, leg. M.R. Brown (ONHM); 1♀, Wadi Shuwaymiyah, under rock on mound of sandy soil, near permanent water seepage site on northern edge of wide vegetated wadi, 17°55.94'N 55°31.47'E, 50 m a.s.l., 25.IX.1995, 19:15 h, leg. G. Lowe, M.D. Gallagher (NHMB); 1 subadult♀, Wadi Shuwaymiyah, small rocky wadi, UV detection on patch of coarse sand on ground, in small side wadi, gravel with rocky walls,

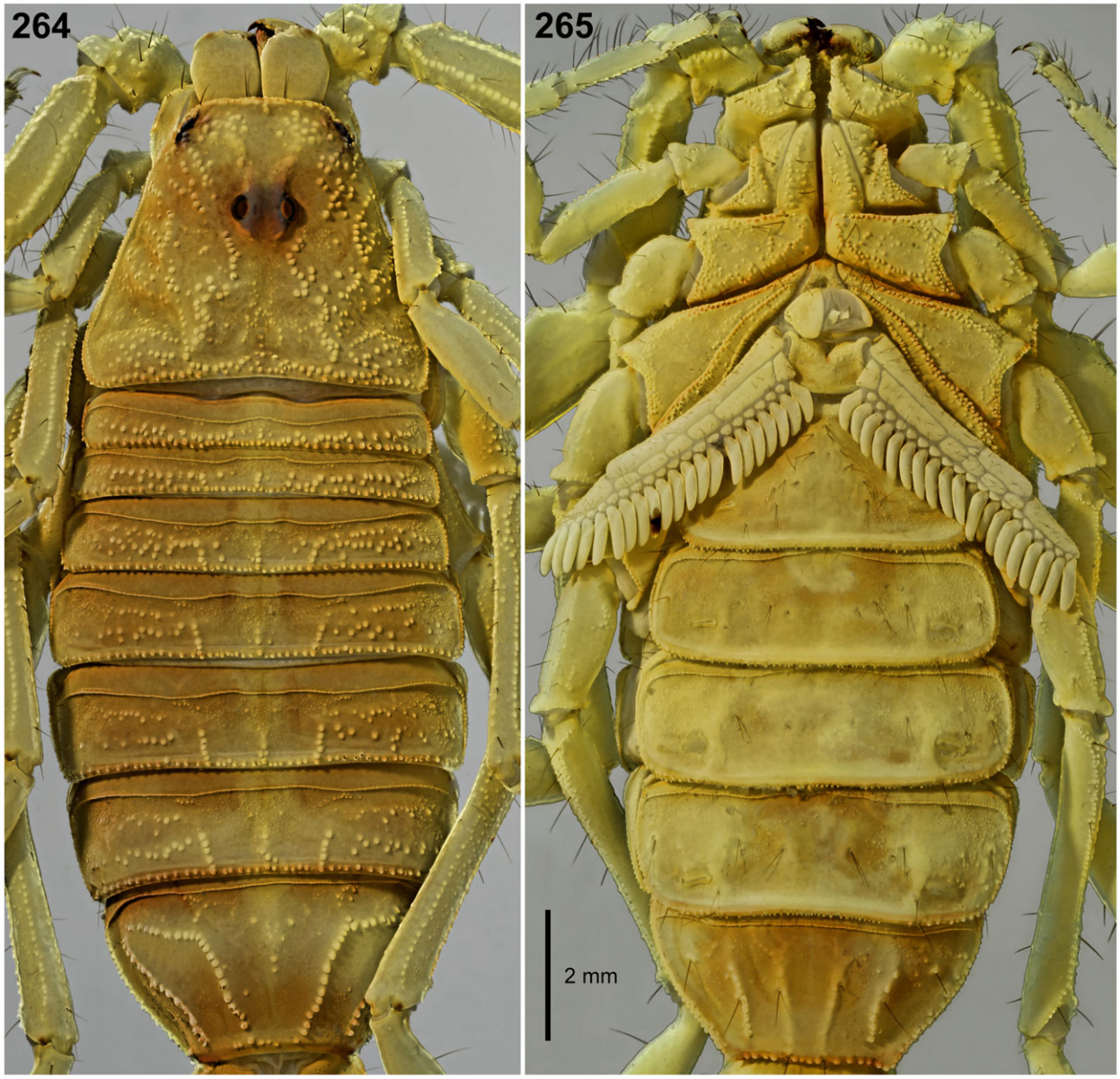

Figures 264–265: Prosoma and mesosoma of male *Xenobuthus* gen. n. *xanthus* sp. n. **Fig. 264.** Dorsal aspect, carapace and tergites. **Fig. 265.** Ventral aspect, coxosternal area and sternites. Holotype male. Scale bar: 2 mm.

17°55.81'N 55°32.98'E, 45 m a.s.l., 25.IX.1995, 21:30 h, leg. G. Lowe, M.D. Gallagher (BMNH); 1 subadult♀, 1 juv♂, east of Jabal Qamr, along coastal wadi, UV detection on slope, vegetated slopes with rocks; soil suitable for burrowing;, 16°53.71'N 53°48.75'E, 15 m a.s.l., 28.IX.1995, 00:30 h, leg. G. Lowe, M.D. Gallagher (NHMB).

DIAGNOSIS**.** A member of the genus *Xenobuthus* differentiated as follows: bicolored, with base color bright yellow, metasomal segments I–III yellow, metasoma IV yellow or dark brown, metasoma V and telson dark brown to black; pedipalp and legs yellow; carapace and tergites with moderately sparse, coarse granulation; metasoma IV without lateral median carinae; metasoma V with ventromedian carina composed of single series of granules, not posteriorly bifurcate, males with ventral intercarinal surface smooth on posterior 1/4 of segment; posterior metasomal segments relatively narrow in male: metasoma III L/W ♂ 1.21; metasoma IV L/W ♂ 1.52; metasoma V L/W ♂ 1.92, L/D 2.44.

ETYMOLOGY. From Greek ξανθός (xanthós) meaning yellow, a reference to the body color.

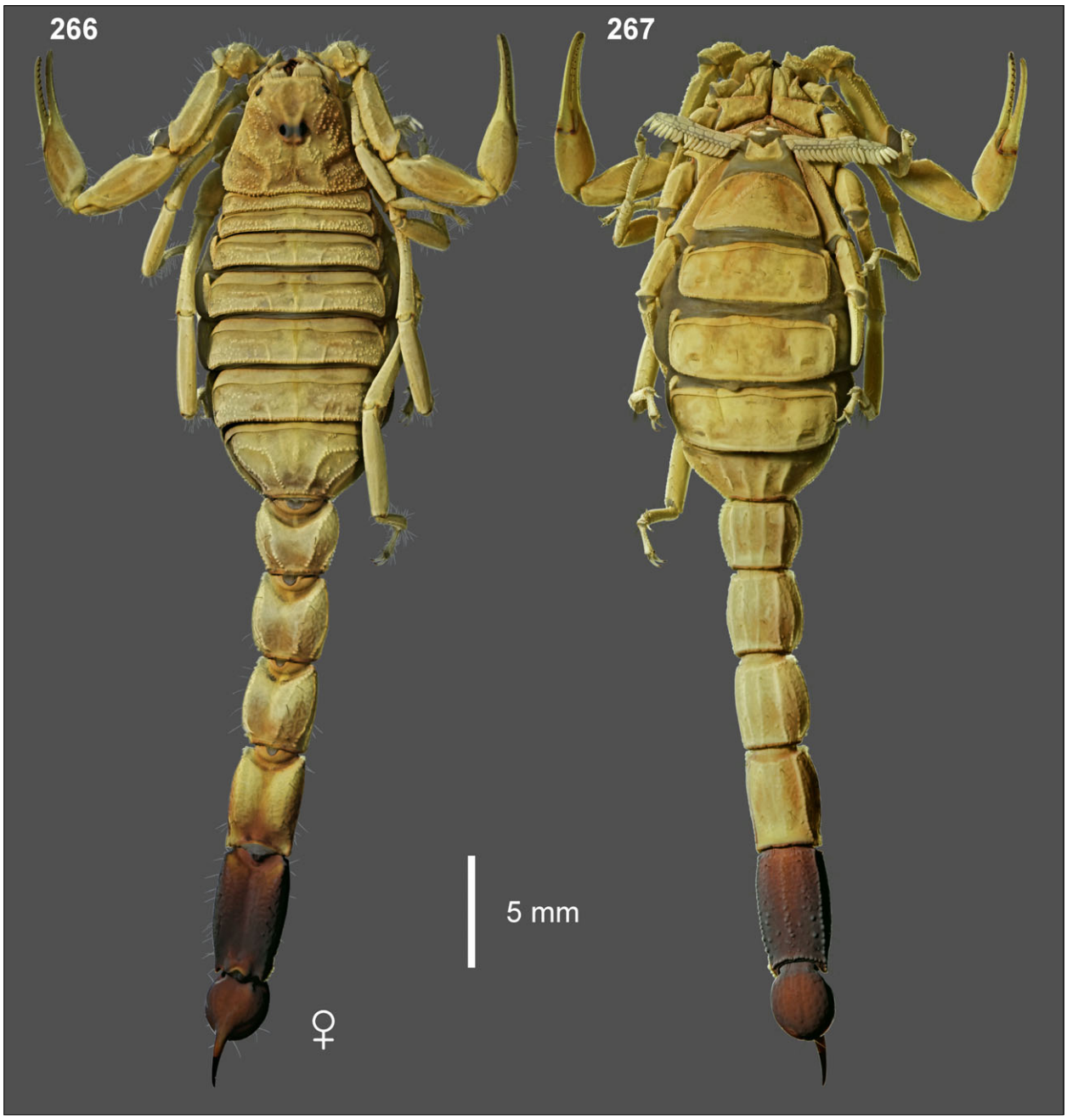

Figures 266–267: Habitus of female *Xenobuthus* gen. n. *xanthus* sp. n. **Fig. 266.** Dorsal aspect. **Fig. 267.** Ventral aspect. Paratype female (♀), #2 in Table 7. Scale bar: 5 mm.

DESCRIPTION.
Based on holotype adult ♂, 3 juv ♂, 2 adult ♀, 3 juv ♀ from Dhofar, Oman.

Coloration (Figs. 260–294, 313–316, 320–325). Bicolored; base color bright yellow with dark brown or black metasoma V and telson; metasoma IV variably pigmented, ranging from bright yellow, to light brown, to dark brown; if dark brown, anterior end may be slightly lighter; median and lateral eyes dark; small brown spots on distal ends of leg femora and patellae marking prolateral articular condyles; chelicerae yellow, without reticulated markings; juveniles may have light fuscous patterns on carapace, tergites and pedipalps (Fig. 270).

Carapace (Figs. 262, 264, 266, 268, 270, 328–329). Strongly trapezoidal, W/L 1.15–1.23, posterior W/ anterior W 2.21–2.41; lateral flanks steeply sloped; median ocular tubercle prominent; postocular area forming tri-

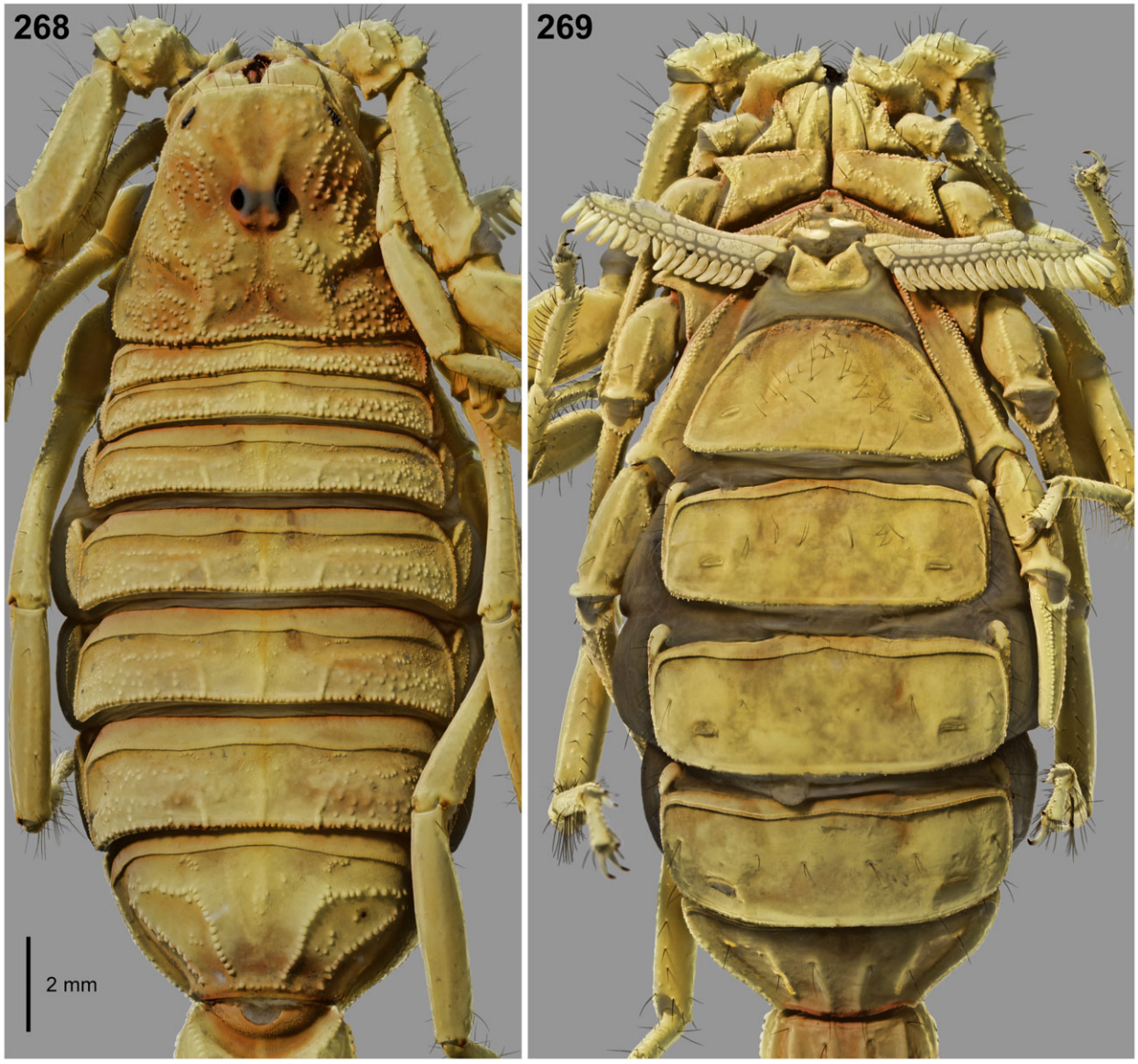

Figures 268–269: Prosoma and mesosoma of female *Xenobuthus* gen. n. *xanthus* sp. n. **Fig. 268.** Dorsal aspect, carapace and tergites. **Fig. 269.** Ventral aspect, coxosternal area and sternites. Paratype female (♀), #2 in Table 7. Scale bar: 2 mm.

angular posteromedial plateau with shallow depressions; interocular triangle gently sloped downwards towards anterior margin, less so in female; anterior margin with 7–9 macrosetae, carapace otherwise devoid of macrosetae; anterolateral margins with 5 pairs of lateral eyes: 3 major ocelli and 1 minor ocellus below granular ridge, and 1 minor ocellus above granular ridge; all carinae of carapace obsolete except for superciliary carinae which may extend slightly anterior to median ocular tubercle; central median and posterior median carinae indicated by granule rows along edges of postocular plateau; surface with sparse to moderate irregular coarse granulation, with extensive smooth areas in postocular plateau, posterior transverse and posterior marginal furrows, and median interocular triangle; superciliary carinae smooth, with a few coarse granules on posterior slopes; granulation of female carapace similar to male, weaker on interocular triangle.

Chelicerae (Figs. 260–261). Dorsal surface of manus smooth, with two short, pale microsetae on apical margin, each with adjacent granules; dorsointernal carina strong, granulate, bearing one long, dark macroseta and one short, pale microseta; fingers robust, movable finger dorsal margin with two large subdistal denticles and two small basal denticles, ventral margin with larger subdistal and smaller basal denticles, fixed finger with

large subdistal denticle and proximal bicusp, two denticles on ventral surface; dorsal surface of movable finger smooth, with 2–3 pale microsetae.

Coxosternal area (Figs. 263, 265, 267, 269). *Holotype male*. Coxa I with medium to coarse granulation, endite smooth on distal third, coarsely granulated on posterior 2/3; coxa II with medium granules concentrated along margins, central surfaces sparsely granulated, endite smooth on anterior end and medial margin, granulated elsewhere; coxa III with strong peg-like granulation concentrated along anterior and distal margins, posterior margin weakly granular in proximal half, central area of sclerite with sparse, fine granulation; coxa IV with dense band of strong peg-like granulation along anterior margin, rimmed with row of similar granules along proximal half of posterior margin, central surface very weakly shagreened; coxae I–III with scattered, mostly anterior macrosetae: coxa I 4–5, II 7–8, III 4–5; coxa IV with single macroseta on anterior proximal limit; sternum with weak fine granulation, subtriangular, with deep posteromedian pit, bearing 2 macrosetae; genital opercula with very weak fine granulation on anterior margin, otherwise smooth, with 2–4 macrosetae, posterolateral margins weakly concave. *Females*. Coxa I with heavy coarse granulation, distal part of endite smooth; coxa II with coarse granules in longitudinal strip on endite, medial half of endite smooth; distal, anterior and posterior margins coarsely granular, central area smooth; coxa III strongly granulated on anterior and distal margins, weakly granulated on proximal posterior margin, central area smooth; coxa IV with dense strip of granules on anterior margin, linear row of granules rimming proximal 2/3 of posterior margin, central area and distal margin smooth; coxal macrosetae: I 5–6, II 7–9, III 4–6, IV 1; sternum similar to male, weakly, finely granulate with larger median pit, 2 setae; genital opercula smooth, bearing 4–7 macrosetae.

Pectines (Figs. 263, 265, 267, 269). Basal piece with anterior margin concave, with deep median pit or groove; surface in male nearly flat, weakly shagreened, bearing 2 setae, in female strongly biconcave posteriorly, sparsely granulated in depressions, more densely along posterior margin, bearing 4–5 setae; pectines with 3 marginal lamellae, 6–8 middle lamellae, extending to distal end of coxa IV in male, falling short of distal end in female; marginal and middle lamellae with sparse cover of short macrosetae; fulcra with 1–4 fine macrosetae (mostly 3); teeth of similar length in both sexes, slightly longer in male; tooth counts: ♂ 18–21, ♀ 18–20.

Hemispermatophore (Figs. 317–319). Flagelliform, with elongate trunk; flagellum with short pars recta bearing anterior marginal lamella, longer pars reflecta gradually tapering to cylindrical hyaline filament; sperm hemiduct tripartite, posterior lobe large, laminate, median lobe small, acuminate, anterior lobe of intermediate length; posterior margin of median lobe overhanging posterior lobe, the two lobes fused along median lobe carina; basal lobe a low, moderately broad, axially oriented, curved scoop with posterior-facing concavity, arising from median lobe carina. The hemispermatophores extracted from the holotype male were soft, not well sclerotized, but the essential capsule structure and form of the basal lobe were visible.

Mesosoma (Figs. 262–270, 335). *Tergites*: pretergites smooth, with weak, fine corrugations on posterior margins; tergites I–VI with lateral areas of coarse granulation and smooth transverse patches, anterior lateral and medial areas weakly shagreened, posterior margins of sclerites rimmed by regular rows of granules; tergite I without distinct carinae, II with weak trace of median carinae; tergites III–VI tricarinate with anteriorly divergent, granulate carinae; granulation and carination pattern of female similar to male, but granules weaker in females; tergite VII with 5 carinae, median carina a weakly granulated hump, lateral carinae strongly granular, inner lateral carinae anteriorly divergent, intercarinal areas smooth except for a few coarse granules and a pair of anterior clusters of small granules; all tergites lacking macrosetae; *sternites*: *holotype male*: sternites III–V lacking carinae, medially smooth, weakly shagreened laterally, III densely shagreened on surface covered by pectines; sternites IV–VI with weak, smooth remnants of outer lateral carinae near posterior margins, adjacent to spiracles; sternites IV–VI with wide, posteromedian smooth patch; posterior margins of sternites III–VI with fringe of small, non-contiguous, digitate denticles; sternite VII smooth except for sparse fine granulation on mediolateral and outer lateral areas, median carinae smooth with trace of granulation, lateral carinae strongly granulose; carinae confined to posterior 2/3 of sternite, only median pairs extending to posterior margin; non-marginal macrosetae: III 18 along edges of pectinal contact area, IV 9, V 6, VI 8, VII 6 including 4 stereotypic isolated macrosetae in middle or anterior near outer sides of carinae; *females*: sternite III smooth except for finely shagreened areas on surface covered by pectines; sternites IV–VI smooth except for very weakly shagreened anterior lateral corners adjacent to presternite borders; sternite VII smooth; carinae obsolete on sternites III–V, reduced to smooth posterior wrinkles on medial sides of spiracles on VI; posterior marginal denticles of sternites III–VI much smaller than in males; sternite VII with two pairs of carinae, medial pair smooth, lateral pair smooth anteriorly, weakly granulate posteriorly; non-marginal macrosetae: III 24–27, IV 10-13, V 6–10, VI 6–7, VII 6; mesosoma wider in female than male.

Metasoma (Figs. 262–263, 266–267, 270, 320–325). Length about equal to prosoma and mesosoma, metasoma + telson L/ carapace L ♂ 5.62, ♀ 4.95–5.07;

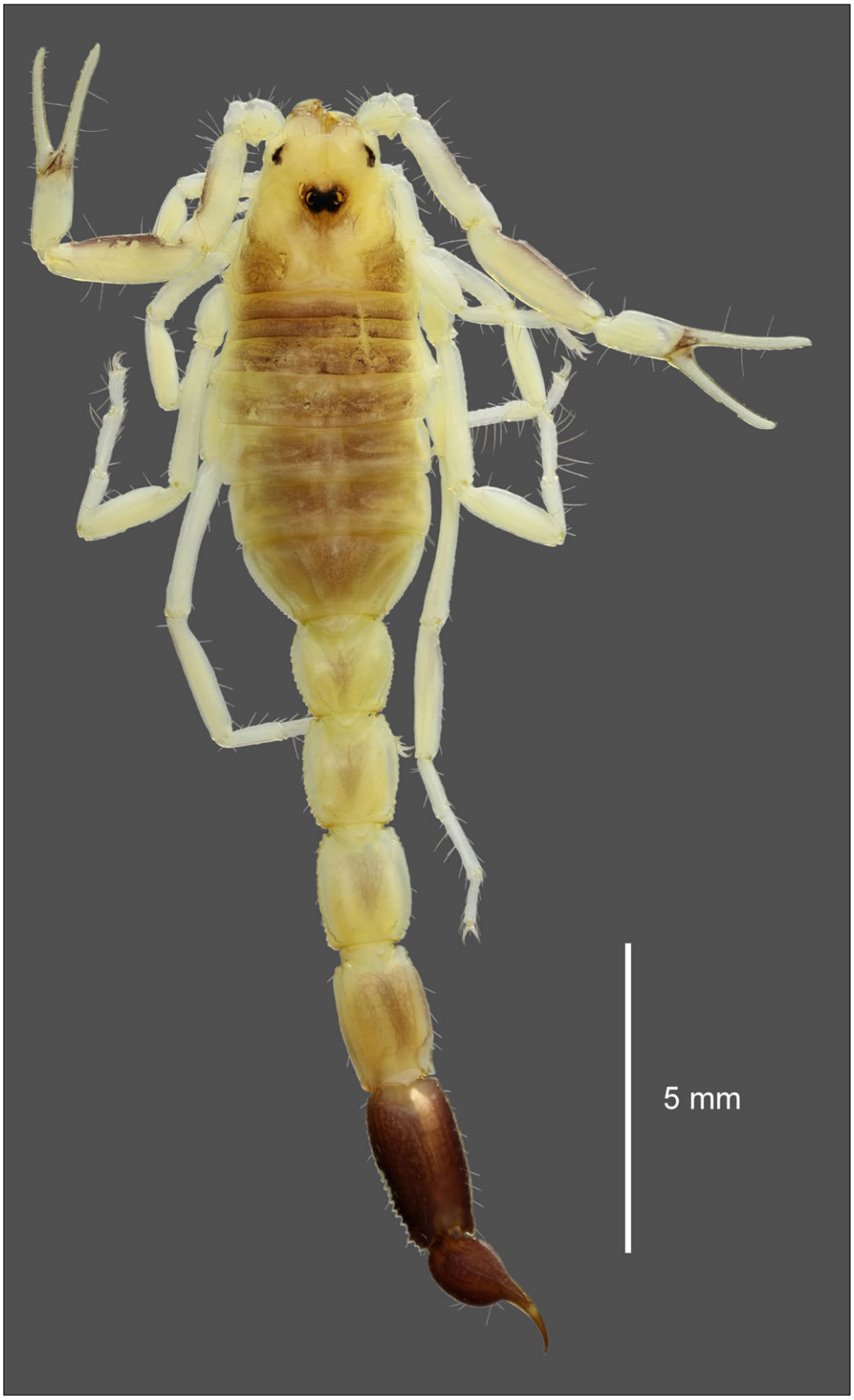

Figures 270: Habitus of juvenile female *Xenobuthus* gen. n. *xanthus* sp. n. Dorsal aspect, showing juvenile color pattern. Oman, east of Jabal Qamr, coastal wadi, 16°53.71'N 53°48.75'E, 28.IX.1995, leg. G. Lowe, M.D. Gallagher. White light illumination. Scale bar: 5 mm.

Figures 271–294: Pedipalp of *Xenobuthus* gen. n. *xanthus* sp. n. **Figs. 271–282.** Holotype male (♂). Dorsal (271–273), external (274–276), ventral (277–279) and internal (280–282) aspect of femur (271, 274, 277, 280), patella (272, 275, 278, 281) and chela (273, 276, 279, 282). **Figs. 283–294.** Paratype female (♀), #2 in Table 7. Dorsal (283–285), external (286–288), ventral (289–291) and internal (292–294) aspect of femur (283, 286, 289, 292), patella (284, 287, 290, 293) and chela (285, 288, 291, 294). Scale bars: 1 mm.

segments moderately robust; *carination*: segment I with 10 complete carinae, II with 10 carinae, 8 complete, lateral median carinae distinct only on posterior 3/4, III with 10 carinae, 8 complete, lateral median carinae distinct only on posterior 1/2, IV with 8 carinae, lateral median carinae absent, V with 3 carinae; most carinae granulate or weakly crenulate; in male, ventrolateral and ventromedian carinae on segment I weakly granular; in females, ventrolateral and ventromedian carinae on segment I smooth, on segment II weakly granular, more smooth anteriorly; ventrolateral carinae on segment V with gradual, slight increase in size of granules posteriorly; segment V with ventromedian carinae composed of linear series of granules, not bifurcating,

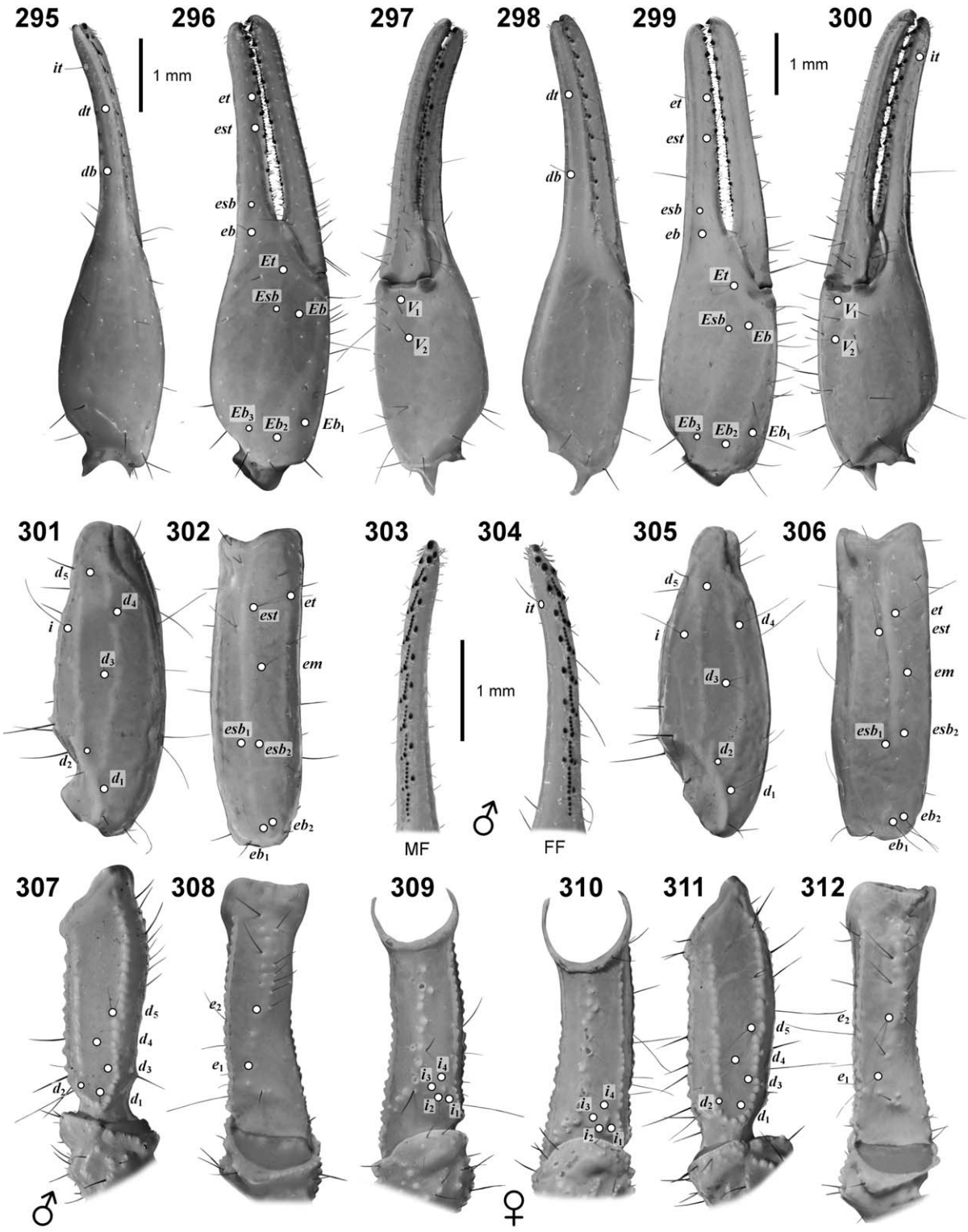

Figures 295–312: Trichobothrial maps and chela finger dentition of *Xenobuthus* gen. n. *xanthus* sp. n. Holotype male (♂): dorsal (295), external (296) and ventrointernal (297) aspect of chela; dorsal (301) and external (302) aspect of patella; dorsal (307), external (308) and internal (309) aspect of femur; dentition of movable finger (MF) (303) and fixed finger (FF) (304). Paratype female (♀), #2 in Table 7: dorsal (298), external (299) and ventrointernal (300) aspect of chela; dorsal (305) and external (306) aspect of patella; internal (310), dorsal (311) and external (312) aspect of femur. Scale bars: 1 mm (♂, ♂ dentition, ♀).

Figures 313–316: Leg tarsi and tibiae of male *Xenobuthus* gen. n. *xanthus* sp. n. Holotype male (♂). Retrolateral aspect, left leg I (313), II (314), III (315), IV (316) tibia, basitarsus and telotarsus. White light illumination. Scale bar: 1 mm.

ventrosubmedian carinae indistinct, positions only indicated by granules; lateral anal margin with 2 blunt granules or lobes, ventral anal margin with 13–20 granules; *intercarinal surfaces*: lateral and ventral aspects of segments I–IV mostly smooth with sparse granulation or isolated granules; dorsolateral and lateral surfaces of segments II–VI weakly rugose; segment V with sparse coarse granulation on ventral surface, smooth on lateral surface, male with posterior 1/4 of ventral surface smooth on either side of ventromedian carina; dorsal surfaces of all segments smooth in male, smooth or weakly rugose in female; *setation*: all segments equipped with scattered long, curved, golden macrosetae on all aspects, most located near or on carinae, setae of similar length in both sexes; metasoma V dorsolateral margins with 15 macrosetae in male, 7–11 in females.

Telson (Figs. 262–263, 266–267, 270, 320–325). Vesicle smooth dorsally and laterally, mostly smooth ventrally except for a few granules at anterior end; small indentations at setal insertion points; bulbous, with steep posterior slope, subaculear tubercle absent, but slight ridge indicates trace of tubercle; several long macrosetae on lateral and ventral surfaces; aculeus slightly shorter than vesicle.

Pedipalps (Figs. 271–312). *Male* (Figs. 271–282, 295–297, 301–304, 307–309). *Femur*: L/W 2.87; dorso-

Figures 317–319: Hemispermatophore capsule region of *Xenobuthus* gen. n. *xanthus* sp. n. Holotype male (♂). Anterior (317), convex (318) and posterior (319) aspects. In convex view (318), the capsule is compressed to show outlines of lobes. White light illumination. Scale bar: 200 µm.

internal, dorsoexternal and ventrointernal carinae strong, with regular coarse granulation; external carina a broad ridge, smooth or with isolated weak granules; internal carina moderate, with coarse granules; intercarinal surfaces smooth; 9–10 accessory macrosetae on distal external surface; *patella*: L/W 2.87; dorsointernal, dorsomedian and external carinae moderate, smooth; dorsoexternal carina weak, smooth; internal carina moderate, weakly granulated; other carinae obsolete, ventromedian and ventroexternal carinae barely visible as smooth traces of thickened integument; intercarinal surfaces smooth; *chela*: slender, L/W 4.26, all carinae obsolete, surface smooth with sparse macrosetae and microsetae; 9 primary denticle subrows on movable fingers, 8 on fixed fingers, total count of non-enlarged primary denticles on movable fingers 43–51 (N = 4 fingers), on fixed fingers 40–52 (N = 3 fingers, 1 malformed finger excluded); denticle subrows except proximal flanked by internal and external accessory denticles, 6–9 internal or external accessory denticles on movable finger, 7–8 on fixed finger. *Female* (Figs. 283–294, 298–300, 305–306, 310–312). *Femur*: slightly more slender than male, L/W 3.00–3.05; carination and surface texture similar to male; 9–11 accessory macrosetae on distal external surface; *patella*: slightly more robust than male, L/W 2.71–2.84; internal carina smooth, other carinae also smooth, as in male; intercarinal surfaces smooth; *chela*: more slender than male, L/W 4.48–4.71, all carinae obsolete, surface smooth with sparse macrosetae and microsetae; 9–10 primary denticle subrows on movable fingers, 8–9 on fixed fingers, total count of non-enlarged primary denticles on movable fingers 47–55 (N = 8 fingers), on fixed fingers 42–52 (N = 8 fingers); 8–9 internal or external accessory denticles on movable fingers, 7–9 on fixed finger. *Trichobothriotaxy*: orthobothriotaxic, type Aβ (Vachon, 1974) (Figs. 295–312).

Legs (Figs. 262–263, 266–267, 313–316). Inferior carinae finely serrate-denticulate on femora, other carinae on femora weakly, finely granulate; prolateral surfaces of femora with sparse fine granulation prox-

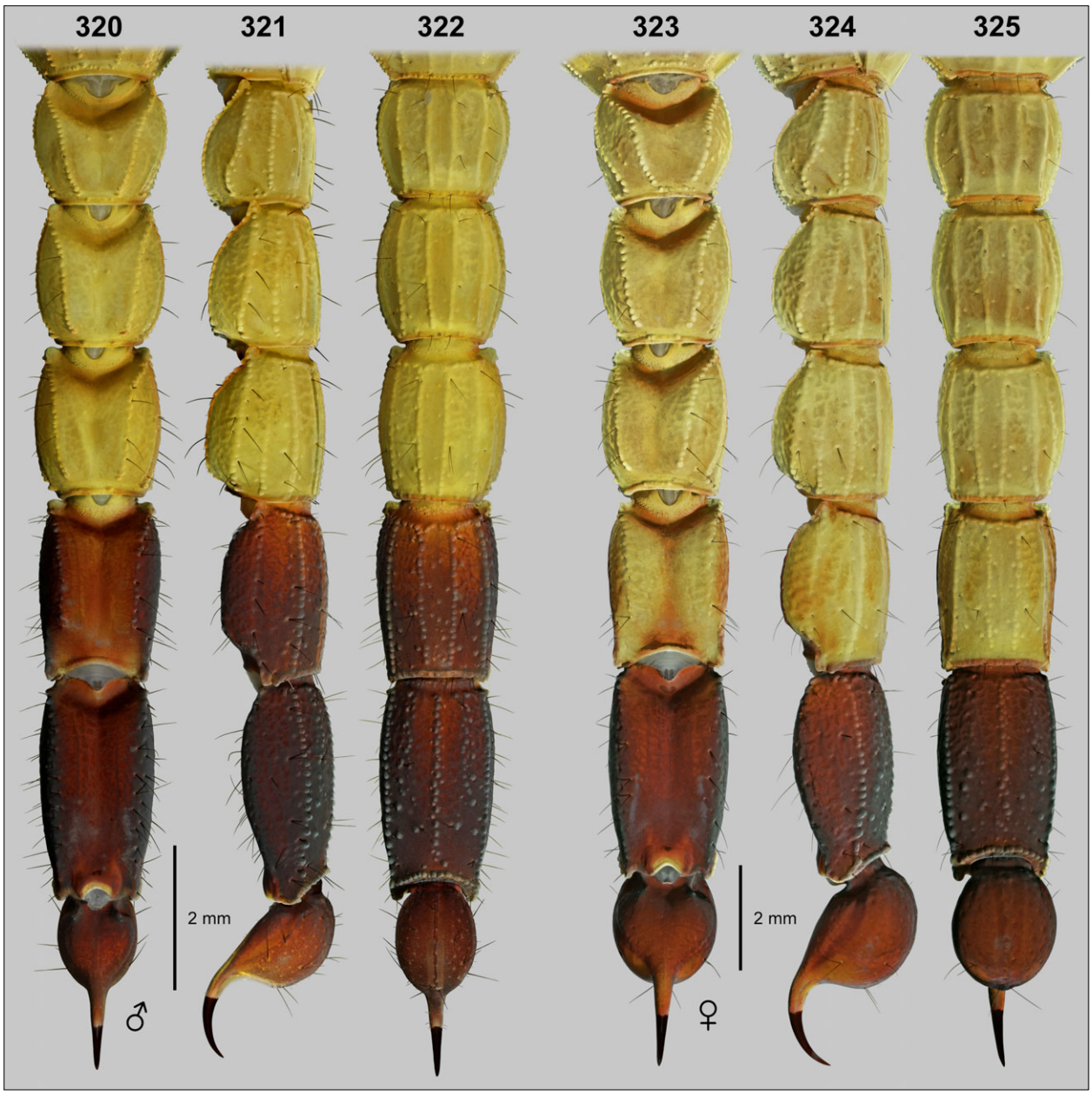

Figures 320–325: Metasoma and telson of *Xenobuthus* gen. n. *xanthus* sp. n. **Figs. 320–322.** Holotype male (♂). Dorsal (320), right lateral (321) and ventral (322) aspects. **Figs. 323–325.** Paratype female (♀), #2 in Table 7. Dorsal (323), right lateral (324) and ventral (325) aspects. Scale bars: 2 mm.

imally, smooth distally, carinae in females becoming indistinct in proximal granular areas; patellae with weakly crenulate-denticulate inferior carinae, other carinae smooth, prolateral surfaces smooth; tibia III–IV with spurs; retrolateral tarsal spurs simple, prolateral tarsal spurs basally bifurcate; basitarsi I/II/III with 7–8/9–12/11–14 long retrosuperior macrosetae arranged in bristle-combs; ventral surface of telotarsi with dual rows of long, fine macrosetae, but dual row condition may often be confined to only basal portion on basitarsi I–III, with single file of setae in distal portion; tarsal ungues moderately long.

Measurements. See Table 7.

Variation. Coloration, morphometric and meristic variation as described above and in Figs. 157–162.

DISTRIBUTION. Known only from Jabal Samhan, Jabal Qara and Jabal Qamr, and adjacent coastal sites in Dhofar Province, Oman.

Measurements (mm)	*Xenobuthus anthracinus* (Pocock, 1895)		*Xenobuthus* gen. n. *xanthus* sp. n.		
	♂	♀	♂ holotype	♀ paratype #1	♀ paratype #2
Total L	36.17	47.80	38.15	39.62	44.75
Metasoma + Telson L	22.20	27.80	24.10	21.86	26.40
Carapace L	4.17	5.27	4.29	4.42	5.21
Carapace anterior W	2.12	2.82	2.12	2.29	2.67
Carapace posterior W	4.54	6.32	5.13	5.08	6.41
Carapace preocular L	1.78	2.38	1.76	1.85	2.41
Metasoma I L/W/D	3.18/ 3.17/ 2.51	3.38/ 4.21/ 3.25	2.93/ 3.17/ 2.58	2.75/ 3.17/ 2.63	3.33/ 3.74 / 3.17
Metasoma II L/W/D	3.23/3.17 /2.59	4.00/ 4.13/3.25	3.46/3.07 /2.67	3.17/ 2.96/ 2.50	3.75/ 3.58/ 3.00
Metasoma III L/W/D	3.50/ 3.21/ 2.58	4.18/ 4.17/ 3.29	3.67/ 3.03/ 2.67	3.29/ 2.92/ 2.50	3.96/ 3.45/ 3.09
Metasoma IV L/W/D	4.08/ 2.96/ 2.42	5.00/ 3.71/ 3.13	4.38/ 2.89/ 2.45	3.83/ 2.85/ 2.38	4.59/ 3.24/ 2.83
Metasoma V L/W/D	4.92/ 2.96/ 2.27	5.93/ 3.71/ 2.92	5.29/ 2.75/ 2.17	4.50/ 2.85/ 2.25	5.67/ 3.25/ 2.64
Telson L	4.58	5.55	4.46	4.71	5.58
Vesicle L/W/D	2.66/ 2.10/ 1.87	3.17/ 2.71/ 2.46	2.54/ 1.94/ 1.78	2.79/ 2.27/ 2.00	3.42/ 2.83/ 2.57
Pedipalp chela L	6.19	7.43	6.08	6.16	7.28
Chela movable finger L	3.79	4.63	3.74	3.75	4.48
Chela fixed finger L	3.00	3.67	2.88	2.92	3.39
Chela manus ventral L/W/D	2.61/ 1.45/ 1.63	2.90/ 1.61/ 1.80	2.57/ 1.43/ 1.57	2.49/ 1.31/ 1.48	2.98/ 1.63/ 1.84
Pedipalp femur L/W	3.33/ 1.10	3.92/ 1.47	3.33/ 1.16	3.42/ 1.14	4.17/ 1.37
Pedipalp patella L/W	4.15/ 1.43	4.85/ 1.88	4.25/ 1.48	4.17/ 1.47	5.01/1.85
Pectine length	3.83	4.33	4.43	3.92	4.58
Pectine teeth (left/ right)	19/ 20	19/ 19	20/ 21	20/19	20/ 18

Table 7: Measurements of adults of *Xenobuthus anthracinus* (Pocock, 1895) and *Xenobuthus* gen. n. *xanthus* sp. n. *X. anthracinus*: male (♂): Oman, S of Thumrait; Nejd Desert, 17°30.77'N 54°2.82' E, 19.X.1993, leg. G. Lowe; female (♀): Oman, S of Thumrait; Nejd Desert, 17°30.76'N 54°2.76' E, 16.X.1993, leg. G. Lowe. *X. xanthus*: holotype male (♂): Oman, Jabal Zulul, 17°57.12'N 55°39.28' E, 26.IX.1995, leg. G. Lowe, M.D. Gallagher; paratype females (♀): #1: Wadi Ara, Jabal Samhan, 17°16'N 54°57'E, 2.II.1994, leg. M.R. Brown; #2, Oman, Wadi Shuwaymiyah, 17°55.94'N 55°31.47'E, 25.IX.1995, leg. G. Lowe, M.D. Gallagher. Abbreviations: L, length; W, width, D depth.

ECOLOGY. It has a preference for mesic habitats, being found in sandy wadis and rocky slopes with vegetation and moisture. Specimens taken by day were sheltering under rocks. The yellow color of the body would blend well with lighter substrates where it was collected, while the dark brown/ black posterior metasoma and telson would stand out in contrast. Similar bicolored patterns seem to have evolved independently in various other buthids (e.g. *Buthacus nigroaculeatus*, *Centruroides bicolor*, *Leiurus* spp., *Hottentotta salei*, *H. saulcyi*, etc.), and may be adaptive in leading visually guided vertebrate predators of scorpions away from the more vulnerable mesosoma, and towards the venom-wielding telson which can deliver mammal-specific defensive toxins. Recorded elevation range was 15–1,050 m. Scorpions that occurred together with *X. xanthus* were: *Butheolus harrisoni* **sp. n.**, *Compsobuthus acutecarinatus* (Simon, 1882), *Hottentotta salei* (Vachon, 1980), *Leiurus haenggii* Lowe et al., 2014, *Microbuthus kristensenorum* Lowe, 2010, and *Nebo whitei* Vachon, 1980.

Key to species of *Butheolus* and *Xenobuthus* gen. n. examined in this study (based on adults)

1 Small to medium sized scorpions, 35–50 mm long; metasomal segments sparsely granular on lateral and ventral sides; basal lobe of hemispermatophore a broad, shallow, curved scoop; pedipalp fingers with 8–10 sub-

rows of denticles; males with macrosetae similar in length to those of females; soles of telotarsi I–III often with single row of setae ..…..... *Xenobuthus* **gen. n.** 5
– Small scorpions, < 36 mm long; metasomal segments densely granular on lateral and ventral sides; basal lobe of hemispermatophore a small, narrow, hook-like process; pedipalp fingers typically with 6–7 subrows of denticles; males with shorter macrosetae than females; soles of telotarsi I–III bearing two rows of setae .....……..... *Butheolus* Simon, 1882 2

2 Pedipalp patella L/W < 2.3, chela manus strongly carinate; telson with large subaculear tubercle, posterior vesicle slope forming acute angle with aculeus base ...……..... *Butheolus thalassinus* Simon, 1882
– Pedipalp patella L/W > 2.3, chela manus smooth or with very weak carinae; telson with subaculear tubercle small or indistinct, posterior vesicle slope forming obtuse angle with aculeus base ...……..... 3

3 Metasoma and telson densely pilose, with abundant macrosetae; basitarsus III with 11–12 retrosuperior setae (bristle-comb) ..... *B. villosus* Hendrixson, 2006
– Metasoma and telson with sparse setation; basitarsus III with 4–10 retrosuperior setae (bristle-comb) …. 4

4 Carapace and tergites coarsely granulated; color of metasoma I–II yellow to light brown; pedipalp patella with complete dorsomedian carina .... *B. harrisoni* **sp. n**.
– Carapace and tergites finely granulated; color of metasoma I–II dark brown; pedipalp patella with dorsomedian carina restricted to distal half of segment .....……..... *B. gallagheri* Vachon, 1980

5 Carapace, mesosoma and metasoma I–III dark brown to black; metasoma IV with 10 carinae, lateral median carinae distinct; ventromedian carina of metasoma V bifurcate; metasoma V in males with ventral intercarinal surface granulated posteriorly .....…..... ……..…… *Xenobuthus anthracinus* (Pocock, 1985)
– Carapace, mesosoma and metasoma I–III bright yellow; metasoma IV with 8 carinae, lateral median carinae obsolete; ventromedian carina of metasoma V not bifurcate; metasoma V in males with ventral intercarinal surface smooth posteriorly .... *Xenobuthus xanthus* **sp. n.**

The above key omits two species, *Butheolus arabicus* Lourenço & Qi, 2006, and *B. hallani* Lourenço & Rossi, 2017 (= *B. pallidus* Lourenço & Duhem, 2012), because the author was not able to loan and examine the types of these two species.

From the published description, and the habitus shown in images on the MNHN website, *B. arabicus* does not fit the diagnosis of *Butheolus* given here. Instead, it complies with certain characters of *Xenobuthus* **gen. n.**: i.e., **1)** large size and general proportion and shape of body and appendages resemble *X. anthracinus* and *X. xanthus*; **2)** 8–9 denticle subrows on pedipalp chela fingers. It is hereby provisionally transferred to that genus: *Butheolus arabicus* Lourenço & Qi, 2006 = *Xenobuthus arabicus* (Lourenço & Qi, 2006) **comb. n.**.

The type locality "East of Khamis Mushayt" suggests the possibility that *X. arabicus* is a junior synonym of *X. anthracinus*, since the latter is also known from Khamis Mushayt (by the AMNH female, examined here and by Hendrixson, 2006). Lourenço & Qi (2006) distinguished *X. arabicus* from *X. anthracinus* as follows:

1) "much larger overall size", i.e. paratype female 40.4 mm vs. 25.3 mm length of a female *X. anthracinus* (cf. their Tab. 1, cited as a 'paratype'): this character is not applicable because: **(i)** adult female *X. anthracinus* can be up to 40–50 mm long (Figs. 198–199, Tab. 7), and the AMNH female is ca. 35 mm long (Hendrixson, 2006). The female studied by Lourenço & Qi (2006) is the same size as the lectotype female (♀ 25 mm, photograph examined) of *X. anthracinus* in ZMUH designated by Kovařík (2004), and is thus likely to be immature or juvenile. It is not a paratype, but either a paralectotype, or possibly the lectotype itself. **(ii)** the holotype male of *X. arabicus* (total L 35.6 mm, carapace L 4.7 mm) is about the same size as the holotype male of *X. anthracinus* (total L 36.5 mm, carapace L 4.4 mm, cf. Pocock, 1895: 295).

2) "strongly marked" (= strongly developed) carinae on tergite VII and metasoma, and granulation of carapace tergites and coxapophysis: this character may not be applicable because adult *X. anthracinus* also have strong carination on tergite VII and metasoma, and strong granulation on carapace, tergites and coxal endites I–II (= coxapophyses) (Figs. 194–201, 252–257). The carination and granulation may not be fully developed in the probably immature or juvenile female used for comparison by Lourenço & Qi (2006).

3) "metasomal segments I to III with 10 carinae in both sexes": this character is not applicable because adult *X. anthracinus* can also have 10 carinae on metasoma I–III in both sexes (Figs. 252–257). Either this character is variable, or the carination is not fully developed in the probably immature or juvenile female used for comparison by Lourenço & Qi (2006).

Another potential difference is in coloration, as the base color of *X. arabicus* was described as "yellow to reddish-yellow", consistent with color photographs of the holotype posted on the MNHN website, which contrasts with the dark reddish-brown to black color of *X. anthracinus*. However, biological pigments can suffer fading or wash out after long storage in alcohol, and coloration is not a very reliable character in old specimens that were not fixed by specific methods that preserve coloration, e.g. heat shock and aldehyde fixation (Williams, 1968). The problem was well dem-

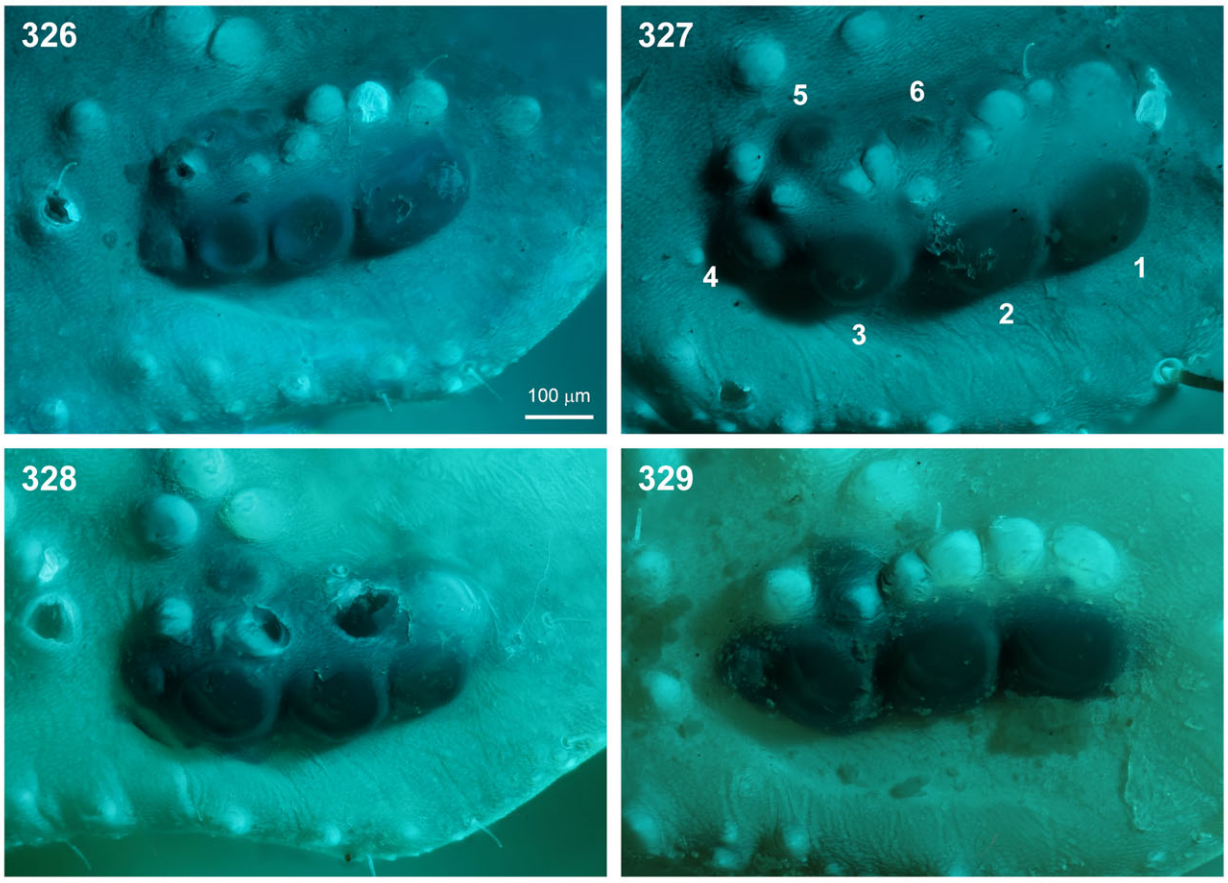

Figures 326–329: Right lateral eye clusters of *Xenobuthus* gen. n. **Figs. 326–327.** *X. anthracinus*, adult male (326) and adult female (327). **Figs. 328–329.** *X. xanthus* sp. n., adult male (328) and adult female (329). Locality data as in Tab. 7. UV fluorescence. Scale bar: 100 µm, for all panels.

onstrated by the holotype of *Butheolus gallagheri* (also in MNHN), that was loaned and examined by the author in 1994, only 14 years after its description by Vachon (1980) as "brun chocolat" (= dark brown natural color, exhibited by live animals and by the aldehyde-fixed materials studied here). By 1994, the holotype had already faded to a pale yellow color on the carapace and tergites, and a pale orange brown color on the metasoma, and the base of the pedipalp fingers had lost the diagnostic melanic pigmentation that was noted by Vachon (1980). The holotype of *X. arabicus* was presumably stored much longer in alcohol (34 years) before it was described.

Although *X. arabicus* and *X. anthracinus* seem similar and were both collected in the vicinity of Khamis Mushayt, they could nevertheless be distinct species. In Dhofar, Oman, similar but distinct species of *Butheolus* and *Xenobuthus* exist in relatively close proximity. Lourenço & Qi (2006) noted that *X. arabicus* only bears 8 carinae on metasoma IV, which is a diagnostic character separating *X. xanthus* from *X. anthracinus*. The question might be addressed by restudying the types of *X. arabicus*, or by further sampling the *Xenobuthus* populations in the region of Khamis Mushayt.

The taxonomic status of *B. hallani*, based on a single holotype male from the United Arab Emirates or adjacent Oman, is also uncertain. It is not clear from the published description, and the general habitus shown in images posted on the MNHN website (reproduced in Lourenço & Rossi, 2017), whether it fits the diagnosis of *Butheolus* given here. In their description, Lourenço & Duhem (2012) noted:

1) "posterior margin of sternites III to VI without denticulations": however, such denticulations are proposed to be diagnostic for both *Butheolus* and *Xenobuthus* (Figs. 332–335), and were present and in all species examined here. Although the sternite denticulations are weaker and may be overlooked in females, they are conspicuous in males, and the holotype of *B. hallani* is male.

2) metasoma V with "lateroventral carinae with a few slightly spinoid granules in the distal region": their Fig. 4 depicts an irregularly dentate posterior carina with two enlarged denticles that are considerably larger than

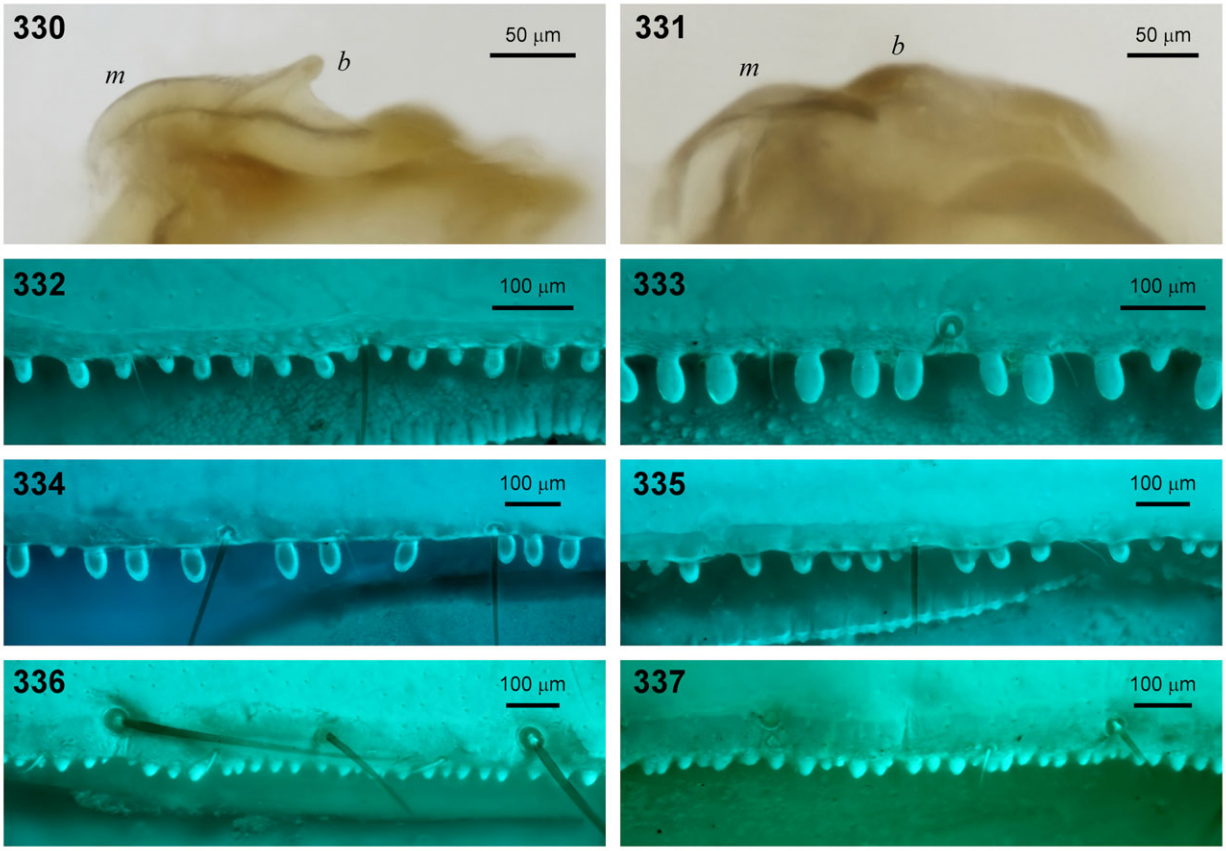

Figures 330–337: Diagnostic characters of genera *Butheolus* and *Xenobuthus* gen. n.. **Figs. 330–331.** Hemispermatophore basal lobes of *B. gallagheri* (330) and *X. anthracinus* (331); axial views of right (330) and mirrored left (331) hemispermatophore. Oriented with convex side up, anterior margin left and posterior margin right. Abbreviations: *b*, basal lobe; *m*, median lobe. Scale bars: 50 µm. **Figs. 332–337.** Dentition of posterior margin of sternite IV in male *B. gallagheri* (332), *B. harrisoni* sp. n. (333), *X. anthracinus* (334), *X. xanthus* sp. n. (335), *Hottentotta jayakari* (Pocock, 1895) (336) and *H. pellucidus* Lowe, 2010 (337). UV fluorescence. Scale bars: 100 µm. Locality data: 330 and 332, as in Tab. 1; 331 and 334, as in Tab. 7; 333, paratype male, same locality as holotype; 335, holotype; 336, Oman, Rte 13, ca. 5.9 km E junction Wadi Mistal Rd, 23°21.33'N 57°38.21'E, 460 m a.s.l., 26.IX.1994, leg. G, Lowe, M.D. Gallagher; 337, Oman, Jabal Bani Jabir, IX.1995, 1800 m a.s.l., leg A. Francois, C. DeLise (ONHM).

the anterior dentition, a pattern that differs from that seen in *Butheolus* and *Xenobuthus*, which have numerous regular denticles gradually increasing in size posteriorly.

These characters, together with the small body size (18 mm), and presence of only 5–6 subrows of denticles on the pedipalp fingers, are more suggestive of *Neobuthus*, than *Butheolus* (Kovařík & Lowe, 2012; Lourenço, 2001, 2005; Lourenço & Qi, 2006; Lowe & Kovařík, 2016). Other key taxonomic characters that could be relevant to its generic affiliation (e.g. position of trichobothrium V_2 on pedipalp manus, number of denticles on ventral aspect of cheliceral fixed finger) have yet to be specified. In any case, the presence of either *Butheolus* or *Neobuthus* in the southeastern corner of the Arabian Peninsula would be a significant range extension for either genus.

Discussion

In his description, Pocock (1895) remarked that *Buthus anthracinus* was most similar to *Butheolus thalassinus*, and Simon (1910) surmised that it may belong to *Butheolus*. On the other hand, in his key Kraepelin (1899) grouped *B. anthracinus* together with *Buthus* species that are now placed in the genus *Hottentotta*, and Birula (1910, 1917a, 1937) suggested in his listings that it might be a member of that genus. That position was also taken by Vachon, according to Lamoral and Reynders (1975), and echoed by Sissom (1994). However, *Buthus anthracinus* differs from *Hottentotta* as follows: **1)** chela trichobothrium *db* positioned proximally on fixed finger, between *esb* and *est* (vs. distal to *est* in many *Hottentotta*, cf. Kovařík, 2007); **2)** chela trichobothrium *eb* positioned on distal

manus (vs. on proximal fixed finger); **3)** 8–10 subrows of primary denticles on pedipalp fingers (vs. 11–16); **4)** basal lobe of hemispermatophore a broad, curved scoop (vs. a small pointed knob or projecting hook, cf. *Hottentotta* basal lobes illustrated in: Lamoral, 1979: 548, fig. 62; Levy & Amitai, 1980: 57, fig. 56; Lowe, 2010b: 6, 13, figs. 17–18, 43–44; Vachon, 1952: 236, fig. 329; Vachon, 1958: 132, fig.13; Vachon & Stockmann, 1968: 87, figs. 5, 7–9); **5)** sternite III–VI posterior margins with fringe of larger non-contiguous, digitate denticles (Figs. 332–335) (vs. smaller, closely spaced, subtriangular denticles in *Hottentotta*, e.g. Figs. 336–337); and **6)** carapace without distinct carinae (vs. strongly carinate).

Buthus anthracinus shares some special features with *Butheolus* that are not found in most other buthids, and hence are potential synapomorphies: **1)** sternite III–VI posterior margins bearing a characteristic fringe of non-contiguous, digitate denticles (Figs. 332–335); **2)** males with prominent peg-like granules on coxae, carapace and tergites; **3)** trapezoidal carapace; **4)** interocular triangle sloped down towards anterior margin of carapace (although not as steeply as in *Butheolus*). These similarities suggest a closer affinity with *Butheolus*, leading Fet & Lowe (2000) to provisionally list *B. anthracinus* under that genus. Here, it is proposed that *B. anthracinus* be moved to its own separate genus *Xenobuthus* **gen. n.**, which also includes *X. xanthus* **sp. n.**, based on the following distinctions from *Butheolus*: **1)** larger size; **2)** more denticle subrows on pedipalp fingers (correlated with character **1**); **3)** lack of dense granulation on metasoma; **4)** lack of sexually dimorphic setation; **5)** pedipalp chela more robust (vs. more slender) in male than female; and **6)** hemispermatophore basal lobe a low, broad, curved scoop (Figs. 248–250, 317–319, 331), differing from the narrow, hook-like structure in *Butheolus* (Figs. 56–58, 124–126, 330). Characters **1–5** are likely to be plesiomorphic states, indicating that *Butheolus* is the more specialized genus. Character **6** could be an autapomorphy for *Xenobuthus*, as this form of basal lobe has not been described in any other member of the *Buthus* group (Fet et al., 2005), the main Palaearctic buthid clade defined by trichobothriotaxy that includes both *Butheolus* and *Xenobuthus*. A low, broad, scoop-like basal lobe was reported in some species of the unrelated genus *Babycurus* (in the *Isometrus* group) (Kovařík et al., 2015: 22, fig. 101; Lowe, 2000: 187, fig. 2), but with a more transverse orientation nearly orthogonal to the median lobe carina, as opposed to the more axial orientation aligned with the median lobe carina in *Xenobuthus*. An alternative hypothesis is to reverse the polarity of this character and assume that the scoop-like lobe is primitive, and the hook-like lobe is derived. In axial view (Fig. 331), the *Xenobuthus* scoop seems to arise as a fin-like, expanded carina along the basal portion of the median lobe. In *Butheolus*, a similar carina can be seen (Fig. 330), but it also has a prominent hook-like basal lobe along its edge. Thus, the *Butheolus* hook could be derived from the simpler scoop by extending a long, narrow process from its margin. As previously noted, the form of the basal lobe is potentially useful for the taxonomy of buthids at the genus level (Kovařík et al., 2016a, 2016b, 2018). A primitive scoop suggests that *Xenobuthus* may occupy a more basal position in the phylogeny of the *Buthus* group.

Xenobuthus xanthus **sp. n.** is quite similar to *X. anthracinus* in size and proportions, but contrasts strikingly in its bright yellow coloration and black tail. It was decided to place it in a separate species rather than regard it as merely a color variant of *X. anthracinus*. Populations with patterns of coloration intermediate between the two species are unknown, and *X. xanthus* exhibits morphometric as well as key structural differences: i.e., metasoma IV lacking the lateral median carina, metasoma V with non-bifurcate ventromedian carina, posteriorly smooth in males. It occurs in mesic environments in the tropical fog oasis region of the coastal plain and mountains of Dhofar (Fig. 338). *X. xanthus* appears to be part of the endemic fauna of the lush monsoon woodlands that flourish on south-facing escarpments in Dhofar and neighboring Yemen. In contrast, *X. anthracinus* was collected further inland on the arid plateau of the Nejd Desert in Dhofar. The five syntypes of *Buthus anthracinus* described by Pocock had imprecise localities in the Hadramaut of Yemen, but could have come from similar habitats. The itinerary of the Hadramaut expedition (XII.1893–III.1894) of British explorers Theodore and Mabel Bent, that collected the specimens, traversed arid wadi systems along the inland plateau at elevations similar to the Nejd Desert locality (Bent, 1895).

An interesting difference between *X. xanthus* and *X. anthracinus* was the presence of six pairs of lateral eyes in the latter species (Figs. 326–327), compared to only five pairs in *X. xanthus* (Figs. 328–329). The five pair configuration (also found in *Butheolus gallagheri*, *B. harrisoni*, *B. thalassinus* and *B. villosus*) is consistent with the 'five-eye' buthid model of Yang et al. (2013), and the 'Type 5' pattern of Loria & Prendini (2014). The six-eye pattern in *X. anthracinus* is unusual in that five pairs was the maximum number found in buthids by Loria & Prendini (2014) in 60 surveyed species, and by Yang et al. (2013) in 77 surveyed species. Loria & Prendini (2014) proposed a six-ocellus model for scorpion lateral eyes, but the basic patterns expressed in various taxa all had five or fewer ocelli. They reported a higher count (7 pairs) only in individual *Opistophthalmus jenseni* (Scorpionidae), which they regarded as an abnormal condition. The six ocelli in *X. anthracinus* were detected by UV fluorescence, and include a lower row of three major ocelli plus one minor ocellus at the

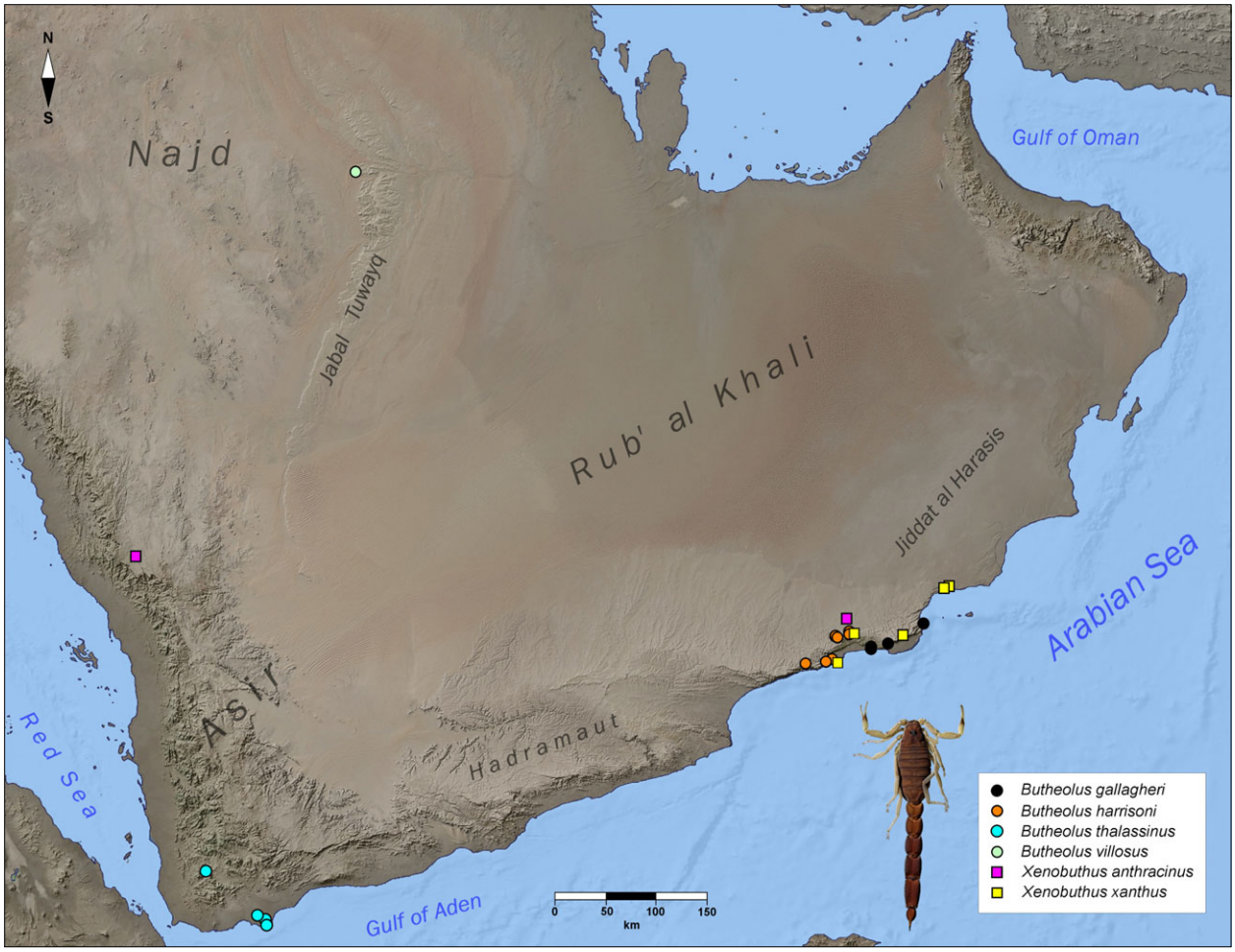

Figure 338. Map of records in the Arabian Peninsula of *Butheolus* and *Xenobuthus* gen. n. Symbols show locations of collection records of species examined in this study. *B. gallagheri*: black circles; *B. harrisoni*: orange circles; *B. thalassinus*: cyan circles; *B. villosus*: light green circle; *X. anthracinus*: magenta squares; *X. xanthus*: yellow squares. Locality data are from specimens examined, except for the type locality and two additional published records of *B. thalassinus*. The indefinite type locality of *X. anthracinus* (Hadramaut "by the way"; Pocock, 1895) is not plotted. Map scale: 150 km.

posterior end, situated below a row of granules, and an upper row of two minor ocelli above the row of granules (Figs. 326–327). The sixth ocellus is not a worn or truncated granule, because these appear very different under UV fluorescence, i.e. as black cavities lacking fluorescent exocuticle (Figs. 326, 328). It was present on the right side in the male (eye count on left side unclear due to abrasion damage) and bilaterally in the female *X. anthracinus* examined here. Its homology under the model of Loria & Prendini (2014) is unclear. Referring to the number labels in Fig. 329, in their 'Type 5' buthid pattern the three major lower ocelli (1–3) would correspond to ALMa, MLMa and PLMa respectively, and the lower minor ocellus (4) to PDMi in a lower position, since the lower minor ocellus PLMi is hypothesized to be lost in buthids. This leaves only ADMi as an upper minor ocellus, to account for two minor ocelli (5 and 6). The upper position of the sixth eye does not match any of the four accessory ocelli of Loria & Prendini (2014). Either it is a supernumerary ocellus not accounted for in their model, or ocelli 5 and 6 are homologous to PDMi and ADMi, and ocellus 4 to PLMi. The latter scheme is inconsistent with derivation of buthid patterns from the six-ocellus model by loss of PLMi. The peculiar six-eye condition was not included here in the diagnosis of *X. anthracinus* due to the small sample size (N = 2 specimens examined from Dhofar), leaving open the possibility that it is an anomaly that may not occur in other individuals or populations of this species. For example, Yang et al. (2013) reported six lateral eyes bilaterally in 1 individual out of 12 *Mesobuthus eupeus mongolicus*, and unilaterally in 1 out

of 21 *M. caucasicus intermedius*, the latter with a different configuration than that seen here (i.e., 5 lower ocelli, 1 upper).

Acknowledgments

The author sincerely thanks many curators and individuals for loans of study materials: Ambros Hänggi, Naturhistorisches Museum, Basel, for loan #NMB20 12/020 of the holotype of *Butheolus villosus*; Jacqueline Heurtault, Muséum National d'Histoire Naturelle, Paris, for loan #94-2 of the holotype of *B. gallagheri*; Paul Hillyard, Natural History Museum, London, for loan #5798 of female *B. thalassinus*; W. David Sissom, Texas, for loan of male *B. thalassinus*; Jan Beccaloni, Natural History Museum, London, for searching for types of *Buthus anthracinus*; Norman Platnick, American Museum of Natural History, New York, for loan of a female *Xenobuthus anthracinus*. Acknowledgments are also owed to many collectors who generously contributed Oman scorpion material over the years, including: J. Dundon, S.M. Farook, M. Fisher, A.S. Gardner, I.D., R & S. Harrison, A. & B. Winkler and A. Ullrich. Thanks to Frantisek Kovařík, Prague, for sharing photographs of the female lectotype and a male of *Xenobuthus anthracinus*. This work is a continuation of systematic studies of scorpions of Oman stemming from fieldwork originally sponsored in 1993–1995 by H.H. The Minister of National Heritage and Culture, Sultanate of Oman, with support from Khair Bin Antar Salim (Director of Museums), Said Ali Said Al-Farsi and Saddiqa Rhamdan at the Ministry of National Heritage and Culture. This study would not have been possible without the enthusiastic support of the late Michael D. Gallagher, friend, mentor and former curator of the Oman Natural History Museum. Lastly, the author thanks two anonymous reviewers for their comments.

References

ACOSTA L.E., CANDIDO D.M., BUCKUP E.H. & BRESCOVIT A.D. 2008. Description of *Zabius gaucho* (Scorpiones, Buthidae); a new species from southern Brazil, with an update of the generic diagnosis. *Journal of Arachnology*, 36 (3): 491–501.

BENT, T. 1895. Expedition to the Hadramut. *Geographical Journal*, 4 (4), 315–331.

BIRULA, A. A. 1898. Miscellanea scorpiologica. III. Zur Synonymie der russischen Skorpione (Forsetzung). *Annuaire du Musee Zoologique de I' Academie Imperiale des Sciences de St.-Petersbourg*, 3: 295–299.

BIRULA, A. 1910. Ueber *Scorpio maurus* Linné und seine Unterarten. *Horae Societatis Entomologicae Rossicae, St Petersburg*, 39: 115–192.

BIRULA, A. A. 1917a. Arachnoidea Arthrogastra Caucasica. Pars I. Scorpiones. *Zapiski Kavkazskogo Muzeya (Mémoires du Musée du Caucase)*, Tiflis, Imprimerie de la Chancellerie du Comité pour la Transcaucasie. ser A, 5, 253 pp. (in Russian; published August 1917). English translation: Byalynitskii-Birulya, A. A. 1964. *Arthrogastric Arachnids of Caucasia. 1. Scorpions.* Israel Program for Scientific Translations, Jerusalem, 170 pp.

BIRULA, A. A. 1917b. *Faune de la Russie et des pays Limitrophes Fondee Principalement sur les Collections du Musée Zoologique de l'Académie des Sciences de Russie. Arachnides (Arachnoidea),* 1(1): xx+227 pp. (in Russian; preface dated October 1917). English translation: Byalynitskii-Birulya, A. A. 1965. *Fauna of Russia and Adjacent Countries. Arachnoidea. Vol. I. Scorpions.* Israel Program for Scientific Translations, Jerusalem, xix, 154 pp.

BIRULA, A. A. 1937. Notes sur les collections des scorpions recuellis dans le Jemen (Arabie S.E.). *Archives du Musée Zoologique de le Université de Moscou*, 4: 101–110. (in Russian).

BORELLI, A. 1915. Gli scorpioni del Museo Civico di Storia Naturale di Milano. *Atti della Societia Italiana di Scienze Naturali e del museo Civico di Storia Natural in Milano. Societia Italiana di Scienze Naturali*, 53: 456–464.

DUPRÉ, G. 2007. Conspectus genericus scorpionorum 1758–2006 (Arachnida: Scorpiones). *Euscorpius*, 50: 1–31.

EL-HENNAWY, H.K. 1992. A catalogue of the scorpions described from the Arab Countries (1758-1990) (Arachnida: Scorpionida). *Serket*, 2 (4): 95–153.

EL-HENNAWY, H.K. 2009. Scorpions of Saudi Arabia. *Serket* 11 (3/4): 119–128.

EL-HENNAWY, H.K. 2014. Preliminary list of spiders and other arachnids of Saudi Arabia (Except ticks and mites). *Serket* 14 (1): 22–58.

FET, V. & G. LOWE. 2000. Family Buthidae. Pp. 54–286 *in* FET, V., W.D. SISSOM, G. LOWE & M.E. BRAUNWALDER. *Catalog of the Scorpions of the World* (1758-1998). The New York Entomological Society.

FET, V. & M.E. SOLEGLAD. 2005. Contributions to Scorpion Systematics. I. On recent changes in high-level taxonomy. *Euscorpius*, 31: 1–13.

FET, V., M.E. SOLEGLAD & G. LOWE. 2005. A new trichobothrial character for the high-level systematics of Buthoidea (Scorpiones: Buthida). *Euscorpius*, 23: 1–40.

FRANCKE, O. F. 1985. Conspectus genericus scorpionorum 1758-1982 (Arachnida: Scorpiones). *Occasional Papers of the Museum, Texas Tech University*, 98: 1–32.

HARADON, R.M. 1984. New and redefined species belonging to the *Paruroctonus baergi* group (Scorpiones, Vaejovidae). *Journal of Arachnology*, 12: 205–221.

HENDRIXSON, B.E. 2006. Buthid scorpions of Saudi Arabia, with notes on other families (Scorpiones: Buthidae, Liochelidae, Scorpionidae). *Fauna of Arabia*, 21: 33–120.

HIRST, S., 1911. Descriptions of new scorpions. *Annals and Magazine of Natural History*, ser.8, 7: 462–473.

KAMENZ, C. & L. PRENDINI. 2008. An atlas of book lung fine structure in the order Scorpiones (Arachnida). *Bulletin of the American Museum of Natural History*, 316: 1–360.

KARSCH, F. 1886. Skorpionologische Beitrage (I. Uebereinen sizilianischen Skorpion.–II. Uebersicht der Gruppe Buthina (Androctonina).–III. Ueber einen neuen *Opisthacanthus* (Peters) Thor). *Berliner Entomologische Zeitschrift*, 30 (1): 75–79.

KÄSTNER, A. 1941. 1. Ordnung der Arachnida: Scorpiones. In: Krumbach, T. (Ed.). *Handbuch der Zoologie*, Walter de Gruyter Verlag, Berlin, 3(1): 117–240.

KOVAŘÍK, F. 1996. *Baloorthochirus becvari* gen. et sp. n. from Pakistan, and taxonomic position of *Orthochirus luteipes* (Scorpiones: Buthidae). *Acta Societatis Zoologicae Bohemicae*, 60: 177–181.

KOVAŘÍK, F. 1998a. Three new genera and species of Scorpiones (Buthidae) from Somalia. *Acta Societatis Zoologicae Bohemicae*, 62: 115–124.

KOVAŘÍK, F. 1998b. *Štírí*. Madagaskar, Jihlava, 175 pp.

KOVARÍK, F. 2003. Scorpions of Djibouti, Eritrea, Ethiopia, and Somalia (Arachnida: Scorpiones), with a key and descriptions of three new species. *Acta Societatis Zoologicae Bohemicae*, 67: 133–159.

KOVAŘÍK, F. 2004. Revision and taxonomic position of genera *Afghanorthochirus* Lourenço & Vachon, *Baloorthochirus* Kovařík, *Butheolus* Simon, *Nanobuthus* Pocock, *Orthochiroides* Kovařík, *Pakistanorthochirus* Lourenço, and Asian *Orthochirus* Karsch, with descriptions of twelve new species (Scorpiones, Buthidae). *Euscorpius*, 16: 1–33.

KOVARÍK, F. 2007. A revision of the genus *Hottentotta* Birula, 1908, with descriptions of four new species (Scorpiones, Buthidae). *Euscorpius*, 58: 1–107.

KOVAŘÍK, F. 2009. Illustrated catalog of scorpions. Part I. Jakub Rolćík – Clairon Production, Prague, 170 pp.

KOVAŘÍK, F. & G. LOWE. 2012. Review of the genus *Neobuthus* Hirst, 1911 with description of a new species from Ethiopia (Scorpiones: Buthidae). *Euscorpius*, 139: 1–25.

KOVAŘÍK, F., G. LOWE, P. JUST, A.I. AWALE, A.S.A. ELMI & F. ŠŤÁHLAVSKÝ. 2018. Scorpions of the Horn of Africa (Arachnida: Scorpiones). Part XV. Review of the genus *Gint* Kovařík et al., 2013, with description of three new species from Somaliland (Scorpiones, Buthidae). *Euscorpius*, 259: 1–41.

KOVAŘÍK, F., G. LOWE, J. PLÍŠKOVÁ & F. ŠŤÁHLAVSKÝ. 2013. A new scorpion genus, *Gint* gen. n., from the Horn of Africa (Scorpiones, Buthidae). *Euscorpius*, 173: 1–19.

KOVAŘÍK, F., G. LOWE, J. PLÍŠKOVÁ & F. ŠŤÁHLAVSKÝ. 2016a. Scorpions of the Horn of Africa (Arachnida: Scorpiones). Part VI. *Compsobuthus* Vachon, 1949 (Buthidae), with a description of *C. eritreaensis* sp. n. *Euscorpius*, 226: 1–21.

KOVAŘÍK, F., G. LOWE, K.B. RANAWANA, D. HOFEREK, V. A. SANJEEWA JAYARATHNE, J. PLÍŠKOVÁ & F. ŠŤÁHLAVSKÝ. 2016b. Scorpions of Sri Lanka (Arachnida, Scorpiones: Buthidae, Chaerilidae, Scorpionidae) with description of four new species of the genera *Charmus* Karsch, 1879 and *Reddyanus* Vachon, 1972 stat. n. *Euscorpius*, 220: 1–133.

KOVAŘÍK, F., G. LOWE, M. SEITER, J. PLÍŠKOVÁ & F. ŠŤÁHLAVSKÝ. 2015. Scorpions of Ethiopia (Arachnida: Scorpiones). Part II. Genus *Babycurus* Karsch, 1886 (Buthidae), with description of two new species. *Euscorpius*, 196: 1–31.

KRAEPELIN, K. 1891. Revision der Scorpione. I. Die Familie der Androctonidae. *Jahrbuch der Hamburgischen Wissenschaftlichen Anstalten Hamburg* 8: 1–144.

KRAEPELIN, K. 1895. Nachtrag zu Theil I der Revision der Scorpione. *Beiheft zum Jahrbuch der Hamburgischen Wissenschaftlichen Anstalten*, 12: 1–24.

KRAEPELIN, K. 1899. Scorpiones und Pedipalpi. In: *Das Tierreich, R. Friedländer und Sohn Verl Berlin*, 8: 1–265.

KRAEPELIN, K. 1903. Scorpione und Solifugen Nordost-Afrikas, gesammelt 1900 und 1901 von Carlo Freiherrn von Erlanger und Oscar Neumann. *Zoologische Jahrbücher, Abtheilung für Systematik* 18: 557–578.

KRAEPELIN, K. 1905. Die geographische Verbreitung der Skorpione. *Zoologische Jahrbücher, Abtheilung für Systematik*, 22(3): 321–364.

LAMORAL, B. H. 1979. The scorpions of Namibia (Arachnida: Scorpionida). *Annals of the Natal Museum*, 23 (3): 497–784.

LAMORAL, B. H. & S. C. REYNDERS. 1975. A catalogue of the scorpions described from the Ethiopian faunal region up to December 1973. *Annals of the Natal Museum*, 22 (2): 489–576.

LAMPE, E. 1917. Katalog der Skorpione, Pedipalpen und Solifugen des Naturhistorischen Museums der Residenzstadt Wiesbaden. *Jahrbucher des Nassauischen Vereine für Naturkunde*, 70(1): 185–203.

LAURIE, M. 1896. Further notes on the anatomy and development of scorpions, and their bearing on the classification of the order. *Annals and Magazine of Natural History* (6), 18: 121–133.

LEVY, G. & AMITAI, P. 1980. *Scorpiones*. *Fauna Palaestina*. *Arachnida* I. The Israel Academy of Sciences and Humanities. Jerusalem, 1980.

LÖNNBERG, E. 1897. Om Skorpionernas och Pedipalpernas geografiska Utbredning. *Entomologisk Tidskrift*, 18: 193–211.

LORIA, S.F. & L. PRENDINI. 2014. Homology of the lateral eyes of Scorpiones: a six-ocellus model. *PLoS ONE* 9(12): e112913. doi:10.1371/journal.pone.0112913.

LORIA, S.F. & L. PRENDINI. 2018. Ultrastructural comparison of the eyespot and ocelli of scorpions, and implications for the systematics of Chaerilidae Pocock, 1893. *Zoologischer Anzeiger*, 273: 183–191.

LOURENÇO, W. R. 2001. Taxonomic considerations on the genera *Butheolus* Simon, *Nanobuthus* Pocock and *Neobuthus* Hirst (Scorpions, Buthidae) with the description of a new species of *Neobuthus* from Ethiopia. *Ecology of Desert Environments*, 2001: 171–183.

LOURENÇO, W. R. 2005. Description of three new species of scorpion from Sudan (Scorpiones, Buthidae). *Boletín Sociedad Entomológica Aragonesa*, 36: 21–28.

LOURENÇO, W. R. & B. DUHEM. 2012. Two new species of scorpions from the Arabian belonging to the genera *Butheolus* Simon and *Compsobuthus* Vachon. *Zoology in the Middle East*, 55: 121–126.

LOURENÇO, W. R. & E.-A. LEGUIN. 2011. Further considerations on the species of the genus *Orthochirus* Karsch, 1891 from Africa, with description of three new species (Scorpiones: Buthidae). *Euscorpius*, 123: 1–19.

LOURENÇO, W. R. & J.-X. QI. 2006. Further considerations on the genus *Butheolus* Simon, 1882 and description of one new species from Saudi Arabia (Scorpiones: Buthidae). *Zoology in the Middle East*, 37: 91–97.

LOURENÇO, W. R. & A. ROSSI. 2017. A new substitute name for *Butheolus pallidus* Lourenço et Duhem, 2012 (Scorpiones, Buthidae), species described from United Arab Emirates/Oman. *Rivista Aracnologica Italiana*, 13: 42–44.

LOURENÇO, W.R. & M. VACHON. 1995. Un nouveau genre et deux nouvelles espèces de scorpions Buthidae d'Iran. *Bulletin du Muséum National d'Histoire Naturelle de Paris*, 17 (3–4): 297–305.

LOWE, G. 2000. A new species of *Babycurus* (Scorpiones: Buthidae) from Northern Oman. *Entomological News*, 111: 185–192.

LOWE, G. 2010a. New picobuthoid scorpions (Scorpiones: Buthidae) from Oman. *Euscorpius*, 93: 1–53.

LOWE, G. 2010b. Two new species of *Hottentotta* Birula, 1908 (Scorpiones: Buthidae) from Northern Oman. *Euscorpius*, 103: 1–23.

LOWE, G. & F. KOVAŘÍK. 2016. Scorpions of the Horn of Africa (Arachnida, Scorpiones). Part V. Two new Species of *Neobuthus* Hirst, 1911 (Buthidae), from Ethiopia and Eritrea. *Euscorpius*, 138: 1–25.

LOWE, G., E.A. YAĞMUR & F. KOVAŘÍK. 2014. A review of the genus *Leiurus* Ehrenberg, 1828 (Scorpiones: Buthidae) with description of four new species from the Arabian Peninsula. *Euscorpius*, 191: 1–129.

NAVIDPOUR, S. & G. LOWE. 2009. Revised diagnosis and redescription of *Apistobuthus susanae* (Scorpiones, Buthidae). *Journal of Arachnology,* 37 (1): 45–59.

NENILIN, A. B. & V. FET. 1992. Zoogeographical analysis of the world scorpion fauna (Arachnida: Scorpiones). *Arthropoda Selecta*, 1 (2): 3–31 (in Russian).

PÉREZ, S.M. 1974. Un inventario preliminar de los escorpiones de la región Paleártica y claves para la identificación de los géneros de la región Paleártica Occidental. *Madrid: Universidad Complutense de Madrid, Facultad de Ciencias, Departamento de Zoología, Cátedra de Artrópodos*, 7: 1–45.

POCOCK, R. I. 1890. A revision of the genera of scorpions of the family Buthidae, with descriptions of some South-African species. *Proceedings of the Zoological Society*, 1890: 114–141.

POCOCK, R. I. 1892. Descriptions of two new genera of scorpions, with notes on some species of *Palamnaeus*. *Annals and Magazine of Natural History*, (6), 9: 38–49.

POCOCK, R. I. 1895. On the Arachnida and Myriopoda obtained by Dr. Anderson's collector during Mr T. Brent's expedition to the Hadramaut, South Arabia, with a supplement upon the scorpions obtained by Dr. Anderson in Egypt and the Eastern Soudan. *Journal of the Linnean Society*, 25: 292–316.

POCOCK, R. I. 1900. *Arachnida. The Fauna of British India, including Ceylon and B*urma. Published under the authority of the Secretary of State for India in Council. London: W. T. Blandford, xii, 279 pp.

PRENDINI, L. 2003. Discovery of the male of *Parabuthus muelleri*, and implications for the phylogeny of *Parabuthus* (Scorpiones: Buthidae). *American Museum Novitates*, 3408:1–24.

PRENDINI, L. & W. WHEELER. 2005. Scorpion higher phylogeny and classification, taxonomic anarchy, and standards for peer review in online publishing. *Cladistics*, 21: 446–494.

SALE, J. B. 1980. The ecology of the mountain region of Dhofar. *Journal of Oman Studies. Special Report,* 2: 25–54.

SANTIAGO-BLAY, J.A., M.E. SOLEGLAD & V. FET. 2004. A redescription and family placement of *Uintascorpio* Perry, 1995 from the Parachute Creek member of the Green River Formation (Middle Eocene) of Colorado, USA (Scorpiones: Buthidae). *Revista Ibérica de Aracnologia*, 10: 7–16.

SIMON, E. 1882. Étude sur les Arachnides de l'Yemen méridional. Viaggio ad Assab nel Mar Rosso, dei Signori G. Doria ed O. Beccari con il R. Avviso 'Esploratore' dal 16 nov. 1879 al 26 feb. 1880. *Annali del Museo Civico di Storia Naturale di Genova*, 18: 207–260.

SIMON, E. 1889. Note sur la piqûre du *Butheolus thalassinus*, par M. Simon. *Bulletin des séances de la Société Entomologiqe de France*, 98.

SIMON, E. 1890. Études arachnologiques. 22e Mémoire. XXXIV. Étude sur les Arachnides de l'Yemen. *Annales de la Société Entomologique de France*, (6) 10: 77–124.

SIMON, E. 1910. Révision des scorpions d'Égypte. *Bulletin de la Sociètè Entomologique d'Égypte* (*Cairo*), 1910: 57–87.

SISSOM, W.D. 1990. Systematics, biogeography and paleontology. Pp. 64–160 *in* Polis, G. A. (ed.). *The Biology of Scorpions*. Stanford University Press, Stanford, California.

SISSOM, W.D. 1994. Descriptions of new and poorly known scorpions of Yemen (Scorpiones: Buthidae, Diplocentridae, Scorpionidae). *Fauna of Saudi Arabia*, 14: 3–39.

SISSOM, W. D., G. A. POLIS & D. D. WATT. 1990. Field and laboratory methods. Pp. 445–461 *in* Polis, G.A. (ed.). *The Biology of Scorpions*. Stanford University Press, Stanford, CA.

SOLEGLAD, M.E. & V. FET. 2003a. The scorpion sternum: structure and phylogeny (Scorpiones: Orthosterni). *Euscorpius*, 5: 1–34.

SOLEGLAD, M.E. & V. FET. 2003b. High-level systematics and phylogeny of the extant Scorpions (Scorpiones: Orthosterni). *Euscorpius*, 11: 1–175.

SREENIVASA-REDDY R.P. 1970. The systematic position of the scorpion genus *Charmus*. *Journal of Natural History*, 4: 17–23.

STAHNKE, H. L. 1971. Scorpion nomenclature and mensuration. *Entomological News*, 81: 297–316.

STAHNKE, H. L. 1972. A key to the genera of Buthidae (Scorpionida). *Entomological News*, 83 (5): 121–133.

TÁBORSKÝ, K. 1934. Sur les especes du genre *Buthus* Leach du Museum National de Prague. *Sbornik Zoologického Oddelení Národniho Muzea v Praze*, 1: 39–40.

VACHON, M. 1952. *Études sur les scorpions*. Institut Pasteur d'Algérie. Alger.

VACHON, M. 1958. The 3rd Danish Expedition to Central Asia. Zoological Results 23. Scorpionidea (Chelicerata) de l'Afganistan. *Videnskabelige Meddelelser fra Dansk Naturhistorisk Forening*, 120: 121–187.

VACHON, M. 1963. De l'utilité, en systématique, d'une nomenclature des dents de chélicères chez les scorpions. *Bulletin du Musèum National d'Histoire Naturelle, Paris*, (2), 35 (2): 161–166.

VACHON, M. 1966. Liste des scorpions connus en Égypte, Arabie, Israël, Liban, Syrie, Jordanie, Turquie, Irak, Iran. *Toxicon*, 4: 209–218.

VACHON, M. 1974. Étude des caractères utilisés pour classe les familles et les genre de Scorpiones (Arachnides). 1. La trichobothriotaxie en Arachnologie. Sigles trichobothriaux et types de trichobothriotaxie chez les scorpions. *Bulletin du Muséum National d'Histoire Naturalle Paris, Zoologie*, (3) 104 (140): 857–958.

VACHON, M. 1975. Sur l'utilisation de la trichobothriotaxie du bras des pedipalps des Scorpions (Arachnides) dans le classement des genres de famille des Buthidae Simon. *Compte rendus hebdomadaires des séances de l'Academie des Sciences, Paris Ser.D Sciences Naturelles*, 281 (21): 1597–1599.

VACHON, M. 1980. Scorpions du Dhofar. The Scientific Results of the Oman Flora and Fauna Survey 1977 (Dhofar). *Journal of Oman Studies. Special Report,* 2: 251–263.

VACHON, M. & R. KINZELBACH. 1987. On the taxonomy and distribution of the scorpions of the Middle East. i*n* Krupp, F., W. Schneider & R. Kinzelbach (eds.). Proceedings of the Symposium on the Fauna and Zoogeography of the Middle East, Mainz, 1985. *Beihefte zum Tübinger Atlas des Vorderen Orients, Reihe A* (*Naturwissenschaften*), 28: 91–103.

VACHON, M. & R. STOCKMANN. 1968. Contribution à l'étude des Scorpions africains appartenant au genre *Buthotus* Vachon 1949 et étude de la variabilité. *Monitore Zoologico Italiano* (*N. S.*) 2 (*Supplemento*): 81–149.

VOLSCHENK, E.S. 2005. A new technique for examining surface morphosculpture of scorpions. *Journal of Arachnology*, 33: 820–825.

WEIDNER, H. 1959. Die entomologischen Sammlungen des Zoologischen Staatsinstituts und Zoologischen Museums Hamburg. I. Teil. Pararthropoda und Chelicerata. I. *Mitteilungen aus dem Hamburgischen Zoologischen Museum und Institut*, 57: 89–142.

WERNER, F. 1934. Scorpiones, Pedipalpi. In: *H. G. Bronns Klassen und Ordnungen des Tierreichs*. Akademische Verlaggesellschaft, Leipzig. 5, IV, 8, Lief. 1-2, Scorpiones, pp. 1–316.

WILLIAMS, S.C. 1968. Scorpion preservation for taxonomic and morphological studies. *Wasmann Journal of Biology*, 26 (1): 133–136.

WOOD, N. 1993. Scorpion Search. *Petroleum Development Oman News*, 4: 12–17.

YANG, X., Y. NORMA-RASHID, W. R. LOURENÇO & M. ZHU. 2013. True lateral eye numbers for extant buthids: a new discovery on an old character. *PLoS ONE*, 8(1): e55125. doi:10.1371/journal.pone.0055125.